The Use of Lab-on-a-chip Devices to Measure the Forces Exerted by Pathogenic Oomycete Species

---

A thesis

submitted in partial fulfilment

of the requirements for the Degree of

Master of Science

in Cellular and Molecular Biology

School of Biological Sciences

University of Canterbury

New Zealand

Heather Shearer

2018

Table of Contents

Table of Figures

Table of Tables

Acknowledgements

Firstly, I would like to thank my supervisory team Ashley Garrill and Volker Nock. The encouragement, support and advice from you both has been extremely valuable throughout my research. Thank you both for all you have both done for me.

I would like to thank my lab group for their support and assistance throughout the year. Steph, Liz and Mona, thank you for your support, encouragement, advice and at times much needed words of motivation. Thank you to Louise for your willingness to create a microscope booking system which benefitted us both. Ayelen and Yiling, thank you both for your roles in device design and fabrication, your contribution is very much appreciated.

Thank you to the lab technicians for their roles in maintaining the 6th floor lab and to all the researchers in the lab for keeping the lab tidy and an enjoyable place to conduct research.

I greatly appreciate and thank the University of Canterbury for their financial assistance.

To my family and friends, thank you for your unfailing support and encouragement throughout this year and all others. I cannot thank you enough for all you have done for me.

Lastly, I would like to thank Michael. Your continued support, encouragement and many hours spent proofreading my drafts has been invaluable and I am forever grateful.

Abstract

Oomycetes in the genus *Phytophthora* cause devastating diseases worldwide, resulting in billions of dollars of economic damage annually. Although the control of these oomycetes is a high priority, a lack of effective control measures has led to their continued success as pathogens. In this thesis, microfluidic Lab-on-a-chip (LOC) devices containing force sensing micropillars were designed to investigate hyphal force production, a key component of invasive growth. The growth rate, width and force exerted by the hyphae of the pathogen *Phytophthora nicotianae* were successfully measured on the designed devices. These variables were also measured in hyphae where the actin cytoskeleton was disrupted with latrunculin B. The results identify the critical importance of the actin cytoskeleton in hyphal growth and morphology. In addition, two other pathogens from the *Phytophthora* genus, *Phytophthora cinnamomi* and *Phytophthora sojae*, were successfully grown on the designed devices. This result identifies the applicability of these devices to investigate the molecular mechanisms responsible for force generation in other pathogenic oomycete species.

The knowledge gained from this research contributes to our understanding of the mechanisms that underlie the invasive growth of pathogenic oomycete species. A greater understanding of these mechanisms is required to improve the control strategies of *Phytophthora* and other pathogenic hyphal organisms. This research highlights the effectiveness of the LOC devices designed in the quest to obtain this knowledge.

Abbreviations and definitions

A. bisexualis	*Achlya bisexualis*
A. cochlioides	*Aphanomyces cochlioides*
ANOVA	Analysis of variance
BMP	Bitmap
C. japonica	*Camellia japonica*
DMSO	Dimethylsulfoxide
F	F statistic
F-actin	Filamentous actin
G-actin	Globular actin
HSD	Honest significant difference
latB	Latrunculin B
LOC	Lab-on-a-chip
min	Minute
ml	Millilitre
mm	Millimetre
MPa	Megapascal
n	Sample size
NA	Numerical aperture
N/A	Not applicable
N. crassa	*Neurospora crassa*
p	Probability value
P. agathidicida	*Phytophthora agathidicida*
P. cinnamomi	*Phytophthora cinnamomi*
P. graminicola	*Pythium graminicola*
P. infestans	*Phytophthora infestans*
P. insidiosum	*Pythium insidiosum*
P. nicotianae	*Phytophthora nicotianae*
P. pluvialis	*Phytophthora pluvialis*
P. radiata	*Pinus radiata*
P. sojae	*Phytophthora sojae*
PDMS	Polydimethylsiloxane

PYG	Peptone yeast glucose
r	Radius
R^2	R-squared
r_s	Spearman's rank correlation coefficient
s	Second
S.E.M.	Standard error of the mean
S. ferax	*Saprolegnia ferax*
USD	United States Dollar
UV	Ultraviolet
v/v	Volume per volume
x	Times
X^2	Chi-square
XML	Extensible Markup Language
µl	Microlitre
µm	Micrometre
µM	Micromolar
µN	Micronewton
%	Percent
°C	Degree Celsius
π	Pi

Chapter 1. Introduction

1.1 Oomycete disease impact

1.1.1 Implications of oomycete disease

In recent years, fungal and oomycete diseases have caused some of the most severe die-offs and extinctions of plant and animal species ever witnessed (Fisher et al 2012). Plant disease epidemics caused by fungal and oomycete infections have altered the course of human history, causing economic and famine tragedies such as the Irish potato famine in 1845 and 1846 (Erwin & Ribeiro 1996, Fisher et al 2012, Money 2006). Currently, food security is being threatened worldwide, with fungal and oomycete infections causing widespread population declines in food crops as well as facilitating declines in other diverse taxa including bees, bats, and amphibians (Bebber et al 2013, Derevnina et al 2016, Fisher et al 2012). While morphologically very similar, oomycetes and fungi have key differences as a result of their differing evolutionary lineages. Oomycetes belong to the Stramenopile lineage in the Chromalveolata supergroup and are therefore more closely related to the brown algae and diatoms than to the fungi, which belong to the Unikonts supergroup (Bouwmeester et al 2009, Keeling et al 2005). Morphological similarities such as the similarities in hyphal growth is therefore thought to be the result of convergent evolution (Money 2007, Money et al 2004).

In 1845, over 40% of the potato crops in Ireland were destroyed from disease caused by the oomycete *Phytophthora infestans*, followed by 90% in the following year (Money 2006). As more than three million people relied upon these crops at the time, this disease led to mass starvation, poverty and emigration (Money 2006). It has been estimated that as a result of the sociological and economic change resulting from this disease, one million of the eight million inhabitants of Ireland were lost through starvation and another million through emigration (Erwin & Ribeiro 1996, Money 2006). This pathogen is still causing disease in potato and tomato plants throughout the world today (Judelson & Blanco 2005). While this pathogen has a narrow host range, limited to tomatoes and potatoes, many other species from the same genus, *Phytophthora*, have much broader host ranges. As such, there is an increasing concern on the potential impact of the species from this genus (Erwin & Ribeiro 1996).

Diseases caused by oomycete species are a threat to both global food security and natural ecosystems (Derevnina et al 2016). Their impact is increasing and unfortunately human activity

is intensifying disease dispersal through environmental modifications which increase the opportunity for the spread of these organisms (Fisher et al 2012). Despite the restrictions that are in place to minimise the dispersal of crop pests and pathogens, biotic homogenisation is occurring at an increasing and alarming rate (Bebber et al 2014, Bebber et al 2013).

Additionally, while the spread of pathogens occurs predominantly through human and animal transportation, there is an increasing concern that climate change is creating opportunities for pathogens to become established in previously unsuitable regions (Bebber et al 2014, Bebber et al 2013). In 2013 it was estimated that as a result of climate change, pests and pathogenic species are migrating towards the Poles at a rate of up to 2.8 kilometres per year (Bebber et al 2013). This increase in pathogen spread and the opportunity for establishment in areas which were previously unsuitable is of great concern.

1.1.2 Control strategies for oomycete disease

Infection of a plant host by a pathogenic species involves an interplay of many defence mechanisms both from the host and from the pathogen that is attempting to infect the plant (Dodds & Rathjen 2010, Fawke et al 2015). To defend against infection, host plants can often detect molecules secreted by the invading species, known as elicitors, the recognition of which triggers immune responses within the host plant (Fawke et al 2015). These responses result in the induction of several plant defence mechanisms such as the release of reactive oxygen species, localised host cell death and expression of other defence related genes (Dodds & Rathjen 2010, Grenville-Briggs & van West 2005, Hardham 2007).

In addition to plant defence responses, humans have introduced measures such as selective breeding and fungicide application to aid plant survival and limit infection by pathogenic species and thereby reduce lost crop yield and economic losses (Dodds & Rathjen 2010). While a combination of these measures is often able to decrease the loss of crops due to infection by pathogenic species, because of the pressures imposed by these measures, the species are often able to develop resistance to chemical treatments as well as adapt and overcome barriers imposed by the host plant (Dodds & Rathjen 2010, Hardham 2007). This is of particular concern for oomycete species that have been shown to have a large genetic flexibility (Tyler 2007).

Many common fungicides used to treat oomycete disease, such as those which inhibit chitin synthase, are ineffective for controlling pathogenic oomycetes whose cell wall is

predominantly composed of β-glucans and cellulose (Grenville-Briggs et al 2008, Hardham 2007, Hua et al 2015). Similarly, azole fungicides which target the sterol biosynthetic pathway are ineffective against oomycetes as they do not synthesise sterols (Hua et al 2015, Latijnhouwers et al 2003, Madoui et al 2009). As these are two of the most common fungicide targets, control of oomycete species can be difficult (Meng et al 2014). An additional problem in addressing oomycete species that infect plants from underground, including many species from the genus *Phytophthora*, is that this treatment is not economically favourable (Tyler 2007). In addition, the use of fungicides and other chemical sprays are becoming less favourable due to the risks associated with pathogen adaptation and the effect they cause on ecosystems and human health (Panabières et al 2016). As such, the development of new management strategies for pathogenic disease control is required.

Although the impact of oomycete diseases is well known, strategies for effective prevention and control of many of these pathogens is limited, identifying the urgent need for an increase in scientific knowledge and development (Derevnina et al 2016, Panabières et al 2016). Although fungicide treatments and breeding measures can be put in place, an increased understanding of the molecular mechanisms behind the invasive growth of pathogenic species is needed to reduce both economic and biodiversity loss. Understanding how invasion occurs and potential ways to reduce this invasive growth could help to protect species which are being targeted by these pathogenic species throughout the world.

1.2 Impact caused by species within the genus *Phytophthora*

1.2.1 National implications of disease caused by species of *Phytophthora*

In New Zealand, oomycete species in the genus *Phytophthora*, particularly the recently introduced species *Phytophthora agathidicida* (previously known as *Phytophthora taxon agathis*) are of concern (Jamieson et al 2014). *P. agathidicida* is a water and soil-borne pathogen that causes kauri dieback, a currently untreatable disease which is having a devastating impact on New Zealand's kauri trees (*Agathis australis*) (Beever et al 2009, Waipara et al 2013). Symptoms of kauri dieback include: root rot, a collar rot causing bleeding and basal lesions, defoliation, severe chlorosis and mortality (Beever et al 2009, Waipara et al 2013). Five species of *Phytophthora* have been recorded from the environment surrounding kauri trees: *Phytophthora cinnamomi*, *Phytophthora cryptogea*, *Phytophthora kernoviae*,

Phytophthora nicotianae and *P. agathidicida*, but it is the latter species that has been identified as the species which is the primary cause of kauri dieback (Beever et al 2009).

In 2008, *P. agathidicida* was classified as an Unwanted Organism under the Biosecurity Act and a management programme for kauri dieback was initiated by the Ministry for Primary Industries, Māori, the Department of Conservation and Regional Councils in order to control the spread of this disease (Jamieson et al 2014, Waipara et al 2013). Measures such as keeping trampers to walking tracks, staying off kauri tree roots and cleaning and disinfecting footwear before entering and leaving forests where kauri trees are located have since been implemented.

Kauri trees are one of the longest living tree species, able to reach over one thousand years in age and with a large trunk around 4.5 meters in diameter (Beever et al 2009). They are known as the kings of the forest and are a taonga, a treasure, to Māori, as well as an iconic species to all New Zealanders and a major tourist attraction (Beever et al 2009, Jamieson et al 2014, Waipara et al 2013). In addition, kauri trees are considered to be a keystone species, altering the soil composition in their immediate environment by generating podsolised soils in which only certain species can grow (Ecroyd 1982). As such, if kauri trees are lost, the whole ecosystem will be altered and these species dependent upon the kauri will likely be lost as well. While provisions to control the spread of the disease have been employed, it is still currently untreatable. An investigation into the invasive growth of *Phytophthora* species is therefore vitally important for conserving this iconic New Zealand species.

Another oomycete species in the genus *Phytophthora* that poses a biosecurity threat in New Zealand is *Phytophthora pluvialis* which causes red needle cast of pine trees (*Pinus radiata*) (Scott & Williams 2014). Red needle cast is a foliar disease that was first identified in 2008, that causes discolouration and lesion formation on *P. radiata* needles followed by premature detachment of the needles from the tree (Dick et al 2014, Scott & Williams 2014). In New Zealand, *P. radiata* represents 90% of the exotic plantation estate, with export earnings of these forests accounting for almost 11% of total national export value (Dick et al 2014). Due to the high economic value of this species in New Zealand, the control of pathogens and pests associated with it is of great importance. While the infection caused by *P. pluvialis* primarily only affects the needles in the lower crown of the trees, heavily affected trees can become fully defoliated (Dick et al 2014). In addition, although *P. pluvialis* has been identified as the causal pathogen of red needle cast, it is thought that given the right environmental conditions, *P.*

radiata may be susceptible to disease caused by other species within the *Phytophthora* genus (Dick et al 2014).

Once established, *Phytophthora* species are nearly impossible to eradicate from the environment, especially in areas such as New Zealand where conditions such as the topography, high rainfall volumes and soil type favour these species (Scott & Williams 2014). As species within the genus *Phytophthora* are abundant and the host range for these species is broad, many plant species are at risk by these organisms. As such, control measures for these species are required to minimise their impact on native species and species of economic importance such as kauri and pine trees in New Zealand.

1.2.2 Impact of the *Phytophthora* species examined in this research

The research described in this thesis is focused on three oomycete species from the *Phytophthora* genus; *P. nicotianae*, *P. cinnamomi* and *Phytophthora sojae*. *P. nicotianae* was the primary focus, while *P. cinnamomi* and *P. sojae* were briefly examined to obtain preliminary data for these species and to allow for a comparison between the three *Phytophthora* species.

As detailed above, species from the genus *Phytophthora* are responsible for causing disease and declines in populations of many species. These include kauri trees in New Zealand (Beever et al 2009, Waipara et al 2013), tobacco plants throughout the world (Jing et al 2017, Wang et al 2013) and jarrah eucalyptus trees in Western Australia (Erwin 1983) among others. While the economic impact of *Phytophthora* species is difficult to calculate due to the many components of pathogenic disease including loss of crops, fungicide/oomycide usage and replacement crops (Panabières et al 2016), it has been estimated that economic damage in the United States alone by *Phytophthora* species is billions of dollars annually (Erwin & Ribeiro 1996). In addition, as the number of recognised *Phytophthora* species is continually expanding, this already substantial cost is likely to continue to increase.

Since the first *Phytophthora* species, *P. infestans*, was described in by Anton de Bary in 1876, the number of described *Phytophthora* species has increased. In 2012, the number of *Phytophthora* species described was approximately 100, a number which had doubled since the previous decade (Kroon et al 2012). Since then, an expanded *Phytophthora* phylogeny has been presented by Yang et al in 2017, which includes 142 named and 43 provisionally recognised species of *Phytophthora* within 10 clades (Yang et al 2017). Within these, both *P.*

sojae and *P. cinnamomi* are in clade 7, while *P. nicotianae* is in clade 1 with *P. infestans* (Kroon et al 2012, Yang et al 2017). As the number of recognised species from the genus *Phytophthora* increases, the ecological and economic importance of these species also increases.

A recent survey by Kamoun et al in 2015 ranked plant-pathogenic oomycetes on their combined scientific and economic importance (Kamoun et al 2015). All three *Phytophthora* species examined in this research were ranked in the top 10, with *P. sojae* ranked 4th, *P. cinnamomi* ranked 7th and *P. nicotianae* ranked 8th equal, with *Pythium ultimum*. However, Panabières et al (2016) believe that *P. nicotianae* should be ranked higher and expect that it will gain an increased ranking in the near future due to its intrinsic characteristics, adaptive potential and the impact of human activities such as climate change.

P. nicotianae, also known as *Phytophthora parasitica*, is a soil-borne plant-pathogenic oomycete well known for its impact on many plant and tree species, in particular tobacco where it causes black shank (Jing et al 2017, Meng et al 2014, Wang et al 2013). Plants at all stages of growth can be infected by *P. nicotianae*, with infection occurring in the roots, crowns, flowers, fruits and leaves (Erwin & Ribeiro 1996). *P. nicotianae* has a large host range and is currently known to be able to infect over 72 plant genera, a number which is still expanding (Meng et al 2015, Meng et al 2014, Panabières et al 2016, Wang et al 2011). Due to this large host range, including the model plants *Arabidopsis thaliana* and *Nicotiana tabacum*, *P. nicotianae* has been identified as an emerging model pathogenic species for the genus *Phytophthora* and oomycete pathogens in general (Meng et al 2015, Meng et al 2014, Wang et al 2011).

P. cinnamomi is a soil-borne oomycete pathogen which also has a broad host range, in Australia alone 3000 species are estimated to be susceptible (Erwin & Ribeiro 1996, Kamoun et al 2015). *P. cinnamomi* is an important pathogen in Australia as it is the causal pathogen of jarrah dieback in Western Australia (Erwin & Ribeiro 1996). Disease caused by *P. cinnamomi* on the native vegetation in Australia impacts whole ecosystems (Chakraborty et al 1998) and has economic impacts in the forestry, horticulture and nursery industries (Kamoun et al 2015).

In contrast to *P. nicotianae* and *P. cinnamomi*, *P. sojae* has a narrow host range, and is limited primarily to soybean (Erwin & Ribeiro 1996). However, even with this narrow host range *P. sojae* has a large economic impact with worldwide losses estimated to be $1-2 billion USD annually (Tyler 2007). All parts of soybean plants are susceptible to infection by *P. sojae*,

although infection typically initiates below ground and spreads up the infected plant (Kamoun et al 2015, Tyler 2007).

While there are many factors which influence disease development in *Phytophthora* species, one of concern is the role of the climate in disease development. The climate has been shown to influence the development of disease caused by *Phytophthora* species by restricting their geographical distribution (Duniway 1983). However, as there are so many species within the *Phytophthora* genus, while one species may be restricted another is likely to be able to thrive (Duniway 1983). This is of particular concern for the species *P. nicotianae* as it has been proposed that it will benefit from global warming as it thrives at a higher temperature than other *Phytophthora* species that infect similar hosts (Erwin & Ribeiro 1996, Kamoun et al 2015).

1.3 Growth and pathogenicity of oomycetes

1.3.1 Initiation of infection

Oomycete plant pathogens grow through one of three lifestyles during infection; biotrophy, necrotrophy or hemibiotrophy (Fawke et al 2015, Park et al 2017). Biotrophic oomycetes keep the host alive during their infection, whereas the assimilation of nutrients from the host cells in necrotrophs results in cell death (Fawke et al 2015). In contrast, hemibiotroph oomycete species, including those in the genus *Phytophthora*, obtain nutrients for growth from both living and dead cells within the host, often growing in an initial biotrophic phase before later changing to a necrotrophic stage (Fawke et al 2015).

A key aspect of oomycete pathogenicity is the ability of their hyphae to grow invasively and thus, overcome the resistance of the substrate of the host (Nezhad & Geitmann 2013). Infection of a plant host by a plant pathogenic oomycete normally begins with either direct or indirect sporangia germination (Fig. 1.1) (Fawke et al 2015, Presti & Kahmann 2017, Tyler 2002). Direct sporangia germination involves the attachment of sporangia to the host surface followed by the invasion of host tissue either through natural openings such as the stomata on a plant leaf or through formation of an appressoria, a specialised structure that forms an initial penetration hypha for host cell penetration (Fawke et al 2015, Grenville-Briggs & van West 2005, Presti & Kahmann 2017, Tyler 2002). In contrast, indirect germination involves the release of zoospores from sporangia which swim to the host surface where they encyst, germinate and produce appressoria for host cell penetration (Fawke et al 2015, Presti &

Kahmann 2017, Tyler 2002). This indirect germination through zoospores is the most important route of infection of roots, especially in saturated soils (Tyler 2002).

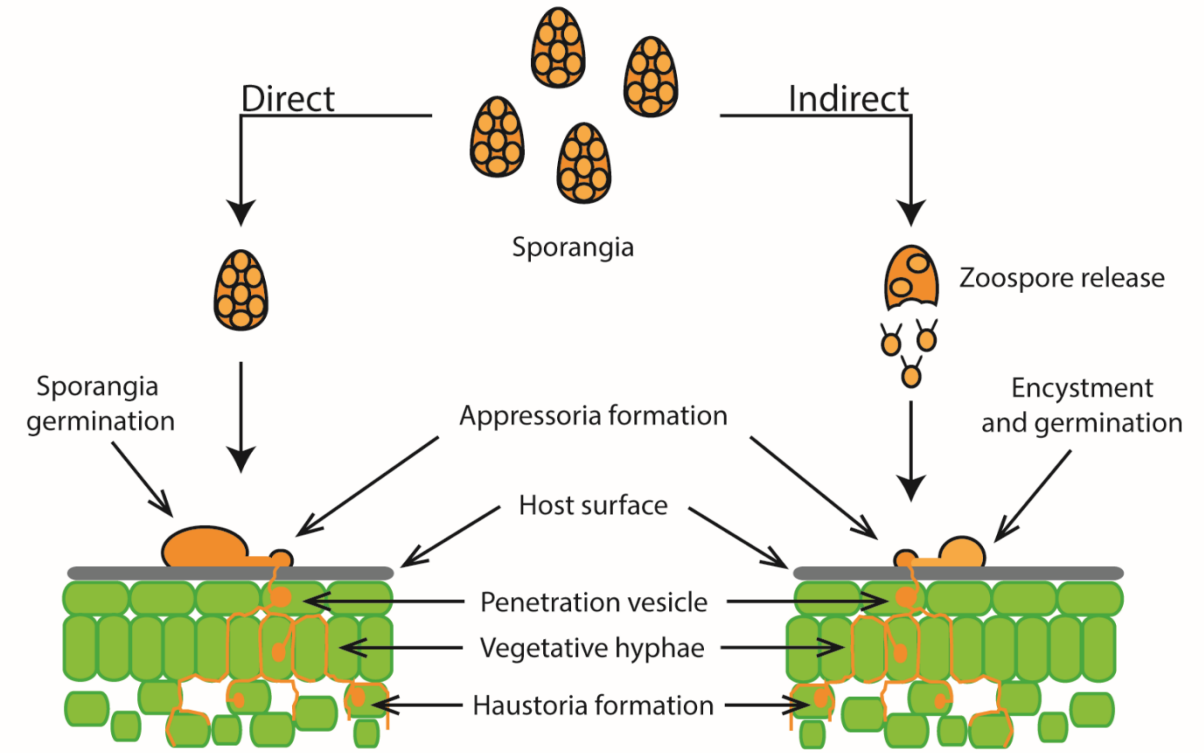

Figure 1.1. Initiation of plant host infection by oomycete species. Initiation of infection of an oomycete species on a host plant can occur through either direct or indirect germination (Fawke et al 2015, Presti & Kahmann 2017, Tyler 2002). In indirect germination, zoospores are released from sporangia following which they encyst to the host surface and germinate. In contrast, direct germination involves the germination of sporangia directly on the host surface. The infection process following germination is the same independent of the initial germination strategy. Adapted from Fawke et al 2015.

Following initial penetration of the host cell wall by appressoria, a primary spherical vesicle is formed from which vegetative hyphae emerge and continue invasive growth (Fawke et al 2015, Kots et al 2017, Presti & Kahmann 2017). The hyphal structures grow both intercellularly and intracellularly through the host cells (Grenville-Briggs & van West 2005). This invasive growth process is also likely to involve the enzymatic breakdown of host tissue, along with protrusive force generation at the tip of the growing hypha (Lew 2011). Lytic enzymes secreted by the invading organism digest host material and thus weaken the substrate for further invasive growth, while also providing the invading organism with nutrients for growth (Sietsma & Wessels 2006).

Most obligate biotrophs and hemibiotrophs also develop haustoria from their intercellular hyphae, which extend into surrounding plant cells, secreting effector molecules and absorbing nutrients (Asai & Shirasu 2015, Fawke et al 2015, Presti & Kahmann 2017). Haustoria enable a close connection with the host cell as they are enveloped by the host cell's plasma membrane (Ackerveken 2017, Asai & Shirasu 2015, Presti & Kahmann 2017).

As plants and their pathogens have co-evolved over millions of years, the host plant has evolved defences against its pathogens while the pathogen has evolved mechanisms to combat and avoid these defences (Asai & Shirasu 2015, Fawke et al 2015). To evade host immune responses and invade the host successfully, pathogenic species produce and secrete effector molecules (Ackerveken 2017, Asai & Shirasu 2015, Fawke et al 2015, Wang et al 2017). How these effector molecules are translocated from the invading hyphal species to the host plant is controversial and not yet fully understood (Ackerveken 2017, Presti & Kahmann 2017).

Two types of effector molecules are produced by plant pathogenic species; apoplastic effector molecules, which act outside of the plant cells to defend the pathogen against the hosts' defence systems and cytoplasmic effector molecules, which are delivered inside the host cells to supress or manipulate intracellular processes (Fawke et al 2015, Wang et al 2017). A recent study on *P. infestans* reported the delivery of both apoplastic and cytoplastic effector molecules from haustoria to the host (Wang et al 2017). The secretion of these effector molecules and their role in nutrient uptake from the host cells highlights the importance of haustoria in plant pathogen infection (Wang et al 2017).

1.3.2 Hyphal growth and pathogenicity

1.3.2.1 The process of tip growth in oomycete species

Oomycetes grow through tip growth, a complex and dynamic process through which filamentous hyphae are extended in a highly polarised manner (Lew 2011). Tip growth is also the mode of growth for many other cell types including fungal hyphae, plant root hairs, pollen tubes, algal rhizoids and moss protonemata (Geitmann et al 2001, Yu et al 2004). In tip growing cells, growth is confined to the tip, or apex of the cell, where new material for growth is deposited (Geitmann et al 2001). The materials required for the formation of new membrane and cell walls during hyphal growth are deposited at this apex via transport along cytoskeletal networks of microfilaments and microtubules (Heath & Kaminskyj 1989, Lamour & Kamoun 2009). Cells that grow through this process grow at rates that are some of the fastest known,

up to 100 micrometres per minute (μm/min) (Geitmann et al 2001). As the cell is extending from the tip relative to the environment, these cells are adapted to produce forces which can penetrate solid substrates, as is observed during invasive growth of fungal and oomycete species (Geitmann et al 2001).

Through the process of tip growth, hyphae move through environments, branching and creating mycelial networks with a high surface area to volume ratio to optimise nutrient uptake (Lew 2011). This is driven by their ability to sense external and internal factors, allowing growth to be directed towards increasingly favourable environments such as those which are nutrient rich (Brand & Gow 2009, Geitmann et al 2001). The uptake of additional nutrients then enables further growth, with the mycelium network continually expanding throughout the host/environment.

1.3.2.2 The role of turgor pressure in oomycete pathogenicity

In cells with a cell wall such as those in plants, fungi and oomycetes, their internal hydrostatic pressure, known as turgor pressure, provides mechanical support as well as providing the force for cell expansion (Lew 2011). In fungal organisms, which can regulate this turgor, the production of the force required for invasive growth is thought to involve an interplay between an increase in turgor pressure in their hyphae and/or modulation of tip yielding (Lew 2011, Lew et al 2004). In contrast, oomycete species have been shown to be unable to regulate or control their turgor (Lew et al 2004). As such, the regulation of their turgor is likely not involved in the invasive growth of oomycetes (Lew et al 2004). Instead, an increase in tip yielding is thought to play a central role (Walker et al 2006).

Tip yielding in fungal and oomycete species is thought to occur through softening of the cell wall as well as modifications to the actin cytoskeleton (Money 2007, Suei & Garrill 2008, Walker et al 2006). In oomycete species, the softening of the cell wall has been shown to occur, at least in part, through the secretion of hydrolase enzymes that cleave cross links in cellulose microfibrils in the cell wall (Money 2007). With increased tip yielding, a greater proportion of the turgor pressure inside the hyphae of these organisms generates the protrusive forces required for invasive growth (Money 2007). Thus, the turgor and the cytoskeletal arrangements within the cell, along with cell wall softening and enzyme secretion, are thought to be vital in force generation and invasive growth in oomycete species.

1.3.2.3 The role of the actin cytoskeleton in hyphal growth and oomycete pathogenicity

The actin cytoskeleton is a major component of the cytoskeleton in almost all eukaryotic cells and is made up of linear actin polymers known as filamentous actin (F-actin) comprised of monomers of globular actin (G-actin) (Chen et al 2000, Meijer et al 2014). When two of these polymers helically intertwine, they form a microfilament. Microfilaments are highly dynamic structures, reorganising continuously based on cellular requirements (Hua et al 2015, Meijer et al 2014). The availability of G-actin monomers, the presence of numerous different actin binding proteins and cellular conditions influence the polymerisation and depolymerisation of these dynamic structures (Meijer et al 2014). Another major component of the cell cytoskeleton are microtubules, both of which are important for delivering material to the hyphal tip for growth. However, the work in this thesis will only focus on the role of microfilaments in hyphal growth and force production.

Although the actin cytoskeleton is conserved in all eukaryotic organisms, playing a key role in many cellular processes, the function has been shown to differ significantly across evolutionary clades (Ketelaar et al 2012, Meijer et al 2014). Recently, *Phytophthora* actin genes have been recognised as different to those from plants, fungi and vertebrates, falling into a distinct, divergent oomycete clade (Ketelaar et al 2012). As little has been researched involving the actin cytoskeleton in oomycete species and due to its divergence from other actin genes, an investigation into the actin cytoskeleton of oomycete species is of interest.

In oomycetes, two dominant F-actin structures have been observed, actin cables and actin plaques (Bachewich & Heath 1998, Deora et al 2008, Kots et al 2017, Walker et al 2006, Yu et al 2004). *P. cinnamomi*, *Achlya bisexualis, Aphanomyces cochlioides* and *Saprolegnia ferax* have also been shown to have an F-actin cap, however this has not yet been observed in *P. infestans* (Bachewich & Heath 1998, Deora et al 2008, Meijer et al 2014, Walker et al 2006, Yu et al 2004). Interestingly, the actin cap in *A. bisexualis* and *P. cinnamomi* hyphae was found to be more common in non-invasive hyphae than hyphae growing invasively (Walker et al 2006). In addition to these structures, two novel actin configurations in *P. infestans* were recently observed; an aster-like actin configuration formed in appressoria and a ring-shaped accumulation of actin filaments formed during cell wall plug deposition (Kots et al 2017).

Rearrangements in the actin cytoskeleton have been observed during invasive growth in both fungi and oomycetes (Suei & Garrill 2008, Walker et al 2006). Walker et al (2006) observed differences in the distribution of F-actin of the oomycetes *A. bisexualis* and *P. cinnamomi*

growing invasively and non-invasively. In this study, an actin cap was predominantly observed at the tips of hyphae in non-invasive conditions while an F-actin depleted zone was observed predominantly under invasive growth conditions. Additionally, an F-actin depleted zone was observed in invasive hyphae of the fungus *Neurospora crassa* (Suei & Garrill 2008) and the size of this increased as a greater penetrative force was required to grow through agar of increasing concentrations. These experiments suggest that along with attachment to and weakening of the host substrate through enzymatic secretions and cell wall softening, the dynamics of F-actin may be important for enabling the invasive growth of fungal and oomycete species (Suei & Garrill 2008, Walker et al 2006).

While the function of all actin structures in oomycetes are yet to be elucidated, the importance of the actin cytoskeleton in their growth is well documented. Due to its importance in many cellular functions such as establishment and maintenance of tip growth and its role in appressoria formation and cyst germination, all of which are involved in invasive growth, the cytoskeleton is an excellent target for agents to control oomycete disease (Bachewich & Heath 1998, Ketelaar et al 2012, Kots et al 2017, Meijer et al 2014). An increase in our knowledge of the cytoskeleton in oomycetes and its role in infection and pathogenicity will be important in the future for the development of potential agents to control oomycete diseases globally.

1.3.2.3.1 Impact of latrunculin B on the actin cytoskeleton in oomycetes

Latrunculin B (latB) is an F-actin polymerisation inhibitor that functions by binding to free G-actin monomers, thus interfering with the cellular roles of microfilaments (Fig. 1.1) (Deora et al 2008, Meijer et al 2014). LatB has been used in previous studies to show the role of the actin cytoskeleton in hyphal growth of the oomycetes *P. infestans*, *S. ferax* and *A. cochlioides* (Bachewich & Heath 1998, Deora et al 2008, Gupta & Heath 1997, Heath et al 2000, Hua et al 2015, Ketelaar et al 2012, Meijer et al 2014). LatB was therefore utilised in this research to observe growth alterations that result from limiting the actin cytoskeleton of *P. nicotianae* and to determine whether the alterations impact hyphal forces generation and if so, to what extent.

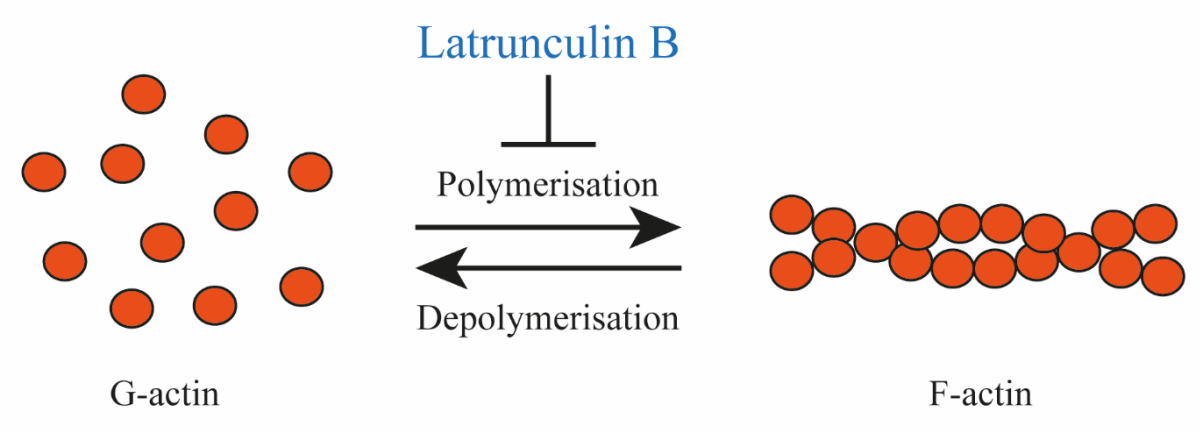

Figure 1.2. The role of Latrunculin B on the actin cytoskeleton. Latrunculin B is an actin polymerising inhibitor which acts by binding to free G-actin monomers, preventing F-actin polymerisation.

1.5 Advancements in cellular force measurement

The ability to measure cellular forces has advanced in recent years, with improvements in the methods used to obtain force values (Eisenstein 2017, Nezhad & Geitmann 2013). While the ability to measure force has been improved, no single method is suitable for all applications as all methods have associated advantages and disadvantages (Nezhad & Geitmann 2013).

Techniques used to measure force in cells have used both indirect and direct methods. Indirect methods can use substrates of a known or calibrated stiffness (e.g. agarose) or various membranes such as gold foil (Miyoshi 1895) and Mylar (polyethylene terephthalate) (Howard et al 1991) through which a cell grows and penetrates (Nezhad & Geitmann 2013). The ability of a cell to grow through the target substrate or membrane gives an indirect estimation of the force generated (Bastmeyer et al 2002). As the force measured using these methods is only an indirect estimation and is heavily reliant on the substrate or membrane resistance, these methods are limited in the accuracy and range of force values that can be obtained.

In contrast, direct methods such as waveguide sensors, optical traps and strain gauge cantilevers can measure and quantify force output directly (Bastmeyer et al 2002, Nezhad & Geitmann 2013). Of these direct methods, micro-strain gauge cantilevers are most suitable for hyphal measurements as they determine forces at a relevant magnitude (Tayagui et al 2017). This method involves placing a cantilever device in front of an advancing cell, contact of which causes the cantilever to bend and force values to be calculated (Bastmeyer et al 2002, Nezhad & Geitmann 2013). However, a risk with using this method is an underestimation of the force

exerted as cellular shape can change upon contact of the tip of the growing cell with the flat surface of the sensor, causing redirection of the growth of the hypha (Money 2007). Furthermore, the applicability of this technique to measure forces in invasive hyphae has been questioned (Walker et al 2006). These are important limitations as a method used to measure a physiologically relevant force must fulfil two key criteria: the measuring tool should not significantly alter the growth behaviour of the cell and the force exerted should be in the dynamic range of the measuring tool (Nezhad & Geitmann 2013). If cellular shape changes on contact with the sensor and causes redirection of hyphal growth, this is an alteration of the growth behaviour of the cell. When this occurs, the results obtained are inconclusive and difficult to use reliably, highlighting a limitation with using micro-strain gauge cantilevers (Nezhad 2014, Nezhad & Geitmann 2013). Additionally, due to the small forces exerted by the hyphae onto a much larger flat surface, the instruments need to be sensitive enough to measure these forces (Money 2007). As such, care needs to be taken when interpreting results obtained using this method.

1.5.1 The use of Lab-on-a-chip devices to measure cellular forces

Recent advancements in force measurement techniques have limited the error associated with collecting force measurement data through the development and use of microfluidic Lab-on-a-chip (LOC) technology. Microfluidic devices are made from polymers, particularly the organic polymer polydimethylsiloxane (PDMS) (Held et al 2011, Jo et al 2000). Microfluidic devices such as the LOC devices used in this research are becoming more frequently used as they allow for the study of whole living organisms and their cellular processes and interactions to be observed in a controllable microenvironment (Stanley et al 2016). There are many benefits for using PDMS; it is optically transparent, biologically and chemically inert, non-toxic, oxygen and carbon dioxide permeable and is fast and easy to fabricate (McDonald et al 2000, Duffy et al 1998, Held et al 2011, Jo et al 2000, Xia & Whitesides 1998). Additionally, the PDMS based method of soft lithography used in LOC device fabrication has been shown to have a lower cost for batch production than other polymer based fabrication methods (Yang et al 2014). However, as PDMS is hydrophobic, it needs to be treated with oxygen plasma before use to increase its hydrophilicity, thereby providing a suitable environment for species to grow (Eddington et al 2006, Jo et al 2000). This is important for the study of oomycetes as their hyphae tend to grow through aqueous environments, not on hydrophobic material (Nock et al 2015).

LOC technology has been developed as an alternative method to micro-strain gauges for cells that easily reorient their growth direction in response to a mechanical trigger (Nezhad et al 2013). Nezhad et al (2013) developed a LOC device with narrow openings called microgaps which were presented as obstacles to pollen tube growth. The design of the microgaps in the growth channels forces the pollen tube to grow through the gaps, the interaction of which allows for force measurements to be collected without compromising cellular growth processes (Nezhad 2014, Nezhad et al 2013).

Additionally, a technically simpler approach to measure forces exerted by cells and organisms was developed for nematodes using PDMS elastomeric micropillar arrays in LOC devices (Ghanbari et al 2010, Ghanbari et al 2012, Johari et al 2012a, Johari et al 2012b, Johari et al 2013, Qiu et al 2015, Qiu et al 2014). In these LOC devices, the spacing between the micropillars as well as the dimensions of the micropillars are critical for successful force measurement. Modifications of these micropillar arrays have been recently utilised for the measurement of forces exerted and directionality of this force by hyphae of the model organisms *A. bisexualis* and *N. crassa* (Nock et al 2015, Sun et al 2018, Tayagui et al 2016, Tayagui et al 2017). The ability to successfully modify these LOC devices for force measurements in hyphal organisms demonstrates the flexibility of these LOC devices, identifying the potential for modifications to suit the organism of interest.

1.6 Aims, hypotheses and objectives

The aim of this research was to design and fabricate microfluidic LOC devices containing force sensing micropillars (referred to as pillars) suitable for the growth and manipulation of pathogenic oomycete species and utilise the devices to measure the forces they exert. Quantification of the forces exerted by the hyphae of oomycete species is of interest because as described earlier, the hyphal force exerted is one of the key components of invasive growth (Lew 2011).

Previous research at the University of Canterbury has used similar LOC devices, which are unique in their ability to measure both the magnitude and direction of the forces exerted by hyphae from filamentous organisms. However, this previous research has focused on two model species: the fungus *N. crassa* and the oomycete *A. bisexualis* (Nock et al 2015, Sun et al 2018, Tayagui et al 2016, Tayagui et al 2017). The research described in this thesis aims to

expand on this previous research using pathogenic oomycete species from the genus *Phytophthora*.

The main hypotheses for this research are:

- *Phytophthora* species will grow on the designed LOC devices.
- The growth rate of *P. nicotianae* hyphae will not be negatively impacted by LOC devices.
- The width of *P. nicotianae* hyphae will not change when grown on LOC devices compared to culture dishes.
- The forces exerted by *Phytophthora* species can be measured using the LOC devices.
- The force exerted by *P. nicotianae* hyphae will increase when actin microfilaments are inhibited.

To address this final hypothesis, comparisons will be made between force measurements collected for *P. nicotianae* under control and experimentally altered conditions. These altered conditions will utilise the cytoskeletal drug latrunculin B to provide information on the underlying cytoskeletal processes occurring during hyphal growth and force generation which are key aspects of invasive growth.

Knowledge gained from this research may therefore aid in understanding the mechanisms that enable pathogenic oomycetes to cause disease. This could impact how we address disease and infection caused by the invasive growth of these organisms and minimise further economic and biodiversity loss.

Chapter 2. Materials and Methods

2.1 Oomycete strains and culture conditions

Three oomycete species from the genus *Phytophthora* were examined in this research; *Phytophthora cinnamomi*, *Phytophthora nicotianae* and *Phytophthora sojae* (Table 2.1). Cultures of *Phytophthora* were maintained weekly on V8-juice agar (referred to as agar), as described by Jung et al (1999) using a low sodium vegetable variant of V8-juice. These cultures were kept in the dark at room temperature.

Table 2.1. *Phytophthora* species used in this research.

Species	Isolation species, location and year of isolation	University of Canterbury culture collection number
Phytophthora nicotianae	Asparagus cv. Lucullus fiel. Rakaia, Mid Canterbury 1986	C218
Phytophthora cinnamomi	*Actinidia deliciosa* Kiwifruit: Chinese Gooseberry; yang-tao-root, Mt Albert Auckland 1979	C222
Phytophthora sojae	*Phebalium squameum* Druce-roots and lower stem, Katikati Bay of Plenty 1986	C223

2.2 Sub-culturing of *Phytophthora* species

Each species was sub-cultured weekly. A 5 millimetre (mm) cork-borer was used to cut mycelial plugs from the growing edge of cultures. The plug was placed hyphae side up onto a fresh agar plate. The new culture was sealed with strips of parafilm and stored in the dark at room temperature.

2.3 LOC device fabrication

LOC devices were fabricated in the Nanofabrication laboratory in the Electrical and Computer Engineering department at the University of Canterbury. LOC devices were fabricated by Yiling Sun, who collaboratively designed and fabricated the devices to suit the requirements for this research. The fabrication process used a similar procedure as described in Sun et al 2018 and Tayagui et al 2017. The devices fabricated in this research were made primarily from PDMS material that comprised the surface of the device, the walls of the channels and the

pillars. Once fabricated, the PDMS chip was sealed between two glass microscope slides for use on the microscope. The completed devices were individually vacuum sealed in food-grade packets until use to keep them clean and enable vacuum-assisted filling (Monahan et al 2001).

As hyphal morphologies differ between different fungal and oomycete species, the LOC devices required refinement throughout the project for the species investigated to allow for optimal growth and force measurement. This led to the fabrication of three different versions of device; these were termed version 1, version 2 and version 3. Pillars were successfully fabricated with diameters of 5 and 7 µm with heights of 13.6 µm for version 1 devices and 11.1 µm for version 2 and 3 devices.

2.4 Seeding LOC devices

2.4.1 Seeding of LOC devices under normal conditions

Seeding of the LOC devices was performed in a sterilised laminar flow cabinet. V8-juice broth (referred to as broth) was used in the device as a nutrient medium. This was made following the same procedure as the V8-juice agar, but without the addition of agar. Due to the particulate matter from the V8-juice, the broth was filtered using a 0.2 µm nylon syringe filter (Sartorius) and a 10 millilitre (ml) plastic syringe (Becton Dickinson) to remove large particles and the cloudy appearance before being added to the device to ensure optimal visualisation of the microchannels (referred to as channels) and pillars on the microscope. As the chip had been plasma-treated during its fabrication it was hydrophilic whilst vacuum sealed. This meant that the broth was filtered before opening the vacuum seal to retain the hydrophilicity. Once the vacuum seal was opened, broth was immediately added to the device using a micropipette.

Once broth had been added, the device was examined through the microscope to check that all channels were filled with broth and that no air bubbles were present. The chip was marked using a permanent marker to identify which of the two holes on the device corresponded to the seeding area. A plug was then cut in a 24-72 hour old culture at the periphery of the growing mycelium using a 3 mm biopsy plunger. A sterilised scalpel was then used to remove the plug and place it into the seeding area on the device with the edge of the plug with the growing hyphal tips positioned towards the channel entrances. When placed into the seeding area, the plug was inverted so that the hyphae were on the bottom side of the plug. The scalpel was then used to cut additional agar from the plug so that it sat cleanly in the device for optimal viewing and focusing through the microscope. Excess broth was then added to the device and

replenished during the experiment to ensure that the hyphae did not dry out due to evaporation of the broth. The device was left to grow in a dark room and was checked every hour for growth until measurements began.

2.4.2 Seeding of LOC devices with addition of latB

The seeding of latB LOC devices was identical to the procedure used when seeding the LOC devices under normal conditions except for the addition of latB and/or dimethylsulfoxide (DMSO) to the broth. Three different experimental conditions and a DMSO control were tested. The final percentage of DMSO in each condition was 0.1% (v/v) and all devices were treated the same irrespective of the conditions.

In experimental conditions containing latB, a stock of latB (Sigma-Aldrich) suspended in DMSO was defrosted from -20 °C for 30 minutes to allow it to equilibrate to room temperature. The latB stock solutions that were defrosted were only used to make up solutions on the day they were defrosted. The remainder of the stock solution was discarded after use. The required volume of latB was then diluted to the desired concentration in filtered broth before being added to the device. In some cases, the latB stock had to be diluted first with DMSO solution before dilution in broth to obtain the final DMSO and latB concentrations required in the final solution.

The volume of the final solutions of broth with latB and/or DMSO were either 5 or 10 ml. A fresh solution was made up for each LOC device used, with the reminder of the solution being discarded after the experiment concluded. The solutions were made up and kept in sterile 50 ml polypropylene Cellstar tubes (Greiner Bio-One) for the duration of each experiment, which were sealed and wrapped with tin foil to prevent light penetration.

As detailed in the Chapter 3, the addition of latB to the broth slowed down growth of hyphae in a dose dependent manner. Because of the very slow rates of growth in these experiments, the device was set up in the evening and left in a dark room to grow until the morning before recording began. To enable these overnight runs, a PHD 2000 infusion syringe pump (Harvard Apparatus) was used to keep the cultures hydrated. A sterile syringe was filled with the broth solution, air bubbles were removed, and using fittings, tubing with an internal diameter of 1 mm (IDEX Health & Science) was attached to the syringe. This tubing was then attached to the top of the LOC device with tape, with the tubing placed in between the seeding hole and the media inlet hole. The device then had excess broth added. The syringe pump was then set

up to infuse the device with 90 µl of broth every hour for 9-10 hours before being checked for growth and measurements being recorded. An image of this setup can be seen in Fig. 2.1.

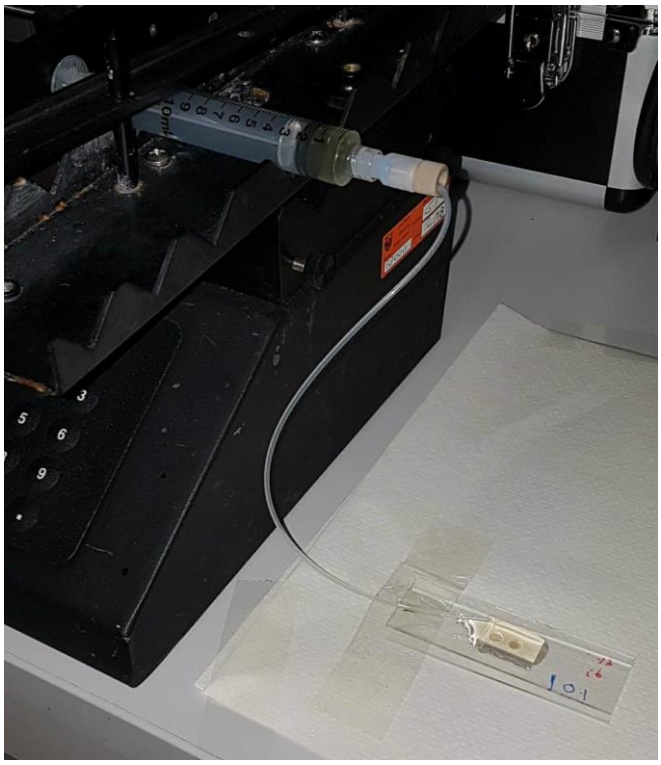

Figure 2.1. Overnight experimental set up for latB experimental LOC devices. A syringe pump was loaded with a syringe containing broth. The syringe then had tubing attached via tubing fittings, with the other end of the tubing taped onto the LOC device. The LOC device then had additional broth added to its surface to ensure there would be an adequate volume of broth on the device at all times for oomycete growth.

2.5 Hyphal imaging

Measurements of hyphal growth rates, widths and forces were made using recordings captured with a Hamamatsu ORCA-flash 2.0 digital camera connected to a Nikon Eclipse 80i fluorescence microscope. Before imaging of LOC devices, excess broth on the top of each device was removed and any remaining residue was wiped with a cotton bud to ensure that the glass slide was clean and dry for optimal imaging.

Once the hyphae had grown out of the seeding area and into the channels, the pillars of interest were brought into focus with a Nikon LU Plan Fluor 50X (0.8 NA) objective lens. Using the programme HCImageLive (Hamamatsu) on a computer, an image from the microscope was brought up and sequential images were set up to be recorded every five seconds. All sequences

were recorded for approximately two minutes after pillar contact. These image sequences were then reduced in length to two minute sequences after image collection, which were used for subsequent analyses. In these image sequences, the first pillar deflection occurred between 20-30 seconds after the beginning of the sequence, obtaining at least 90 seconds of force measurement data.

2.6 Calculation of hyphal growth rates

2.6.1 Hyphal growth rate on LOC devices

Adobe Photoshop (CC 2014) was used to calculate the growth rate of *Phytophthora* hyphae on LOC devices. The first image in a recorded sequence and an image close to, but prior to actual hyphal contact with the pillar, was opened in Adobe Photoshop. These two images were overlaid and using the measuring tool, the number of pixels between the growth points of the hyphae were measured and recorded in an Excel spreadsheet (Microsoft 2016). The number of pixels for one micrometre was calculated using images from a micrometre slide. The pixels for hyphal growth were then divided by the number of pixels per micrometre to calculate micrometres of growth. This was then divided by the time it took the hyphae to grow that distance to achieve micrometres of growth per minute. These values were calculated for all hyphae on each device that had measured force values to produce an average growth rate in micrometres per minute on the LOC devices.

2.6.2 Growth rate of *P. nicotianae* on culture dishes

The growth rate of *P. nicotianae* hyphae was calculated on 100 mm diameter cell culture dishes (Corning) under three conditions; 10 ml of agar, 10 ml of filtered broth and 10 ml of broth and a thin layer of PDMS.

To make the PDMS dishes for the broth and PDMS condition, 6 ml of pre-mixed degassed PDMS mixture was poured into each culture dish and swirled to leave a thin layer of PDMS across the bottom of the dish. The dishes were then left to bake on a hotplate for 6 hours.

To set up the agar growth rate dishes, 10 ml of agar was pipetted into Ultraviolet (UV) light sterilised culture dishes and left to set. Once set, a sterilised cork-borer and scalpel were used to cut a plug in a culture plate and place it into the centre of the culture dish which was then sealed with parafilm. This was repeated for all three replicates.

To set up the broth growth rate dishes, a plug was taken from a culture plate and placed into the centre of a UV sterilised culture dish. Following this, 10 ml of broth was carefully pipetted around the plug. The dish was then sealed with parafilm and the process repeated for all three replicates.

Before placing a plug onto the broth and PDMS dishes, the PDMS dishes were UV sterilised and plasma-treated by a hand plasma treatment device (Electro-Technic Products) to ensure that the PDMS layer was hydrophilic. The hand plasma treatment took between 1.5 and 2 minutes, following which the same method for the broth dishes was carried out for all three broth and PDMS dishes. All nine experimental dishes were then placed into a polystyrene box that was open slightly to allow for airflow and kept in the dark at room temperature.

After 48 hours, all dishes were imaged on a Nikon Eclipse 80i fluorescence microscope. Images were taken at time 0 and again after 10 minutes with a Nikon LU Plan Fluor 10X (0.3 NA) objective lens. After the first image was taken, the light on the microscope was turned off until 30 seconds before the second image was taken, at this time the microscope was carefully refocused.

Adobe Photoshop was used to calculate the growth rate of the hyphae on the culture dishes. For this, a similar procedure as for the growth rate on the chips was used. The growth in pixels between the first and second images were measured using pixel values calculated for the 10X objective lens to calculate growth rates in micrometres per minute for all hyphae which were in focus. This was repeated for all experimental dishes.

2.6.2.1 Growth rate on culture dishes with the addition of latB

Growth rate experiments on culture dishes with latB followed the same procedure as the broth and PDMS growth rate dishes, except for the addition of latB or DMSO to the broth before it was added around the plug. The concentrations of latB and DMSO in these dishes were the same as those used in the LOC device experiments. Three replicates were set up for each of the experimental conditions and all dishes had the same treatment.

2.7 Calculation of hyphal widths

2.7.1 Hyphal width on LOC devices

Adobe Photoshop was used to calculate the width of hyphae in LOC devices. Hyphal widths were calculated from hyphae that were close to, but not touching the pillar and were measured

approximately 10 µm back from the tip of the hyphae. This was calculated using the pixel-to-micrometre conversion calculated for the 50X objective lens during the growth rate analysis. The number of pixels for widths were input into an Excel spreadsheet and converted into micrometres using these calculation values. Hyphal widths were calculated for all hyphae per device that force values had been quantified for. Hyphal width, growth rate and the forces exerted by these hyphae could then all be compared.

2.7.2 Width of *P. nicotianae* hyphae on culture dishes

To calculate the width of *P. nicotianae* hyphae on culture dishes, a similar procedure to the growth rate calculation on culture dishes was used. Using Adobe Photoshop, the hyphal width in pixels was measured approximately 10 µm back from the hyphal tip for the second image taken during growth rate measurements. Hyphal widths in micrometres were calculated using the pixel-to-micrometre conversion calculated for the 10X objective lens during the growth rate analysis. Hyphal widths were calculated for all hyphae which were in focus and had growth rates calculated for across all experimental dishes.

2.8 Determination of force magnitude and direction from pillar deflection

2.8.1 Detection of pillar deflection using FIJI and the plugin TrackMate

To calculate force measurements, two programs were used; FIJI (Schindelin et al 2012) and MATLAB (2016a, Mathworks). In FIJI, images from each recorded sequence were imported and converted to an 8-bit grey-scale format. The images were then cropped to 368 x 368 pixels and saved as BMP files in a new analysis folder. Following this, a plugin called TrackMate (Tinevez et al 2017) in FIJI was used to track pillar movement through time and detect pillar deflections.

TrackMate creates circles of a size set by the user in all areas where it detects that a circle is present. In this research, the size of the circle was set so that it matched the size of the pillar which was being analysed. This size varied depending on the version of chip used and the and pillar size in the chip, ranging from 17-31 pixels. A threshold value was also set in the plugin to help filter out artefactual circles and ensure that the circles detected were not too close to one another. This value was set between one and three depending on the LOC device. Pillar 7 devices typically had a threshold value of one and pillar 5 typically devices had a threshold of three. All circles that were detected, other than the circle on the pillar, were then filtered out

using the plugin functions so that the single pillar could be accurately tracked throughout the entire sequence.

It was not always possible to remove all unwanted circles with filtering. In these instances, the remaining detected circles were left in this initial step. The track made by these circles was then removed by filtering out the track at a later step. Once only the desired track made from the circle on the pillar remained, the tracking data was saved and exported as an XML file into the analysis folder with the corresponding BMP image sequence.

2.8.2 MATLAB force value quantification

Once the TrackMate file had been exported, two customised MATLAB script files (Ghanbari et al 2010, Ghanbari et al 2012, Tayagui et al 2017) were copied into the analysis folder for each sequence. The main script file was then opened in MATLAB. This script file contained code which applied a linear-spring force deflection model (Ghanbari et al 2012), where the force exerted by the hypha corresponds to the deflection of the pillar. This model accounted for various contributing factors to force output including the height of the contact point on the pillar (approximated to be half the pillar height, confirmed using confocal imaging (unpublished data)), the moment of inertia, the Youngs modulus and the Poisson's ratio for PDMS (Ghanbari et al 2012). Additional parameters in the script were set for each hyphal sequence including specifying the start and end of the sequence, the pillar height and the pillar diameter.

After running the script, MATLAB produced three graphical outputs and a text file containing total force values as well as forces in both X and Y directions for each image in the sequence. A copy of each image was also saved by MATLAB with the middle point of the pillar marked by a cross, a scale bar and an arrow showing both the direction and magnitude of the forces exerted at each time point in the sequence.

2.8.3 Manual data processing in Excel to remove by-products of drift

Although sequences were manually sorted to contain two minutes of force value data, with the pillar deflection point at approximately 20-30 seconds from the start of the sequence, small force values were obtained in this initial period where the pillar was not being deflected. These values were likely due to small movements of the microscope slide during image sequence collection or other irregularities during data collection. As such, an additional step in the

analysis was carried out. All total force measurement data was imported into Excel spreadsheets with each experimental set up in a spreadsheet of its own (e.g. all DMSO force measurements from pillar 5 devices in one sheet and all DMSO force measurements from pillar 7 devices in another). The total force values recorded across the first 15 seconds were then averaged. This averaged value was then subtracted from all following measurements. The values for the first 15 seconds were then set to zero before further analysis was carried out. This additional step increased the accuracy of the force measurement data and limited inaccuracies caused by drift that was associated with device movement or other uncontrollable factors during data collection.

2.9 Determination of squeezing and hyphal tip forces

Force measurements were separated into two types of forces visually; squeezing forces and hyphal tip forces. Squeezing forces were defined as forces where hyphae deflected the pillar but without direct contact of the hyphal tip with the pillar. In contrast, hyphal tip forces were defined as forces where the hyphal tip directly contacted the pillar.

While squeezing force data analysis could utilise all force measurements collected over the two minute time frame, hyphal tip force analysis could only utilise force measurements that were collected for the time that the hyphal tip was pushing against the pillar. Once the hyphal tip moved off the pillar and the hypha moved into a squeezing force, all subsequent force values were excluded. As such, force measurements for hyphal tip forces varied in sequence length.

2.10 Calculations of hyphal pressures

Hyphal pressures were calculated for hyphae that produced hyphal tip deflections using Equations 2.1 and 2.2. The percentage of total turgor pressure generating the protrusive force exerted on the pillar was calculated using Equation 2.3. This equation used a turgor pressure value of 0.69 MPa, approximated through a comparison of turgor pressure values in other oomycete species (Money et al 2004).

Equation 2.1

$$Contact\ area = 2\pi r^2\ ,$$

where r is half the width of hyphal tip contact on the pillar at the time point that the corresponding force value in Equation 2.2 was recorded.

Equation 2.2

$$Pressure = \frac{Force}{Contact\ area},$$

where force is hyphal tip force values.

Equation 3.3

$$Percentage\ of\ total\ turgor\ pressure = \frac{Pressure}{Turgor\ pressure} \times 100,$$

where turgor pressure is the approximated value of 0.69 MPa.

2.11 Maximum and half point force value determination

Force values were examined in two ways; maximum force values and half point force values. The maximum force value for each hypha was the maximum force value calculated in the corresponding sequence. The half point force value for squeezing force hyphae was the force value at 70 seconds in the sequence. A time point of 70 seconds was used as the half point as deflection recordings began 20-30 seconds into each sequence and continued for a total of two minutes. As such, 70 seconds was approximately the half point in force data collection in these sequences. As hyphal tip deflection data had varied time points, 40 seconds was chosen as the half point.

2.12 Statistical analysis

Statistical analysis was performed primarily using R (3.4.3). Excel was used to calculate means and standard error of the means.

To determine statistical significance between conditions, two-tailed t-tests and analysis of variance (ANOVA) tests followed by post hoc Tukey HSD tests were used. The alpha value used for all significance testing was 0.05. Before carrying out ANOVA analysis, the data was tested for the assumptions of normality and homogeneous variances. These assumptions were tested using the Shapiro-Wilk normality test and the Levene's test for homogenous variances. If the data did not meet these assumptions and data transformation did not fix the ANOVA violations, a Kruskal-Wallis non-parametric test, followed by post hoc analysis using the Dunn's test was carried out.

The Spearman's rank correlation test was used for correlation analysis. This test was used as the Shapiro-Wilk normality test indicated that the data was not normally distributed. For regression analysis, linear and multiple regression tests were carried out in Excel.

Once data was analysed, OriginPro (OriginLab) was used to generate graphical outputs. Adobe Illustrator (CS6) was used to create and label figures.

Chapter 3. Results

3.1 LOC device design

To measure hyphal forces, three versions of LOC devices were designed and fabricated; version 1, version 2 and version 3. All three versions had a similar overall design (Fig. 3.1), with minor changes in channel width, gap size and pillar diameter.

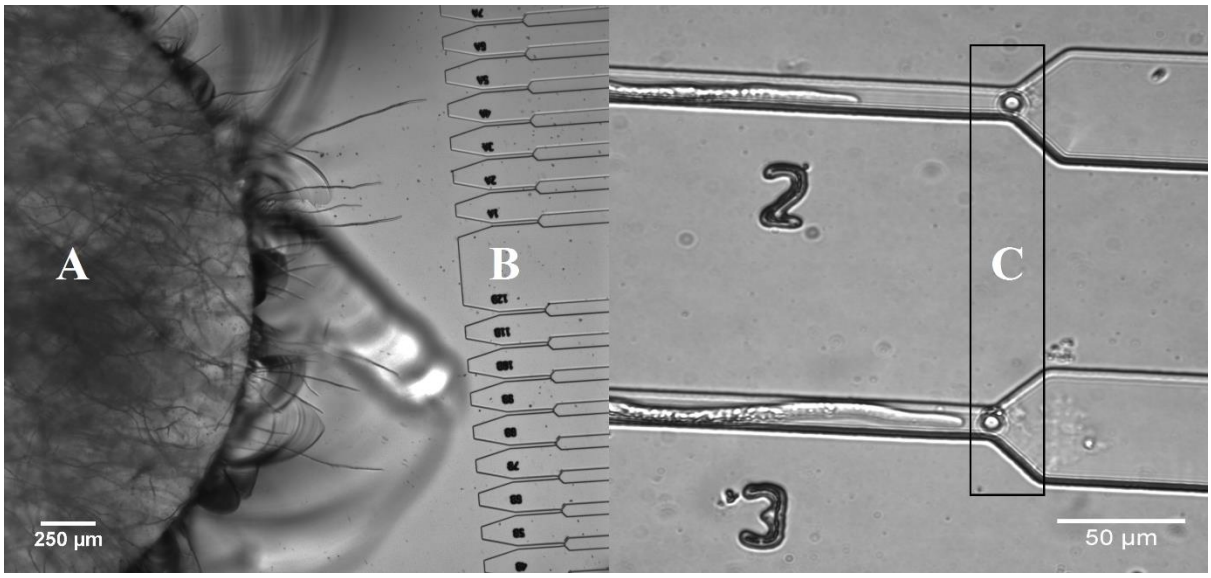

Figure 3.1. LOC device design. (A) Seeding area of LOC devices with a hyphal plug, (B) measurement channels, (C) measurement pillars within channels. Hyphae can be seen growing on the device and in the channels.

3.1.1 Version 1 LOC devices

Version 1 LOC devices were fabricated with pillar diameters of either 5 or 7 µm (referred to as pillar 5 and pillar 7 devices respectively) and a height of 13.6 µm. These devices had 24 parallel channels with a width of 15 µm, located between the seeding area where the hyphal plug was added and the media inlet area for the addition of liquid medium (Fig. 3.2). The gap size between the pillar and the channel walls differed between version 1 devices. In devices with a pillar diameter of 7 µm, this gap size was 4 µm (referred to as gap 4). In contrast, devices with a pillar diameter of 5 µm had gap sizes of either 3 or 5 µm (referred to as gap 3 and gap 5, respectively) (Fig. 3.3). The different gap sizes in pillar 5 devices were tested to determine which gap size was most suitable, as previous preliminary research had shown that hyphae could grow along the channel wall, effectively avoiding the pillar in the centre.

Figure 3.2. Version 1 and version 3 LOC devices. (A) seeding area, (B) media inlet area. The left image is a version 1 device with 24 parallel channels. The right image is a version 3 device, indicative of version 2 and 3 device designs with 12 parallel channels. Red dye was used to fill the channels for visualisation.

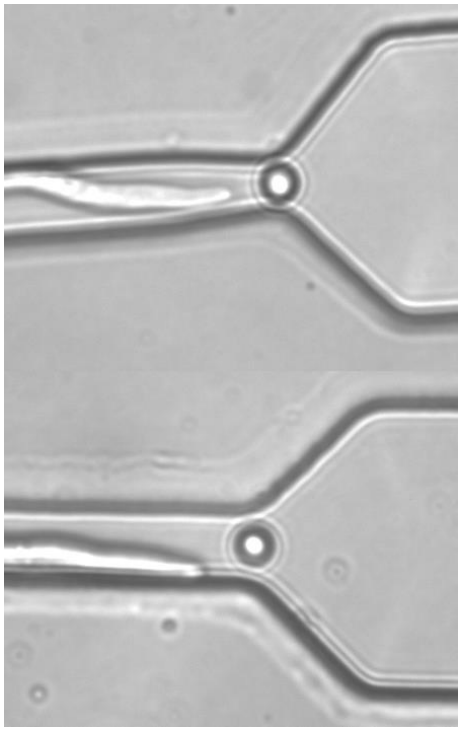

Figure 3.3. Gap size variation in version 1 pillar 5 chips. The top channel has a gap size of 3 µm between the pillar and the channel walls. The bottom channel has a gap size of 5 µm. Hyphae can be seen growing in the channels.

While the forces exerted by the hyphae and the directionality of these forces were able to be measured using these devices, the hyphae of *P. nicotianae* grew very quickly. As a result, many of the pillars deflected by the hyphae in the version 1 devices were unable to be recorded as the deflections were occurring concurrently with other pillars that were being recorded. The design was therefore streamlined to have half the number of channels while still maintaining

the same pillar diameters and general design. Additionally, the two gap sizes in version 1 pillar 5 devices (gap 3 and gap 5) were combined into both pillar 5 and 7 devices, with half the channels having a gap of 3 µm and half with a gap of 5 µm. These were called version 2 devices.

3.1.2 Version 2 LOC devices

Version 2 LOC devices had 12 channels (Fig. 3.2) with a width of 17 µm and pillar heights of 11.1 µm. Within these channels, two differing channel designs were trialled. Channels 1-6 had a gap size of 3 µm while channels 7-12 had a gap of 5 µm (Fig. 3.4). Devices with pillar sizes of 5 and 7 µm were designed, both which had the two gap sizes. Having two gap sizes on the same device created the opportunity to compare between gap sizes on one device with hyphae from the same mycelium, as opposed to version 1 devices that had gap size variations between the devices but not within. This would reduce variation between devices such as temperature, light exposure and handling conditions. However, due to limitations with the scale of the device, the pillars in channels 1-6 were found to be adhering to the walls of the channel. This meant that the pillars were not freely moving and as such these channels could not be used for force measurement collection. However, pillars in channels 7-12 were found to work well in the device. As a gap size of 5 µm was found to work effectively in both version 1 and version 2 devices, this gap size was implemented into the final device design, version 3.

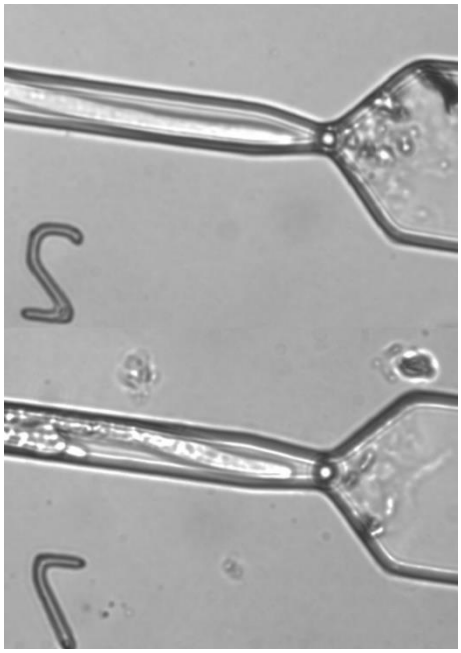

Figure 3.4. Gap size variation in version 2 pillar 5 chips. The top channel, channel 2, had a gap size of 3 µm. The bottom channel, channel 7, had a gap size of 5 µm. Hyphae can be seen growing in the channels.

3.1.3 Version 3 LOC devices

Version 3 LOC devices were designed to remove the adhering pillars that were present in version 2 devices. Version 3 devices used a similar design to the version 2 devices, maintaining the 12 channel design (Fig. 3.2), pillar heights and channel widths, altering only the gap size in channels 1-6 so that the gap size was identical for all 12 channels. The gap size in all channels within version 3 devices was 5 µm, which had been successfully implemented in channels 7-12 in the version 2 devices. Pillar diameters of 5 and 7 µm were used successfully, as in both version 1 and 2 devices.

3.2 Growth rates of *P. nicotianae* hyphae

The growth rates of *P. nicotianae* hyphae were calculated for growth on culture dishes and on LOC devices. This determined whether the device parameters were affecting the growth rate of the hyphae. Whether the presence of PDMS or the cytoskeletal inhibitor latB affected the growth rate of the hyphae on culture dishes and devices was also examined.

3.2.1 Growth rates on culture dishes

The growth rates of *P. nicotianae* hyphae on culture dishes were compared under various conditions. To determine whether PDMS had a significant effect on the growth rate of *P. nicotianae* hyphae, the hyphal growth rates were compared under three conditions; agar, broth and broth with PDMS (Fig. 3.5). This comparison identified that there was a statistically significant difference in the growth rate of *P. nicotianae* hyphae under these conditions ($F_{2,54} = 15.08$, $p < .0001$). Post hoc analysis determined that the growth rate was significantly faster when grown in a liquid medium compared to a solid medium. The results also identified that there was no significant difference in the growth rate of the hyphae when grown in liquid medium with or without PDMS.

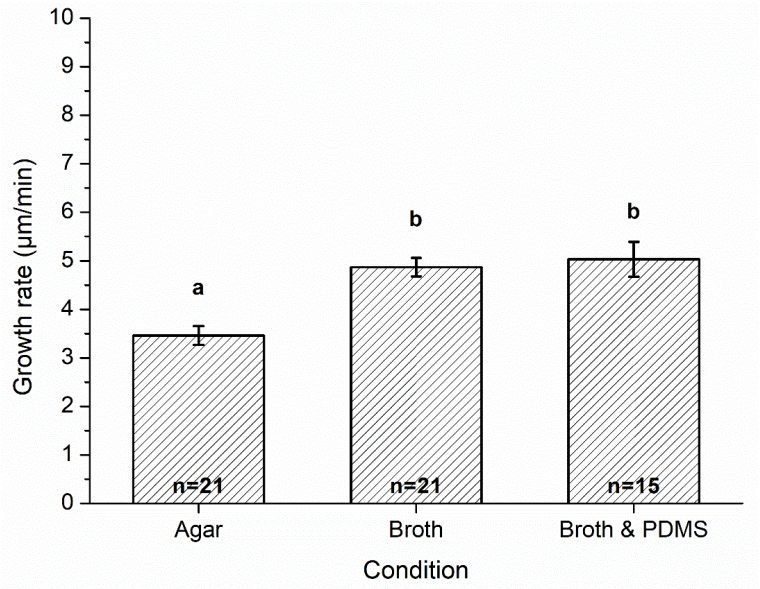

Figure 3.5. *P. nicotianae* growth rate is not altered by the presence of PDMS. Error bars represent the standard error of the mean and n corresponds to the number of individual measurements. Values with the same letter are not significantly different to each other ($p > .05$).

To determine whether a significant difference in the growth rate of *P. nicotianae* hyphae exists when grown in the presence of latB, five conditions were tested in PDMS layered culture dishes (Fig. 3.6). These conditions were; broth (referred to as normal), 0.1% DMSO (referred to as DMSO), 0.05 µM latB + 0.1% DMSO (referred to as 0.05 µM latB), 0.075 µM latB + 0.1% DMSO (referred to as 0.075 µM latB) and 0.1 µM latB + 0.1% DMSO (referred to as 0.1 µM latB). Both the normal and DMSO conditions were controls, with broth being compared to 0.1% DMSO to determine whether the DMSO present in the medium was affecting the hyphae.

When grown in culture dishes under these conditions, there was a statistically significant difference in the hyphal growth rate between conditions ($X^2 = 75.91$, $p < .0001$). Post hoc analysis determined that there was a significant difference in growth rate between normal and 0.1 µM latB, DMSO and 0.05 µM latB, DMSO and 0.075 µM latB, DMSO and 0.1 µM latB conditions and between 0.05 µM latB and 0.1 µM latB. Experimental analysis identified that the DMSO condition did not differ significantly to normal conditions and was therefore a valid control. This was found in the analysis of all latB experiments (growth rate, hyphal width and force analysis). As such, the effects observed were the result of latB treatment and not DMSO.

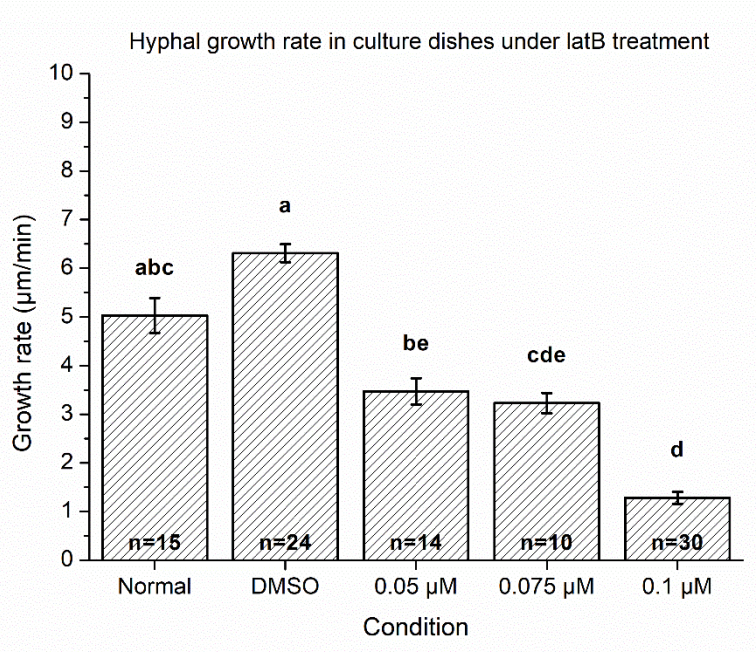

Figure 3.6. *P. nicotianae* growth rate differs in the presence of latB. Error bars represent the standard error of the mean and n corresponds to the number of individual measurements. Values with the same letter are not significantly different to each other ($p > .05$).

3.2.2 Growth rates on LOC devices

Hyphal growth rates on LOC devices were determined throughout all experiments, under all conditions. This allowed for a comparison of the growth rate of *P. nicotianae* hyphae when grown on devices with different channel widths, in the presence of various latB concentrations and when grown on devices compared to on culture dishes where growth was physically unrestrained.

To determine whether channel width in LOC devices affected the growth rate of hyphae, the growth rate in version 1 devices (width = 15 µm) was compared to version 2 and 3 devices (width = 17 µm) (Fig. 3.7). The results showed that there was no statistically significant difference in the growth rate of *P. nicotianae* hyphae when grown in channels with widths of 15 and 17 µm ($p > .05$).

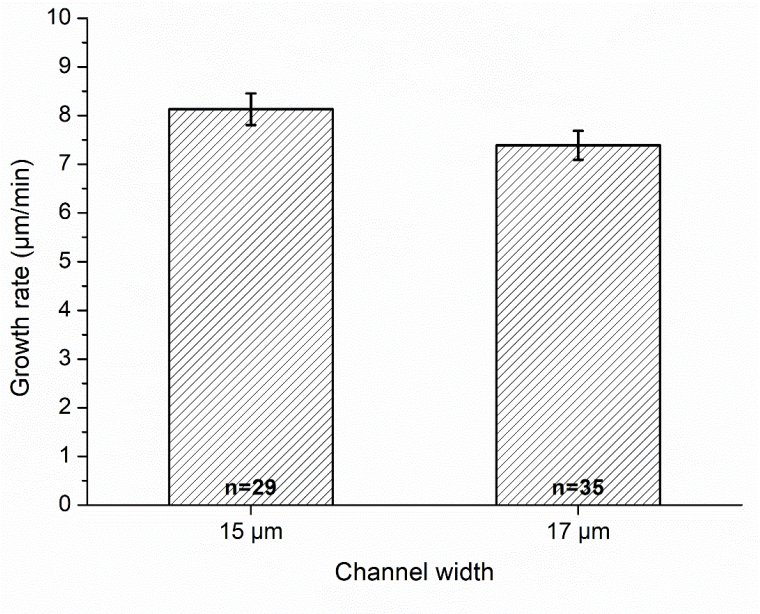

Figure 3.7. *P. nicotianae* growth rate does not differ in LOC device channels with widths of 15 and 17 µm. Error bars represent the standard error of the mean and n corresponds to the number of individual measurements.

To determine whether the presence of latB affected the growth rate of *P. nicotianae* hyphae on LOC devices, the growth rates under each condition were compared (Fig. 3.8). The conditions were the same five conditions tested in the latB culture dishes experiment; normal, DMSO, 0.05 µM latB, 0.075 µM latB and 0.1 µM latB. The results showed a statistically significant difference in the growth rate between the conditions tested ($F_{4,116} = 29.1$, $p < .0001$). Post hoc analysis determined that there was a significant difference in growth rate between all conditions except for between normal and DMSO, between 0.05 µM latB and 0.075 µM latB and between 0.075 µM latB and 0.1 µM latB.

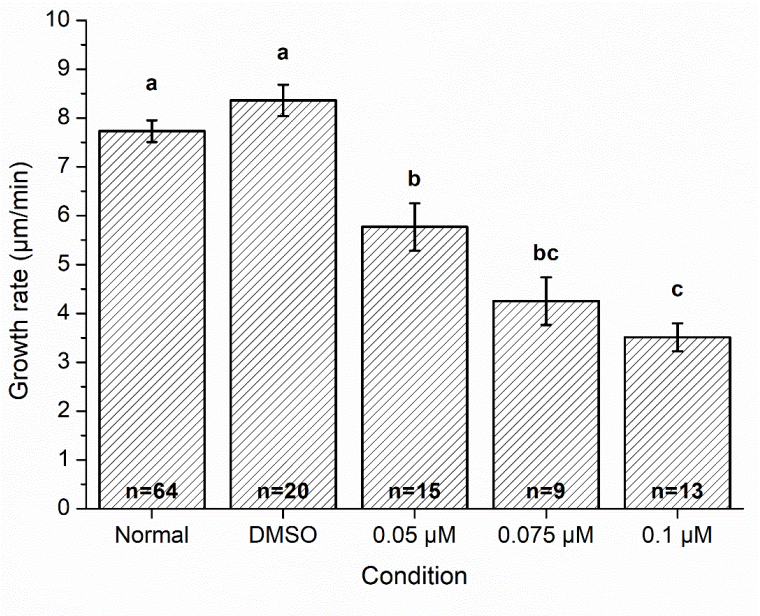

Figure 3.8. *P. nicotianae* growth rate differs on LOC devices in the presence of latB. Error bars represent the standard error of the mean and n corresponds to the number of individual measurements. Values with the same letter are not significantly different to each other ($p > .05$).

To determine whether the physical restraints of the LOC devices affected the growth rate of *P. nicotianae* hyphae, growth rates under all conditions on culture dishes and devices were compared (Fig. 3.9). A statistically significant difference in growth rate was identified for all conditions, with hyphae growing at a significantly faster rate in channels compared to in culture dishes, except for in the presence of 0.075 µM latB.

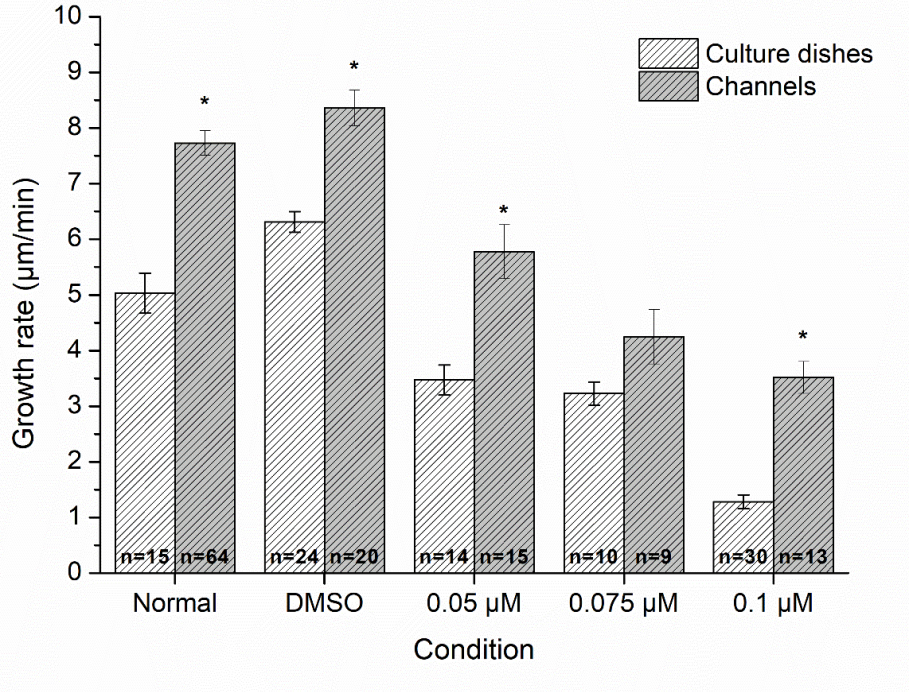

Figure 3.9. *P. nicotianae* growth rate differs on culture dishes compared to LOC devices in the presence of latB, except for in the presence of 0.075 µM latB. Error bars represent the standard error of the mean and n corresponds to the number of individual measurements. Asterisks identify a significant difference between culture dishes and devices within the condition ($p < .05$).

3.3 Hyphal widths of *P. nicotianae*

The widths of *P. nicotianae* hyphae were calculated on culture dishes and on LOC devices. This determined whether the device parameters were affecting the widths of the hyphae. Whether the presence of PDMS or the cytoskeletal inhibitor latB affected the width of the hyphae on culture dishes and devices was also examined.

3.3.1 Hyphal widths on culture dishes

The widths of *P. nicotianae* hyphae on culture dishes were compared under various conditions. To determine whether PDMS had a significant effect on the width of *P. nicotianae* hyphae, the hyphal widths were compared under three conditions; agar, broth and broth with PDMS (Fig. 3.10). This comparison identified that there was a statistically significant difference in the width of *P. nicotianae* hyphae under these conditions ($F_{2,54} = 49.8$, $p < .0001$). Post hoc analysis determined that the hyphal width was significantly wider when grown on a solid medium

compared to a liquid medium. The results also identified that there was no significant difference in the width of the hyphae when grown in liquid medium with or without PDMS.

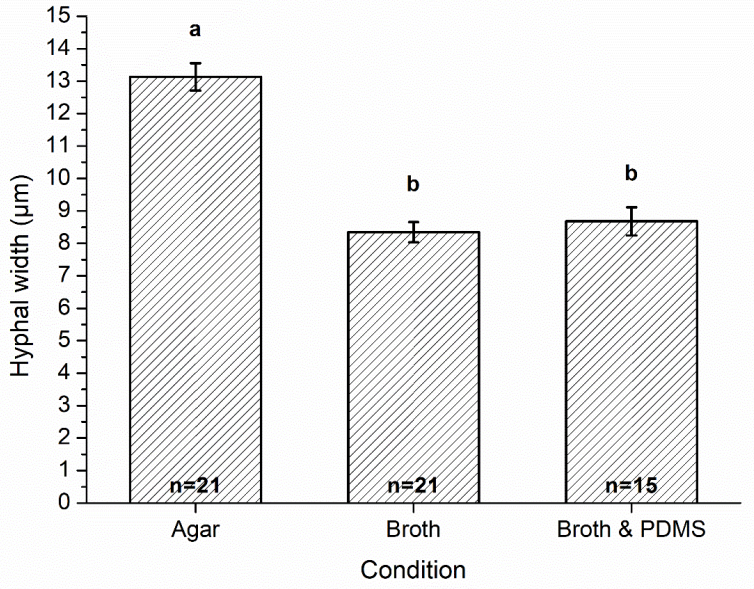

Figure 3.10. *P. nicotianae* hyphal width is not altered by the presence of PDMS. Error bars represent the standard error of the mean and n corresponds to the number of individual measurements. Values with the same letter are not significantly different to each other ($p > .05$).

To determine whether a significant difference in the width of *P. nicotianae* hyphae exists when grown in the presence of latB, five conditions were tested in PDMS layered culture dishes (Fig. 3.11). These conditions were the same five conditions used previously for latB experiments. When grown in culture dishes under these conditions, there was a statistically significant difference in the hyphal width between conditions ($F_{4,88} = 4.7$, $p < .005$). Post hoc analysis determined that there was a significant difference in hyphal width between normal and 0.075 µM latB and normal and 0.1 µM latB conditions.

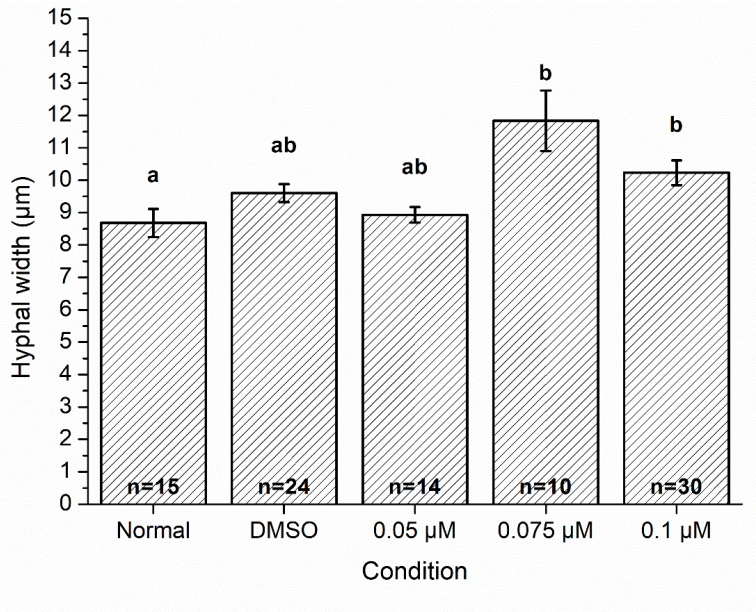

Figure 3.11. *P. nicotianae* hyphal width differs in the presence of latB. Error bars represent the standard error of the mean and n corresponds to the number of individual measurements. Values with the same letter are not significantly different to each other ($p > .05$).

3.3.2 Hyphal widths on LOC devices

Hyphal widths on LOC devices were determined throughout all experiments, under all conditions. This allowed for a comparison of hyphal width of *P. nicotianae* hyphae when grown on devices with different channel widths, in the presence of various latB concentrations and when grown on devices compared to on culture dishes where growth was physically unrestrained.

To determine whether channel width in LOC devices affected the hyphal width, the width of hyphae in version 1 devices (width = 15 µm) was compared to version 2 and 3 devices (width = 17 µm) (Fig. 3.12). The results showed that there was no statistically significant difference in the width of *P. nicotianae* hyphae when grown in channels with widths of 15 and 17 µm ($p > .05$).

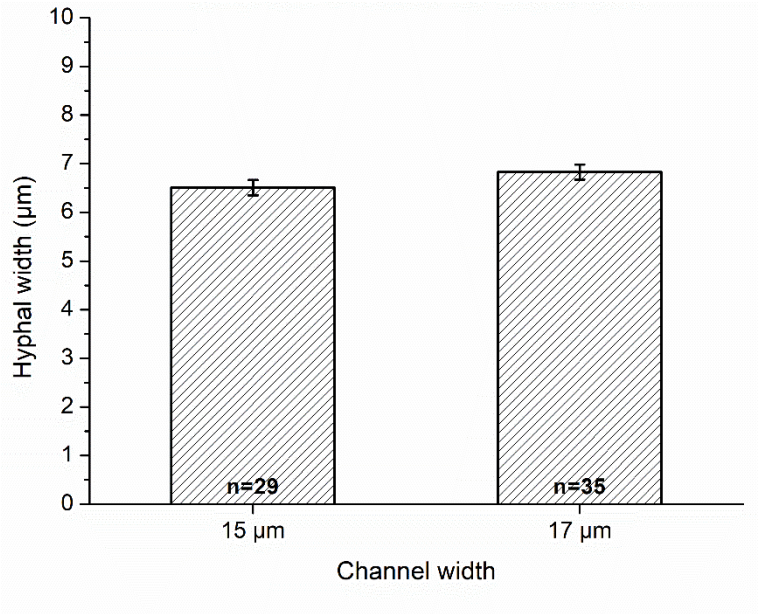

Figure 3.12. *P. nicotianae* hyphal width does not differ in LOC device channels with widths of 15 and 17 µm. Error bars represent the standard error of the mean and n corresponds to the number of individual measurements.

To determine whether the presence of latB affected the width of *P. nicotianae* hyphae on LOC devices, the widths of the hyphae under each condition were compared (Fig. 3.13). The conditions were the same five conditions used previously for latB experiments. The results showed that there was no statistically significant difference in the width of *P. nicotianae* hyphae between the conditions tested ($p > .05$).

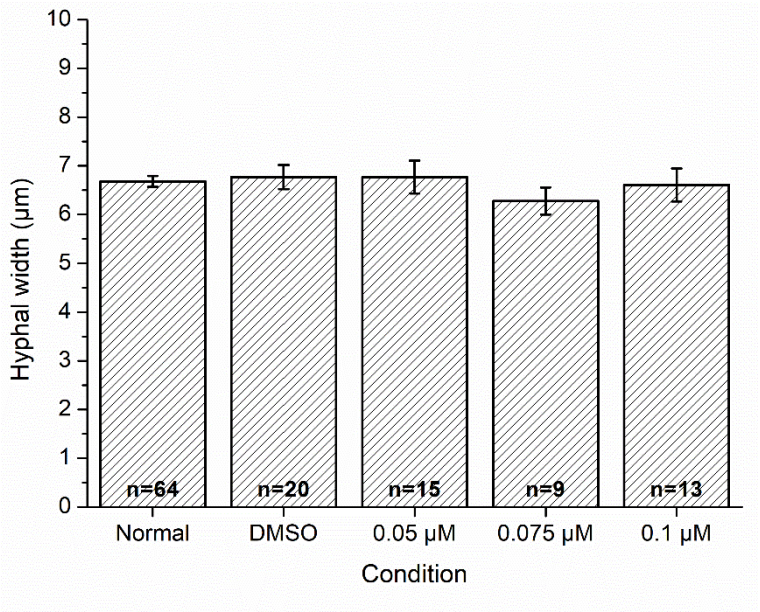

Figure 3.13. *P. nicotianae* hyphal width does not differ on LOC devices in the presence of latB. Error bars represent the standard error of the mean and n corresponds to the number of individual measurements.

To determine whether the physical restraints of the LOC devices affected the width of *P. nicotianae* hyphae, hyphal widths under all conditions on culture dishes and devices were compared (Fig. 3.14). A statistically significant difference in hyphal width was identified for all conditions, with hyphae being significantly wider when grown in culture dishes compared to in channels.

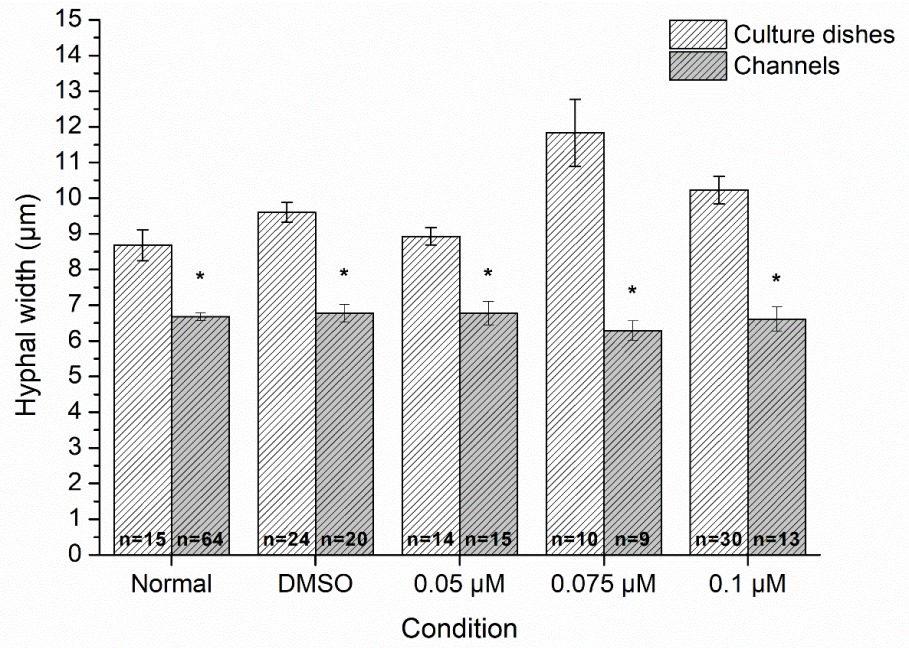

Figure 3.14. *P. nicotianae* hyphal width differs on culture dishes compared to LOC devices in the presence of latB. Error bars represent the standard error of the mean and n corresponds to the number of individual measurements. Asterisks identify a significant difference between culture dishes and devices within the condition ($p < .05$).

3.4 Force measurements for *P. nicotianae* on LOC devices

Force measurements were obtained on version 1, 2 and 3 LOC devices. The force measurements were separated into pillar size 5 and pillar size 7 for each version, then further separated into hyphal squeezing and tip deflection forces (Fig. 3.15). This separation allows for comparisons between forces produced from different sized pillars and the different forces that can be collected from the LOC devices for each pillar size. More squeezing force data was collected than tip deflection data as the latter required a direct contact of the tip apex with the pillar.

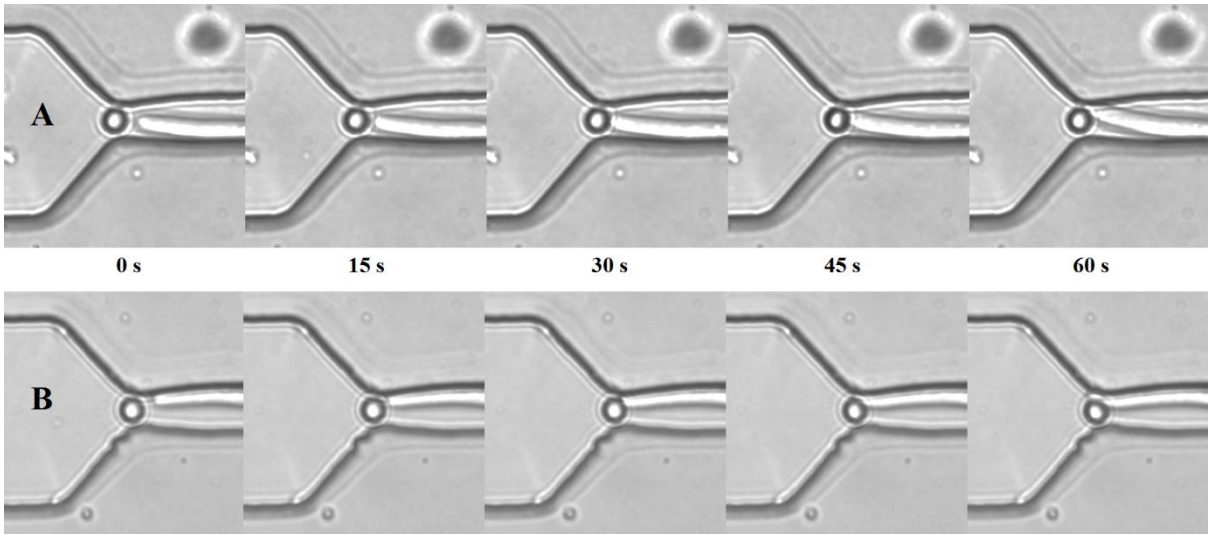

Figure 3.15. Hyphal tip and squeezing force deflections over time. (A) hyphal tip deflection over time. Hyphal tip deflection is shown in images 0-45 s, in the last image the tip has moved off the pillar and the hypha has moved into a squeezing force. (B) squeezing force deflection over 60 s.

3.4.1 Force measurements from version 1 LOC devices

In version 1 LOC devices, both pillar 5 and pillar 7 designs were tested. Devices with a pillar size of 5 had a gap size of either 3 or 5 µm. As such, hyphal squeezing and tip deflection force measurements were separated into pillar 5 gap 3 (Fig. 3.16), pillar 5 gap 5 (Fig. 3.17) and pillar 7 (Fig. 3.18).

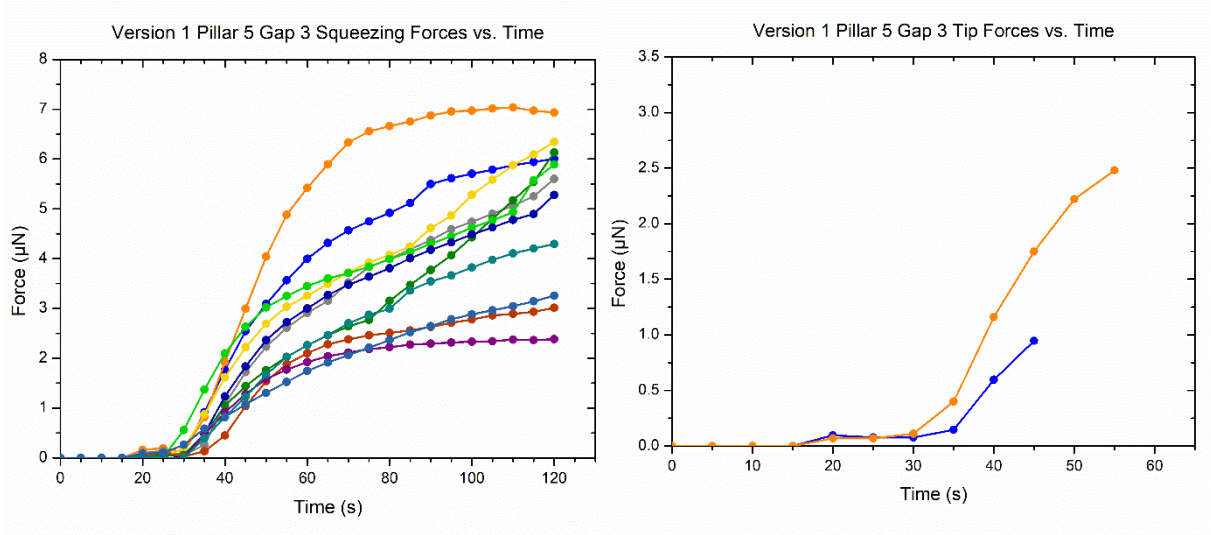

Figure 3.16. Version 1 pillar 5 gap 3 hyphal squeezing and tip deflection force measurements over time. A total of 11 squeezing forces and 2 tip deflection forces were recorded for *P. nicotianae* hyphae.

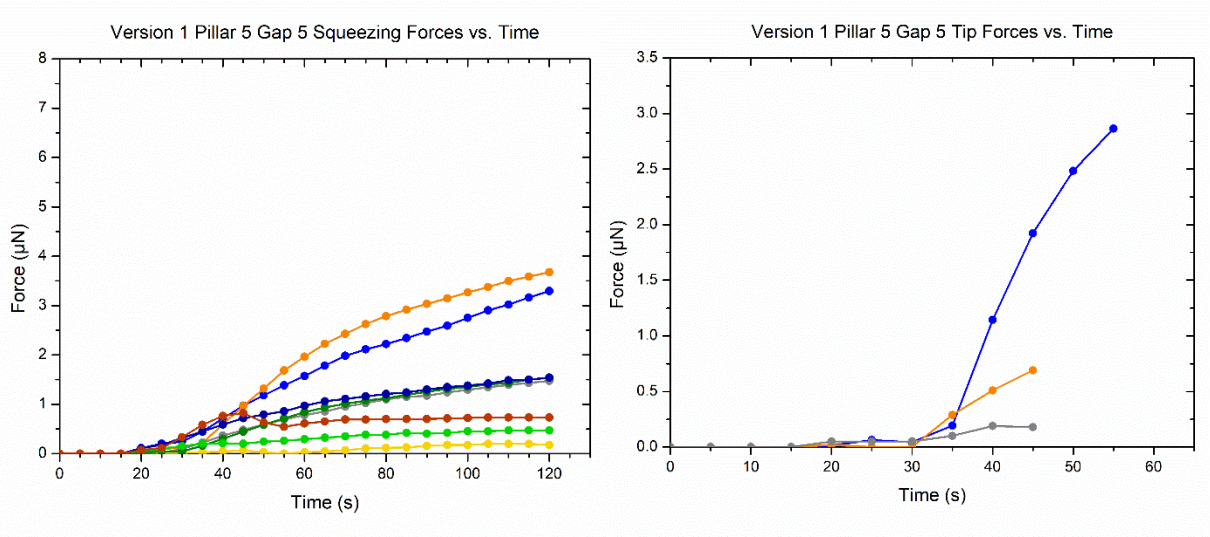

Figure 3.17. Version 1 pillar 5 gap 5 hyphal squeezing and tip deflection force measurements over time. A total of 8 squeezing forces and 3 tip deflection forces were recorded for *P. nicotianae* hyphae.

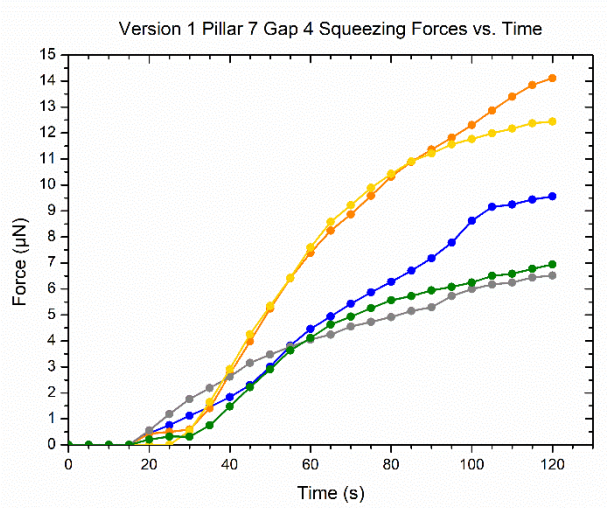

Figure 3.18. Version 1 pillar 7 hyphal squeezing force measurements over time. A total of 5 squeezing forces were recorded for *P. nicotianae* hyphae.

3.4.2 Force measurements from version 2 LOC devices

In version 2 LOC devices, both pillar 5 and pillar 7 designs were tested. There were no differences in gap width in version 2 devices. Hyphal squeezing and tip deflection force measurements were separated into pillar size 5 (Fig. 3.19) and pillar size 7 (Fig. 3.20).

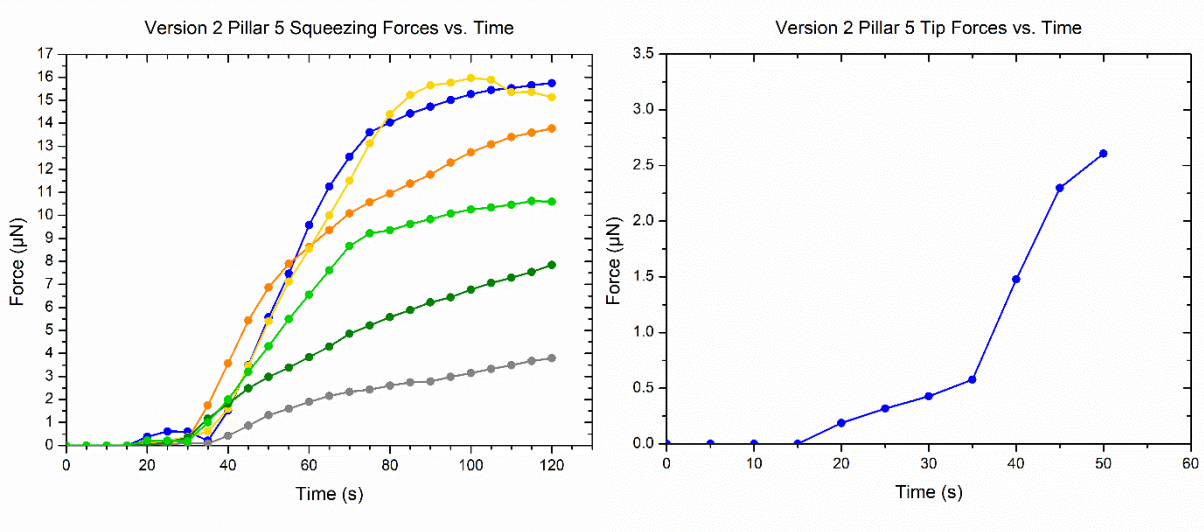

Figure 3.19. Version 2 pillar 5 hyphal squeezing and tip deflection force measurements over time. A total of 6 squeezing forces and 1 tip deflection force were recorded for *P. nicotianae* hyphae.

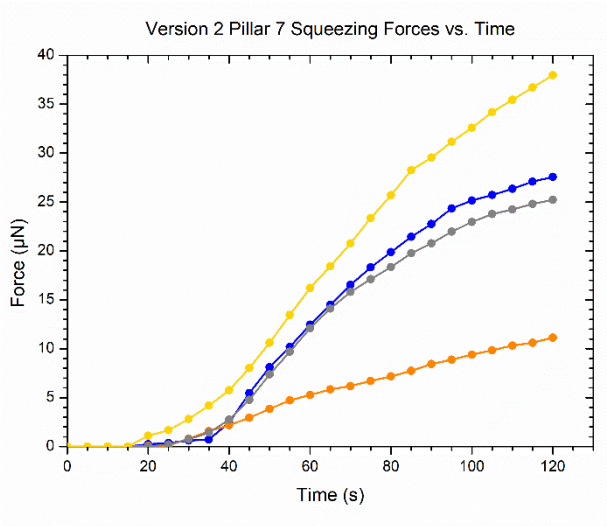

Figure 3.20. Version 2 pillar 7 hyphal squeezing force measurements over time. A total of 4 squeezing forces were recorded for *P. nicotianae* hyphae.

3.4.3 Force measurements from version 3 LOC devices

In version 3 LOC devices, both pillar 5 and pillar 7 designs were tested. There were no differences in gap width in version 3 devices. Hyphal squeezing and tip deflection force measurements were separated into pillar size 5 (Fig. 3.21) and pillar size 7 (Fig. 3.22).

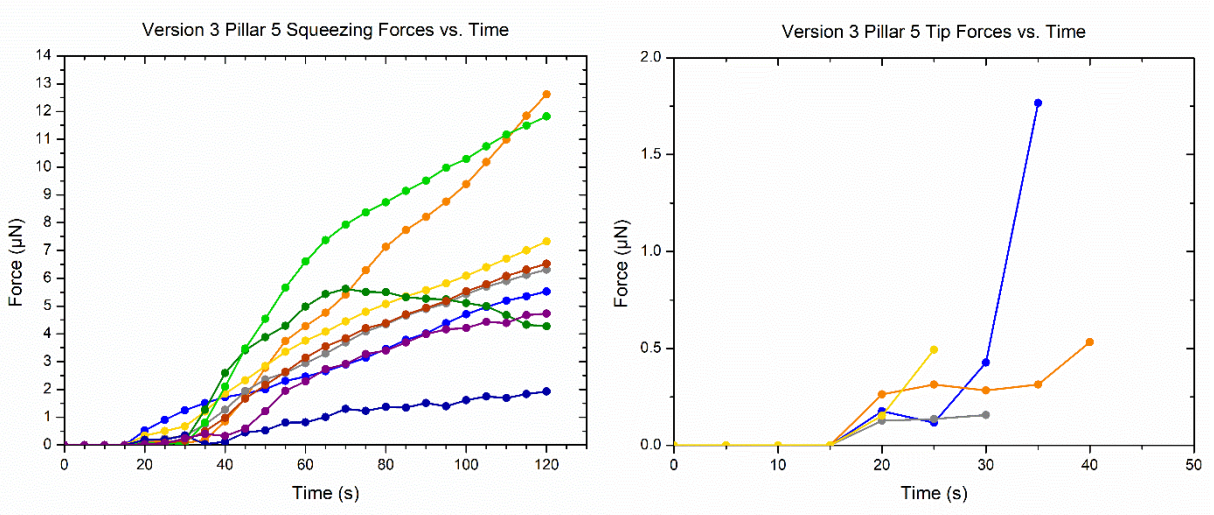

Figure 3.21. Version 3 pillar 5 hyphal squeezing and tip deflection force measurements over time. A total of 9 squeezing forces and 4 tip deflection forces were recorded for *P. nicotianae* hyphae.

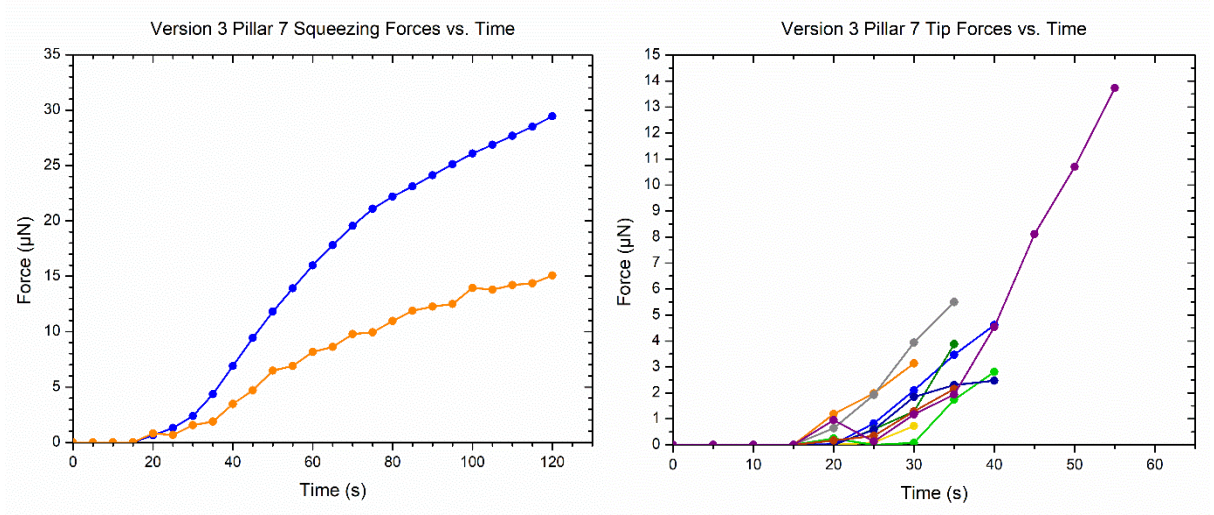

Figure 3.22. Version 3 pillar 7 hyphal squeezing and tip deflection force measurements over time. A total of 2 squeezing forces and 9 tip deflection forces were recorded for *P. nicotianae* hyphae.

3.5 Force measurements from version 3 LOC devices with addition of latB

The force measurements obtained for version 3 LOC devices under latB conditions were separated into each condition. For each condition, force measurements were separated into pillar size 5 and pillar size 7, then further separated into hyphal squeezing and tip deflection forces. This separation allows for comparisons between forces exerted at different concentrations of latB, between forces produced from different sized pillars and between hyphal squeezing and tip deflection forces.

The latB conditions were the same conditions used previously for latB experiments; DMSO (Fig. 3.23 and Fig. 3.24), 0.05 µM latB (Fig. 3.25 and Fig. 3.26), 0.075 µM latB (Fig. 3.27 and Fig. 3.28) and 0.1 µM latB (Fig. 3.29 and Fig. 3.30).

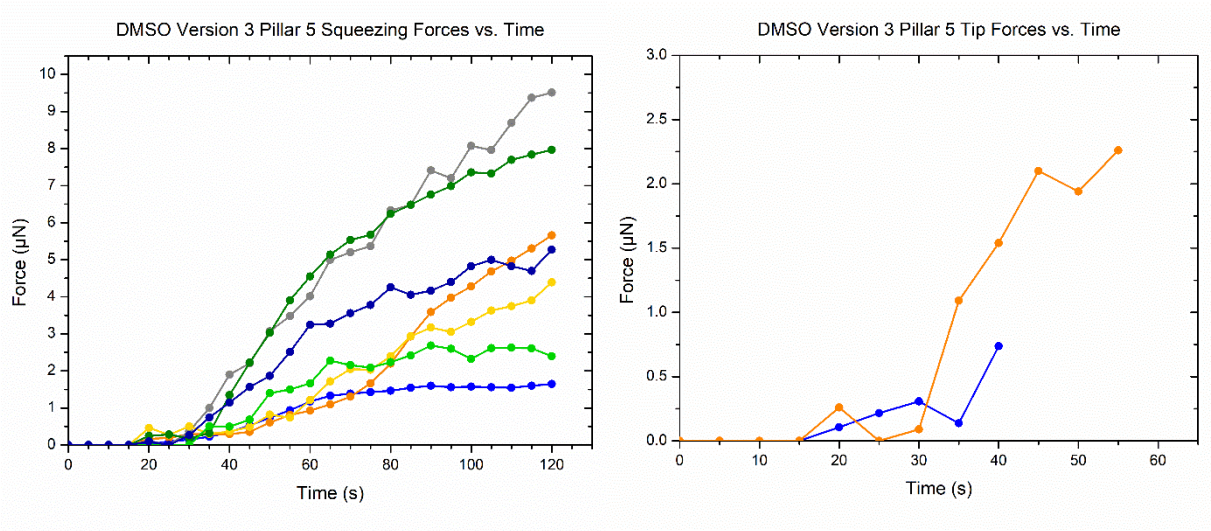

Figure 3.23. Version 3 pillar 5 hyphal squeezing and tip deflection force measurements over time with 0.1% DMSO. A total of 7 squeezing forces and 2 tip deflection forces were recorded for *P. nicotianae* hyphae.

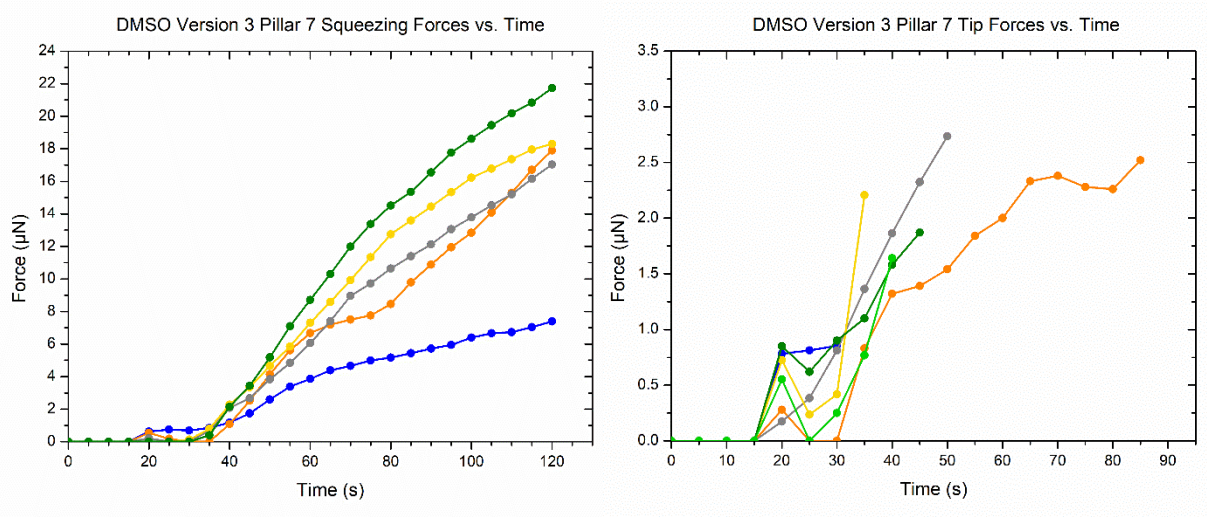

Figure 3.24. Version 3 pillar 7 hyphal squeezing and tip deflection force measurements over time with 0.1% DMSO. A total of 5 squeezing forces and 6 tip deflection forces were recorded for *P. nicotianae* hyphae.

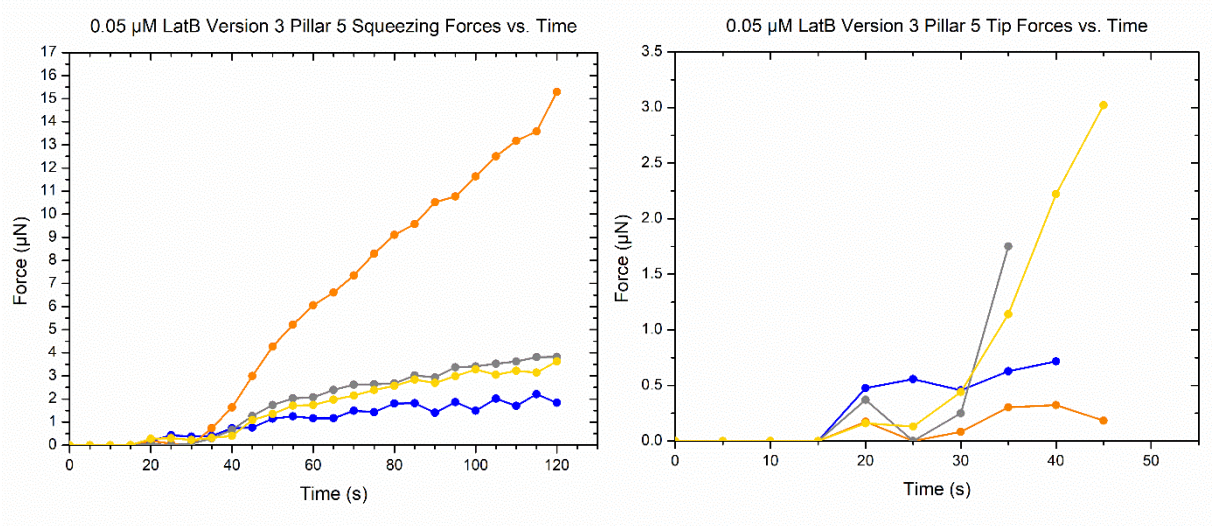

Figure 3.25. Version 3 pillar 5 hyphal squeezing and tip deflection force measurements over time with 0.05 µM latB. A total of 4 squeezing forces and 4 tip deflection forces were recorded for *P. nicotianae* hyphae.

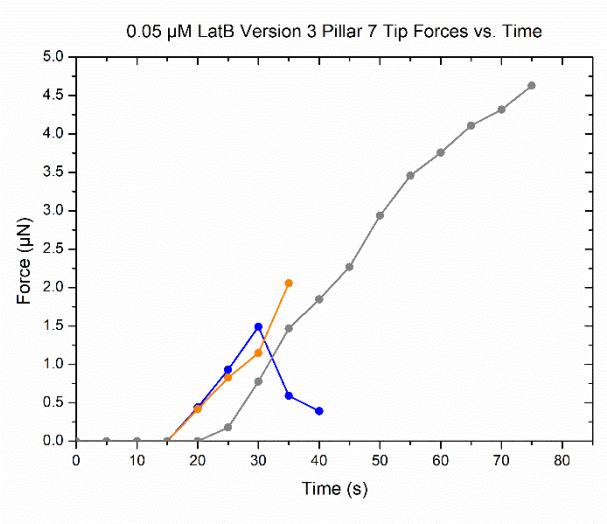

Figure 3.26. Version 3 pillar 7 hyphal tip deflection force measurements over time with 0.05 µM latB. A total of 3 tip deflection forces were recorded for *P. nicotianae* hyphae.

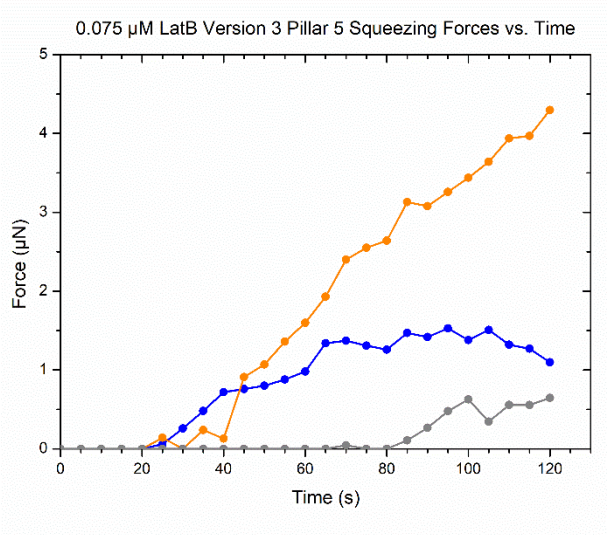

Figure 3.27. Version 3 pillar 5 hyphal squeezing force measurements over time with 0.075 µM latB. A total of 3 squeezing forces were recorded for *P. nicotianae* hyphae.

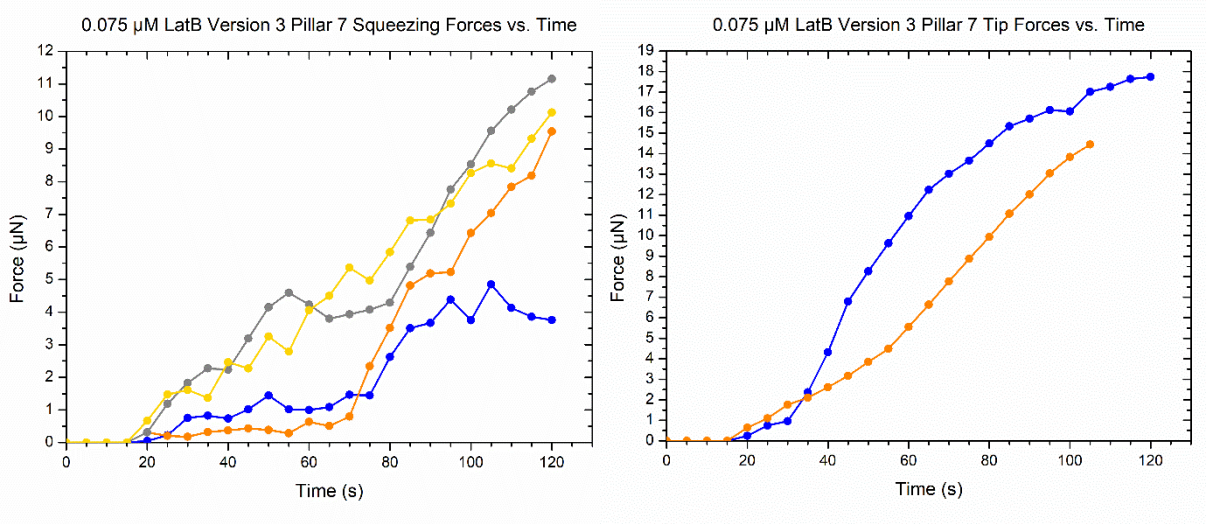

Figure 3.28. Version 3 pillar 7 hyphal squeezing and tip deflection force measurements over time with 0.075 µM latB. A total of 4 squeezing forces and 2 tip deflection forces were recorded for *P. nicotianae* hyphae.

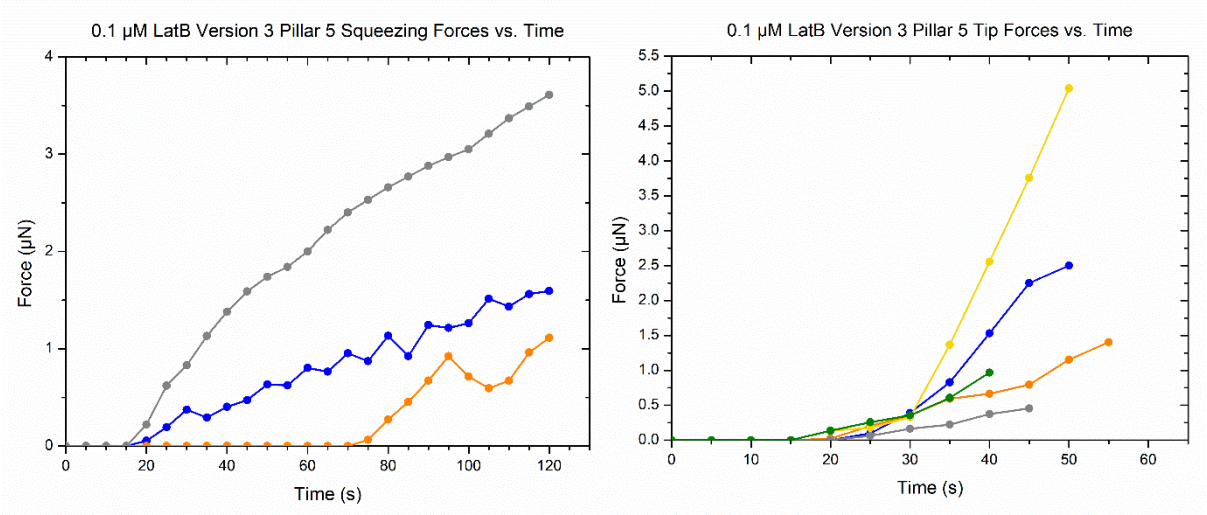

Figure 3.29. Version 3 pillar 5 hyphal squeezing and tip deflection force measurements over time with 0.1 µM latB. A total of 3 squeezing forces and 5 tip deflection forces were recorded for *P. nicotianae* hyphae.

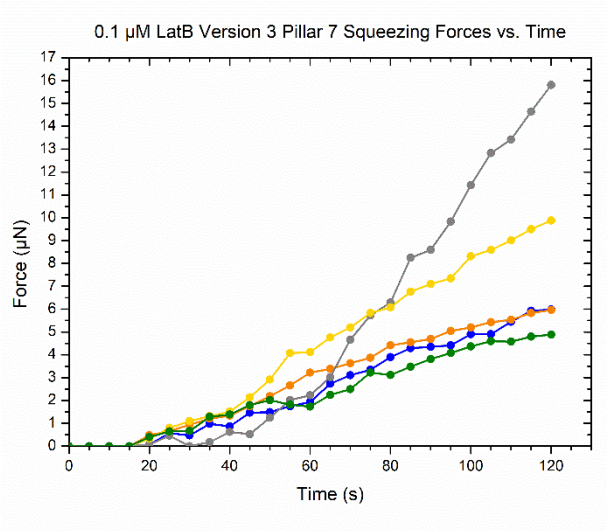

Figure 3.30. Version 3 pillar 7 hyphal squeezing force measurements over time with 0.1 µM latB. A total of 5 squeezing forces were recorded for *P. nicotianae* hyphae.

3.6 Force measurements from version 2 LOC devices for *P. cinnamomi* and *P. sojae*

Force measurements were obtained from version 2 pillar 5 LOC devices for *P. cinnamomi* and *P. sojae* (Fig. 3.31). This identified that these species can grow on LOC devices and that force data can be collected using the existing LOC devices designed and fabricated in this research. The *P. cinnamomi* and *P. sojae* hyphae for which force measurements were recorded also had their growth rates and hyphal widths calculated (Table 3.1).

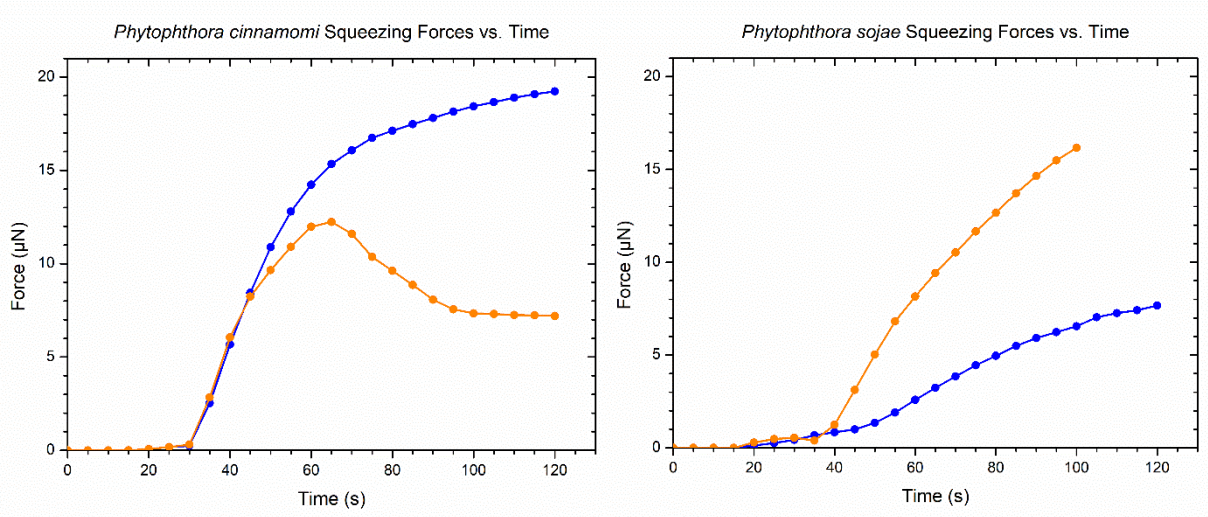

Figure 3.31. *P. cinnamomi* and *P. sojae* hyphal squeezing force measurements over time. A total of 2 squeezing forces were recorded for both *P. cinnamomi* and *P. sojae* hyphae.

Table 3.1. Growth rates and hyphal widths for *P. cinnamomi* and *P. sojae* hyphae.

Species	Hypha number	Growth rate (µm/min)	Hyphal width (µm)
P. cinnamomi	1	6.89	7.96
	2	6.78	5.00
P. sojae	1	4.23	7.64
	2	3.96	5.38

3.7 Comparison between maximum and half point force measurements in LOC devices

Force measurements under normal and latB conditions were compared to determine whether latB was affecting the forces produced by *P. nicotianae* hyphae. Both hyphal squeezing and tip deflection forces were compared which were separated into pillar size 5 and pillar size 7 to determine whether pillar size affected hyphal force production under all conditions tested. Hyphal squeezing and tip deflection force values were calculated using the averaged maximum and half point force values obtained by each hypha under each condition.

3.7.1 Squeezing force measurements

3.7.1.1 Comparison between squeezing force measurements in version 1 LOC devices

Version 1 force values were examined separately to version 2 and 3 measurements as version 1 LOC devices differed in device design from version 2 and 3 devices. As version 1 pillar 5 LOC devices were designed to test two gap sizes (3 or 5 µm), squeezing forces between devices with different gap sizes was tested. To test whether gap size had an impact on the obtained forces, maximum and half point squeezing forces were compared (Fig. 3.32). This showed a statistically significant difference in forces exerted by *P. nicotianae* hyphae when both maximum ($p < .0001$) and half point ($p < .0005$) force values were analysed. Devices with a gap size of 3 µm led to the production of significantly higher force values by *P. nicotianae* hyphae than devices with a gap size of 5 µm. This highlights the importance of device design for force data collection.

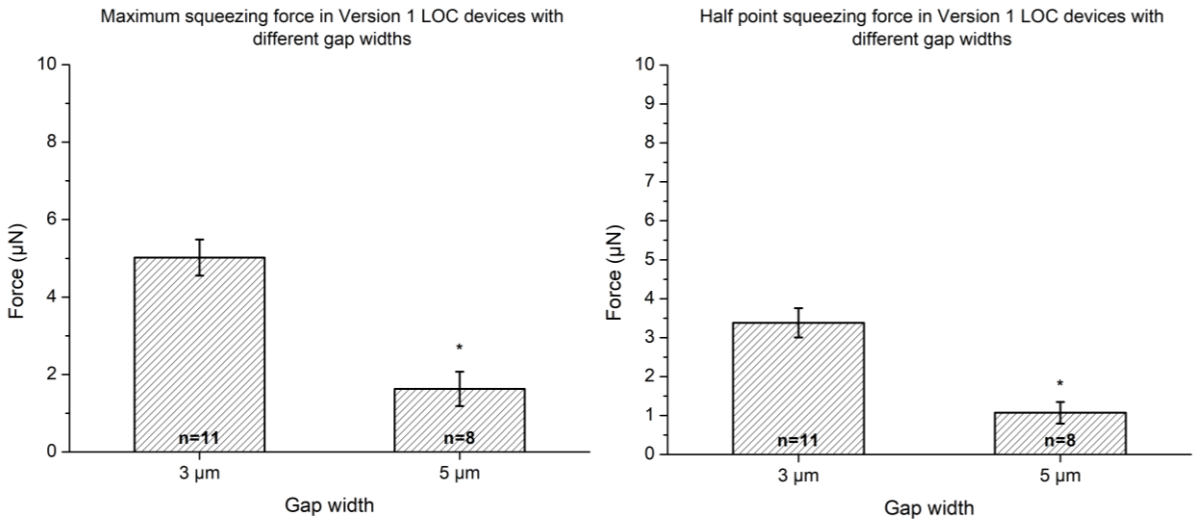

Figure 3.32. Gap size between the pillar and the channel walls affects the maximum and half point squeezing forces in pillar 5 LOC devices. Error bars represent the standard error of the mean and n corresponds to the number of individual measurements. Asterisks identify a significant difference between 3 and 5 µm gap size ($p < .05$).

3.7.1.2 Maximum and half point squeezing forces on pillar 5 LOC devices under latB treatment

To determine whether *P. nicotianae* squeezing forces differed under latB conditions in pillar 5 devices, maximum and half point values were examined under all conditions (Fig. 3.33). This analysis determined that in pillar 5 devices, there was a statistically significant difference in the squeezing forces exerted by *P. nicotianae* hyphae when both maximum ($F_{4,27} = 3.0$, $p < .05$) and half point ($F_{4,27} = 3.4$, $p < .05$) force values were analysed. However, when post hoc analysis was carried out for both data sets, no significant difference was identified.

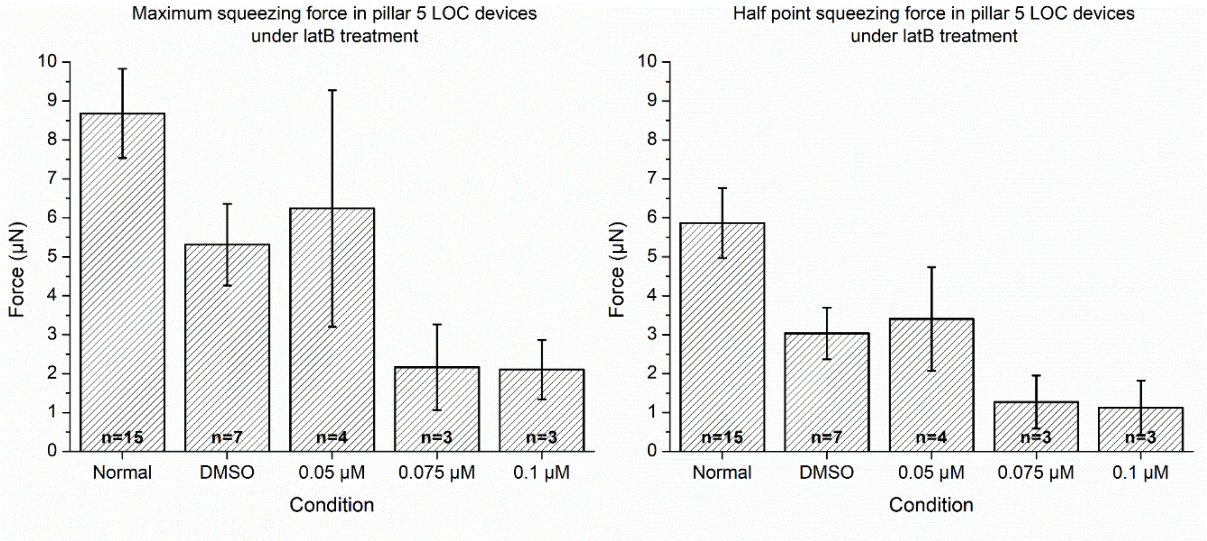

Figure 3.33. LatB treatment does not affect the maximum and half point squeezing forces in pillar 5 LOC devices. Error bars represent the standard error of the mean and n corresponds to the number of individual measurements.

3.7.1.3 Maximum and half point squeezing forces on pillar 7 LOC devices under latB treatment

To determine whether *P. nicotianae* squeezing forces differed under latB conditions in pillar 7 devices, maximum and half point values were examined under all conditions (Fig. 3.34). This analysis determined that in pillar 7 devices, there was a statistically significant difference in the squeezing forces exerted by *P. nicotianae* hyphae when both maximum ($F_{4,19} = 5.9$, $p < .005$) and half point ($F_{4,19} = 10.1$, $p < .0005$) force values were analysed. Post hoc analysis for maximum force values identified a significant difference between normal and 0.075 µM latB and between normal and 0.1 µM latB. Post hoc analysis for half point force values identified an additional significant difference between normal and 0.05 µM latB in addition to between normal and 0.075 µM latB and between normal and 0.1 µM latB.

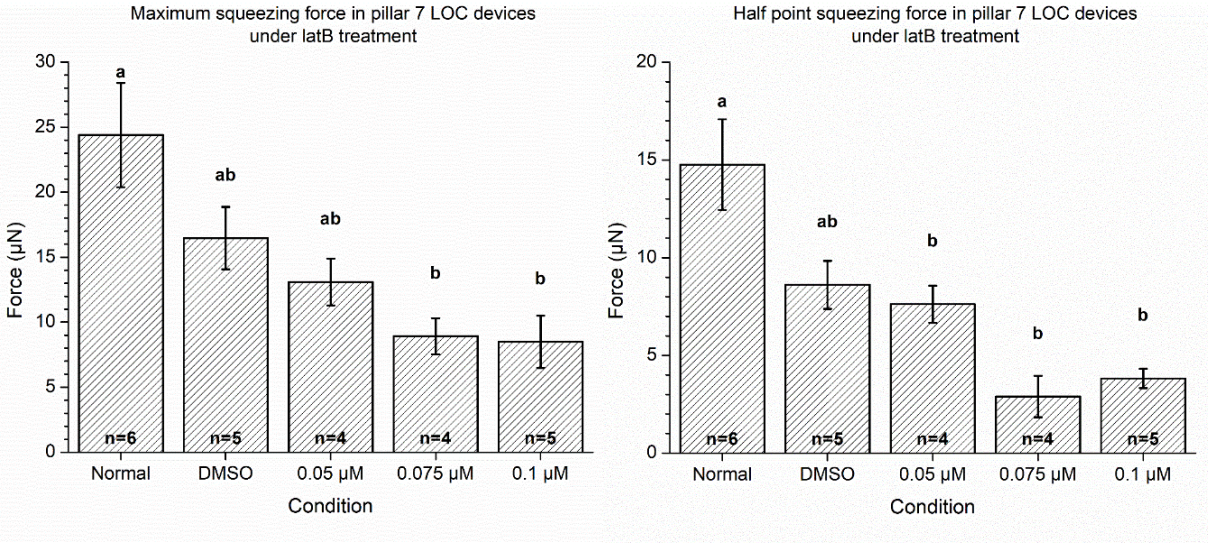

Figure 3.34. LatB treatment affects the maximum and half point squeezing forces in pillar 7 LOC devices. Error bars represent the standard error of the mean and n corresponds to the number of individual measurements. Values with the same letter are not significantly different to each other ($p > .05$).

To determine whether *P. nicotianae* squeezing forces differed under latB conditions between pillar 5 and pillar 7 devices, pillar 5 and pillar 7 maximum and half point values were examined under all conditions (Fig. 3.35). This analysis determined that there was a statistically significant difference between pillar 5 and pillar 7 squeezing forces exerted by *P. nicotianae* hyphae under most conditions when both maximum and half point force values were analysed. For maximum squeezing forces there was a significant difference between pillar 5 and pillar 7 forces under all conditions except for 0.05 µM latB and 0.1 µM latB. For half point squeezing forces there was a significant difference between pillar 5 and pillar 7 forces under all conditions except for 0.075 µM latB.

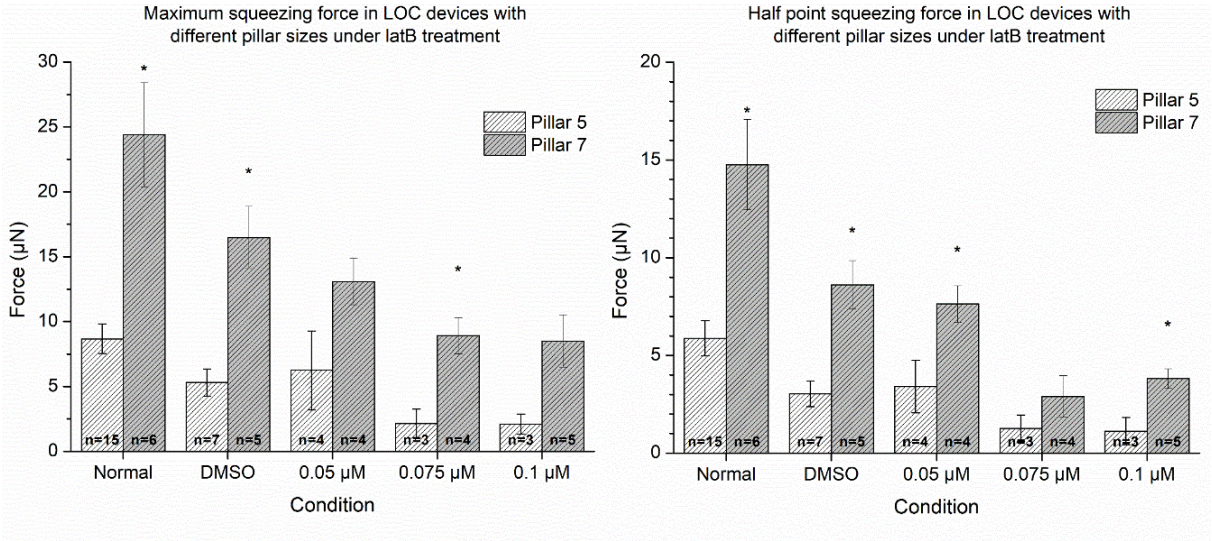

Figure 3.35. Maximum and half point squeezing forces differ in pillar 5 LOC devices compared to pillar 7 LOC devices in the presence of latB. Error bars represent the standard error of the mean and n corresponds to the number of individual measurements. Asterisks identify a significant difference between pillar 5 and pillar 7 squeezing forces within the condition ($p < .05$).

3.7.2 Hyphal tip force measurements

3.7.2.1 Maximum and half point hyphal tip forces on pillar 5 LOC devices under latB treatment

To determine whether *P. nicotianae* hyphal tip forces differed under latB conditions in pillar 5 devices, maximum and half point values were examined under all conditions (Fig. 3.36). As no data was obtained for pillar 5 with 0.075 μM latB, this condition was not included. This analysis determined that in pillar 5 devices, there was no statistically significant difference in the hyphal tip forces exerted by *P. nicotianae* hyphae when both maximum ($F_{3,12} = 0.4$, $p > .05$) and half point ($F_{4,7} = 0.2$, $p > .05$) force values were analysed.

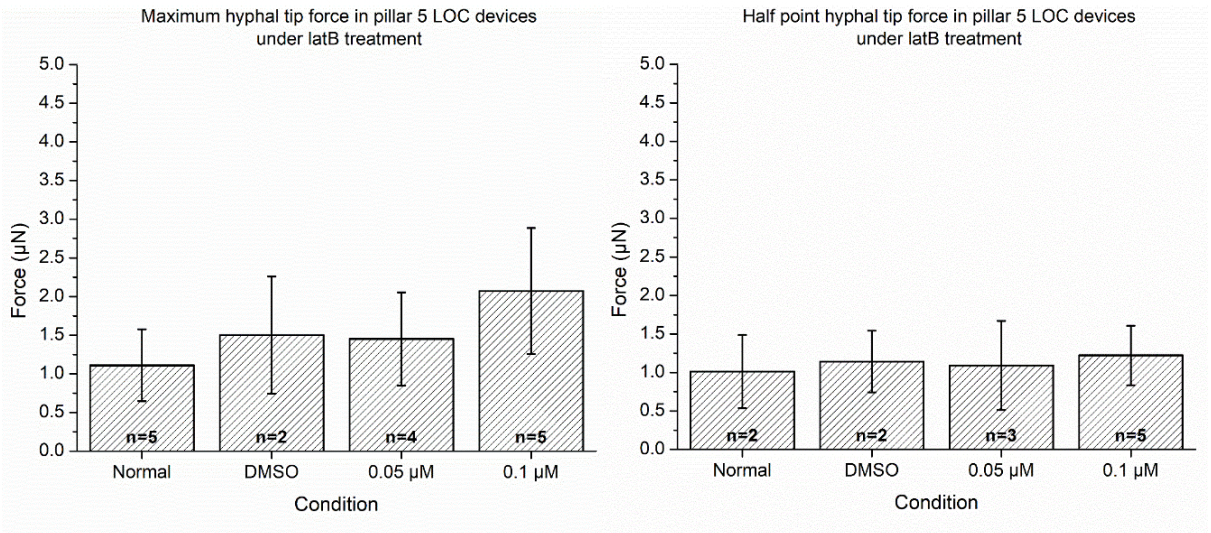

Figure 3.36. LatB treatment does not affect the maximum and half point hyphal tip forces in pillar 5 LOC devices. Error bars represent the standard error of the mean and n corresponds to the number of individual measurements.

3.7.2.2 Maximum and half point hyphal tip forces on pillar 7 LOC devices under latB treatment

To determine whether *P. nicotianae* hyphal tip forces differed under latB conditions in pillar 7 devices, maximum and half point values were examined under all conditions (Fig. 3.37). As no data was obtained for pillar 7 with 0.1 µM latB, this condition was not included. This analysis determined that in pillar 7 devices, there was a statistically significant difference in the hyphal tip forces exerted by *P. nicotianae* hyphae when both maximum ($F_{3,16} = 8.41$, $p < .005$) and half point ($X^2 = 8.4$, $p < .05$) force values were analysed. Post hoc analysis for maximum force values identified a significant difference between normal and 0.075 µM latB, between DMSO and 0.075 µM latB and between 0.05 µM latB and 0.075 µM latB. Post hoc analysis for half point force values identified that there was no significant difference between latB conditions.

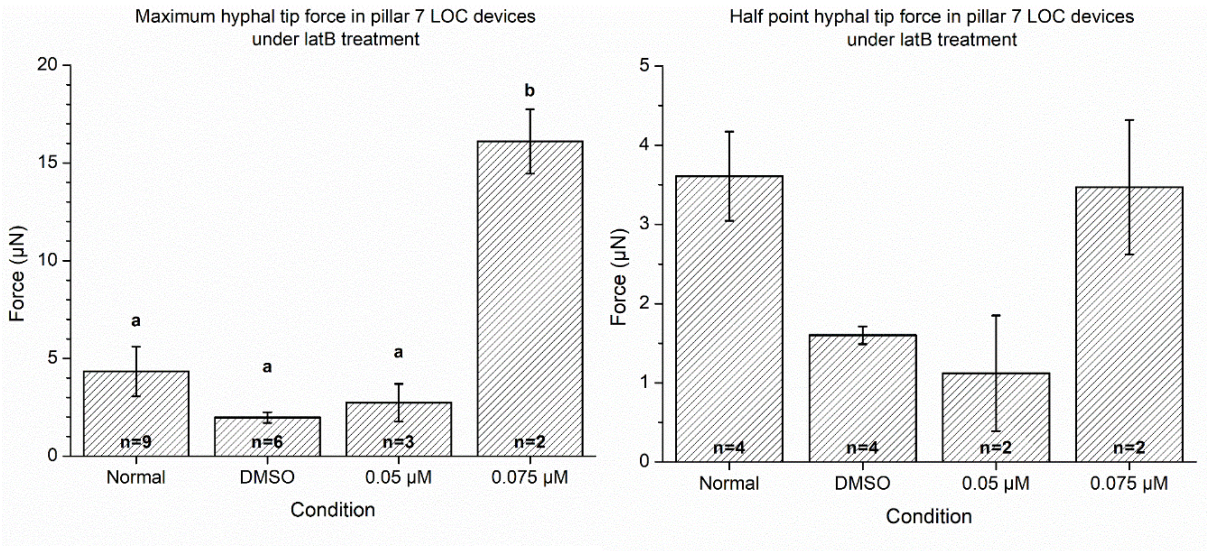

Figure 3.37. LatB treatment affects the maximum hyphal tip forces in pillar 7 LOC devices but not the half point hyphal tip forces. Error bars represent the standard error of the mean and n corresponds to the number of individual measurements. Values with the same letter are not significantly different to each other ($p > .05$).

To determine whether *P. nicotianae* hyphal tip forces differed under latB conditions between pillar 5 and pillar 7 devices, pillar 5 and pillar 7 maximum and half point values were examined under all conditions (Fig. 3.38). As no data was obtained for both pillar 5 with 0.075 µM latB and pillar 7 with 0.1 µM latB, these conditions were not included. This analysis determined that there was a statistically significant difference between pillar 5 and pillar 7 hyphal tip forces exerted by *P. nicotianae* hyphae only under normal conditions when both maximum and half point force values were analysed.

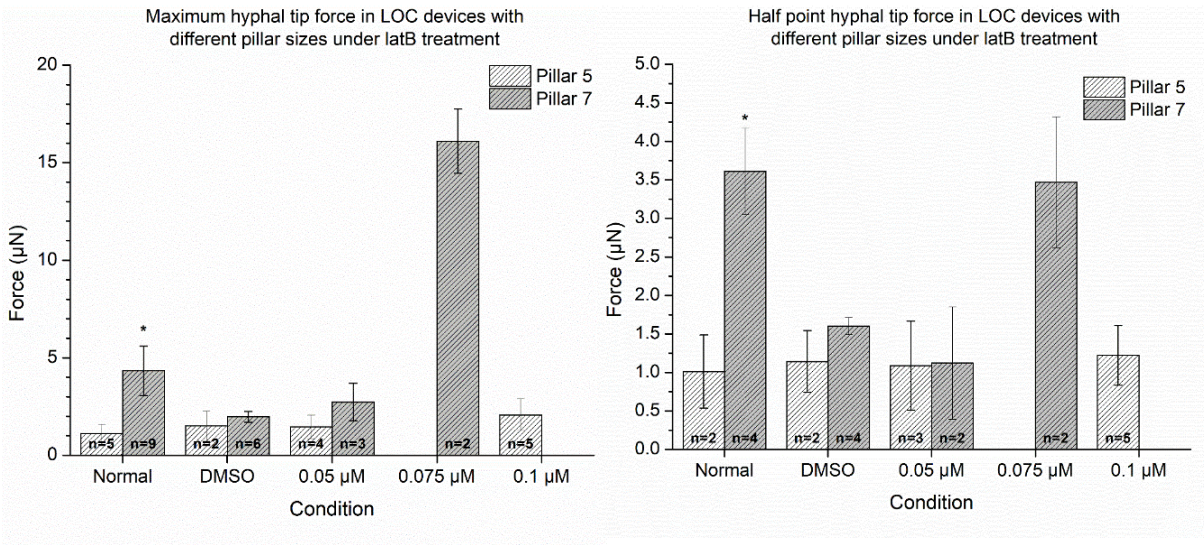

Figure 3.38. Maximum and half point hyphal tip forces differ in pillar 5 LOC devices compared to pillar 7 LOC devices under normal conditions but not in the presence of latB. Error bars represent the standard error of the mean and n corresponds to the number of individual measurements. Asterisks identify a significant difference between pillar 5 and pillar 7 hyphal tip forces within the condition ($p < .05$).

3.8 Comparison between maximum and half point pressure measurements in LOC devices

3.8.1 Pressure measurements in pillar 5 LOC devices

To determine whether *P. nicotianae* hyphal tip pressures differed under latB conditions in pillar 5 devices, pressures were calculated using maximum and half point force values and examined under all conditions (Fig. 3.39). As no data was obtained for pillar 5 with 0.075 µM latB, this condition was not included. This analysis determined that in pillar 5 devices, there was no statistically significant difference in the pressure exerted by *P. nicotianae* hyphae when both maximum ($F_{3,12} = 0.4$, $p > .05$) and half point ($F_{3,8} = 0.2$, $p > .05$) pressure values were analysed.

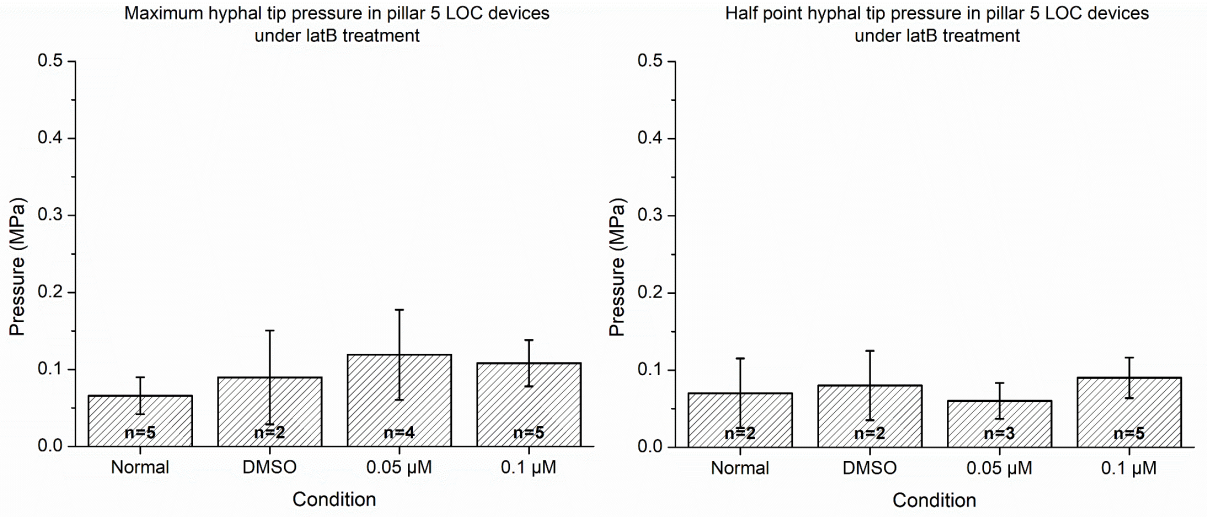

Figure 3.39. LatB treatment does not affect the maximum and half point hyphal tip pressures in pillar 5 LOC devices. Error bars represent the standard error of the mean and n corresponds to the number of individual measurements.

3.8.2 Pressure measurements in pillar 7 LOC devices

To determine whether *P. nicotianae* hyphal tip pressures differed under latB conditions in pillar 7 devices, pressures were calculated using maximum and half point force values and examined under all conditions (Fig. 3.40). As no data was obtained for pillar 7 with 0.1 µM latB, this condition was not included. This analysis determined that in pillar 7 devices, there was a statistically significant difference in the pressure exerted by *P. nicotianae* hyphae when half point ($F_{3,8}$ = 6.2, p < .05) pressure values were analysed, but no statistically significant difference when maximum pressure values were analysed ($F_{3,16}$ = 1.63, p > .05). Post hoc analysis for half point pressure values identified a significant difference between DMSO and 0.075 µM latB and between 0.05 µM latB and 0.075 µM latB.

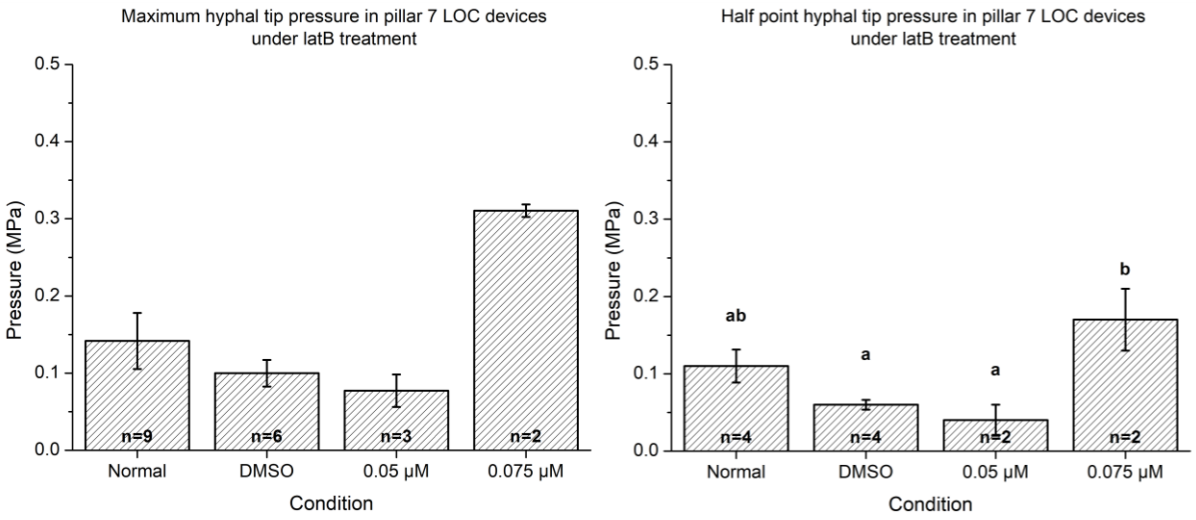

Figure 3.40. LatB treatment affects the hyphal tip pressures in pillar 7 LOC devices. Error bars represent the standard error of the mean and n corresponds to the number of individual measurements. Values with the same letter are not significantly different to each other (p > .05).

To determine whether *P. nicotianae* hyphal tip pressures differed under latB conditions between pillar 5 and pillar 7 devices, pressures calculated from maximum and half point force values on pillar 5 and pillar 7 devices were examined under all conditions (Fig. 3.41). As no data was obtained for both pillar 5 with 0.075 µM latB and pillar 7 with 0.1 µM latB, these conditions were not included. This analysis determined that there was no statistically significant difference in the pressure exerted by *P. nicotianae* hyphae between pillar 5 and pillar 7 devices when both maximum and half point pressure values were analysed.

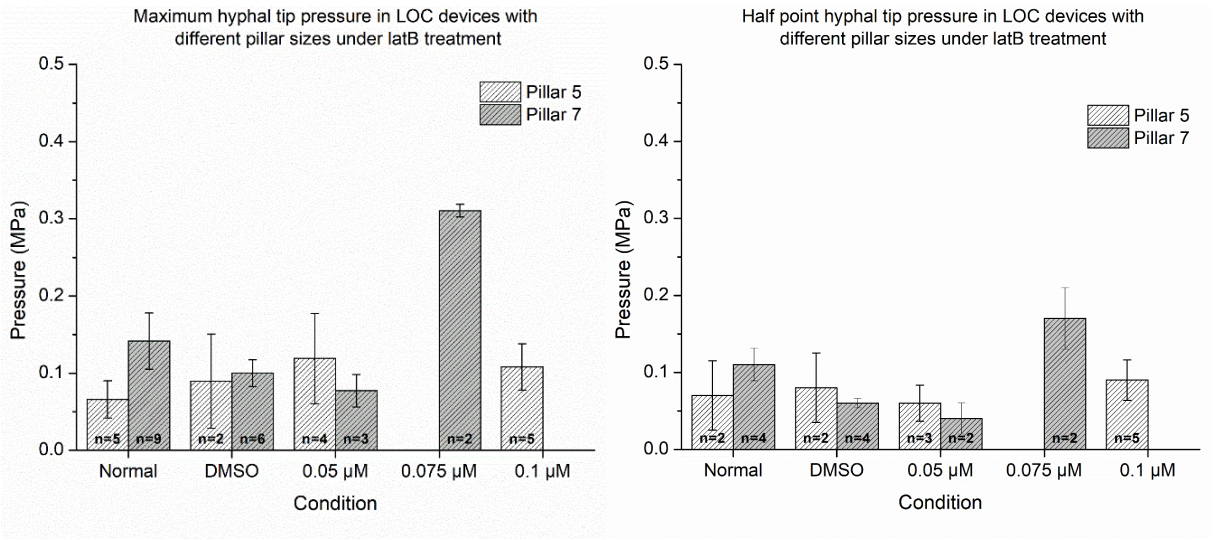

Figure 3.41. Pillar size does not affect hyphal tip pressures in the presence of latB. Error bars represent the standard error of the mean and n corresponds to the number of individual measurements.

3.8.3 Hyphal tip pressure measurements as a percentage of total turgor pressure

Pressure measurements were converted into percentages of total turgor pressure using a turgor pressure of 0.69 MPa. As turgor pressure has not been measured for *P. nicotianae*, this value approximated from turgor values in other oomycete species, as mentioned in Chapter 2. These percentages calculated were compared to determine whether the percentage of total turgor pressure exerted by *P. nicotianae* hyphae differed within and between latB conditions in pillar 5 and pillar 7 devices. Pressure percentages were calculated using pressures from maximum and half point force values and were examined under all conditions (Table 3.2). As no data was obtained for pillar 5 with 0.075 µM latB and pillar 7 with 0.1 µM latB, these conditions were not included. Graphical representations of this data (not shown) produced the same trends as seen in pressure Figs. 3.39-3.41.

Table 3.2. Percentage of total turgor pressure exerted by *P. nicotianae* hyphae on LOC device pillars.

Condition	Pillar 5 maximum average (%)	Pillar 5 half point average (%)	Pillar 7 maximum average (%)	Pillar 7 half point average (%)
Normal	10	11	21	15
DMSO	13	12	14	9
0.05 µM	17	9	11	6
0.075 µM	N/A	N/A	45	24
0.1 µM	16	14	N/A	N/A

Analysis determined that in pillar 5 devices, there was no statistically significant difference in the percentage of total turgor pressure exerted by *P. nicotianae* hyphae when half point pressure values were analysed ($F_{3,8} = 0.2$, $p > .05$) or when maximum pressure values were analysed ($F_{3,12} = 0.4$, $p > .05$). In contrast, in pillar 7 devices there was a statistically significant difference in the percentage of total turgor pressure exerted by *P. nicotianae* hyphae when half point pressure values were analysed ($F_{3,8} = 65.9$, $p < .05$), but no statistically significant difference when maximum pressure values were analysed ($F_{3,16} = 1.7$, $p > .05$).

To determine whether the percentage of total turgor pressure exerted by *P. nicotianae* hyphae differed within latB conditions in pillar 5 and pillar 7 devices, pressures calculated from maximum and half point force values on pillar 5 and pillar 7 devices were examined under all conditions. This analysis determined that there was no statistically significant difference in the percentage of total turgor pressure exerted by *P. nicotianae* hyphae between pillar 5 and pillar 7 devices when both maximum and half point pressure values were analysed.

3.9 Relationships between growth rate, hyphal width, force production and pressures of *P. nicotianae* hyphae in LOC devices

As force measurements, pressures, growth rates and widths of *P. nicotianae* hyphae were collected throughout the experiments, an investigation into whether these variables had a relationship was tested using regression and correlation analysis. This analysis examined whether there were relationships between combinations of these variables and if so, how strong they were.

3.9.1 Relationship between growth rate and hyphal width

To determine whether there was a relationship between growth rate and hyphal width, both correlation and regression analysis were performed. Spearman's correlation analysis ($r_s = 0.04$, $p > .05$) and regression analysis ($R^2 = 1.48 \times 10^{-4}$, $p > .05$) identified that there was no statistically significant relationship between the growth rate and width of *P. nicotianae* hyphae when grown on LOC devices.

3.9.2 Relationship between growth rate and hyphal tip pressures

To determine whether there was a relationship between growth rate and hyphal pressures, both correlation and regression analysis were performed. Regression analysis identified that there was a statistically significant relationship between the growth rate and pressure exerted by *P. nicotianae* hyphae when using maximum ($R^2 = 0.11$, $p < .05$) and half point force values to calculate pressure ($R^2 = 0.16$, $p < .05$). In contrast, Spearman's correlation analysis identified that there was no statistically significant relationship between the growth rate and pressure exerted by *P. nicotianae* hyphae when using maximum ($r_s = -0.24$, $p > .05$) and half point force values to calculate pressure ($r_s = -0.34$, $p > .05$).

While a statistically significant relationship was detected during regression analysis, the R^2 value for this data is low. This model shows that growth rate explains 11 or 16% of the variation in pressure and vice versa when calculated with maximum and half point force values respectively. As this R^2 value is low and only a small proportion of the variance can be explained by this model it is likely that there is no meaningful relationship between the growth rate and pressure, consistent with the results obtained for correlation analysis.

3.9.3 Relationship between growth rate, hyphal width and force

To determine whether there was a relationship between growth rate, hyphal width and force, multiple regression analysis was performed. Analysis identified that there was a relationship between hyphal growth rate and width and the production of squeezing forces in both pillar 5 and pillar 7 devices and the production of hyphal tip forces in pillar 7 devices.

3.9.3.1 Relationship between growth rate, hyphal width and squeezing force

The relationship between growth rate, hyphal width and squeezing forces in pillar 5 devices was statistically significant when using both maximum ($R^2 = 0.39$, $p < .001$) and half point

force values (R^2 = 0.34, p < .005). However, while this relationship was significant, the R^2 values were low, with the hyphal width and growth rate accounting for 39 or 34% of the variation in squeezing force.

Similarly, the relationship between growth rate, hyphal width and squeezing forces in pillar 7 devices was statistically significant when using both maximum (R^2 = 0.32, p < .05) and half point force values (R^2 = 0.34, p < .05). However, while this relationship was significant, the R^2 values were low, with the hyphal width and growth rate accounting for 32 or 34% of the variation in squeezing force.

3.9.3.2 Relationship between growth rate, hyphal width and hyphal tip force

The relationship between growth rate, hyphal width and hyphal tip forces in pillar 7 devices was statistically significant when using maximum force values (p < .001). Similar to the squeezing force relationships, the R^2 value was low, with the hyphal width and growth rate accounting for 46% of the variation in hyphal tip force.

In contrast, there was no relationship between growth rate, hyphal width and hyphal tip forces in pillar 5 devices when using maximum force values (p > .05) or between growth rate, hyphal width and hyphal tip forces in pillar 5 and 7 devices when using half point force values (p > .05).

3.10 Hyphal morphological observations on LOC devices

When treated with latB and when grown on version 2 devices with pillars adhered to the channel walls, notable changes in hyphal morphologies were observed. During latB treatment, disruptions of hyphal polarity and directionality were observed while hyphal growth into adhered pillars formed appressoria-like structures.

3.10.1 Hyphal morphologies observed with latB treatment

Treatment of *P. nicotianae* hyphae with latB in LOC devices caused morphological changes (Table 3.3), representative images of which can be seen in Fig. 3.42. These morphological changes were not observed in normal or DMSO conditions. Furthermore, a greater number of changes were observed under higher latB concentrations, suggesting that the morphological changes were a direct result of latB concentration. Of course, the absence of particular changes in a given condition does not mean that they never occurred, only that they were not observed

in the images obtained during data collection. Concentrations of 0.25 µM latB and 0.5 µM latB were added to devices, as seen in Table 3.3. However, due to the slow growth rate of *P. nicotianae* hyphae at these concentrations, these devices were only used to observe morphological changes as a result of latB treatment.

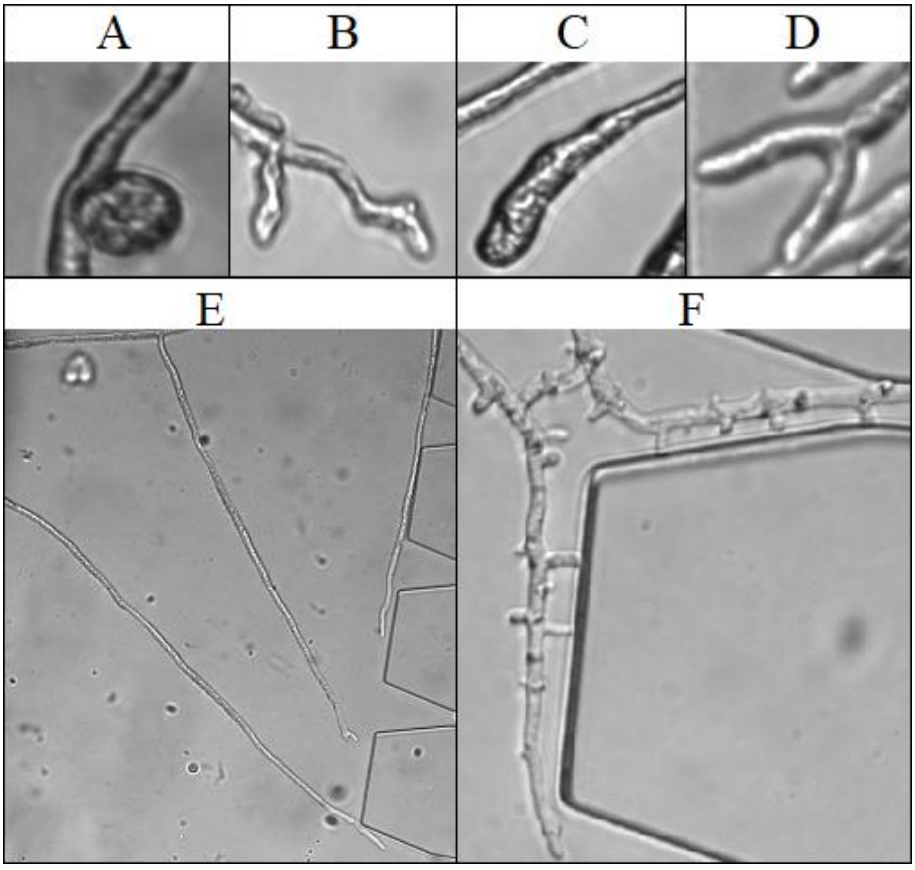

Figure 3.42. Hyphal morphologies observed in LOC devices with latB treatment. (A) hyphal curling, (B) irregular hyphal diameter, (C) hyphal swelling, (D) hyphal bifurcation, (E) reduced hyphal branching, (F) excessive branch initiation/formation.

Table 3.3. Hyphal morphologies observed in LOC devices with latB treatment. Tick marks indicate the presence while cross marks indicate the absence of each morphological change. N/A indicates that the growth pattern did not allow for these changes to be observed.

Condition	A	B	C	D	E	F
Normal	×	×	×	×	×	×
DMSO	×	×	×	×	×	×
0.05 µM	×	✓	✓	✓	✓	✓
0.075 µM	✓	✓	✓	×	✓	✓
0.1 µM	✓	✓	✓	✓	✓	✓
0.25 µM	N/A	✓	✓	N/A	N/A	✓
0.5 µM	✓	✓	✓	✓	✓	✓

3.10.2 Appearance of appressoria-like structures

As pillars were found to adhere to the channel walls in channels 1-6 of version 2 devices, the force values obtained for these deflections were unable to be used. However, when recording data for these channels, an interesting morphological change was occasionally observed as the hyphae were able to exert enough force to push past the pillar by forming an appressoria-like structure (Fig. 3.43).

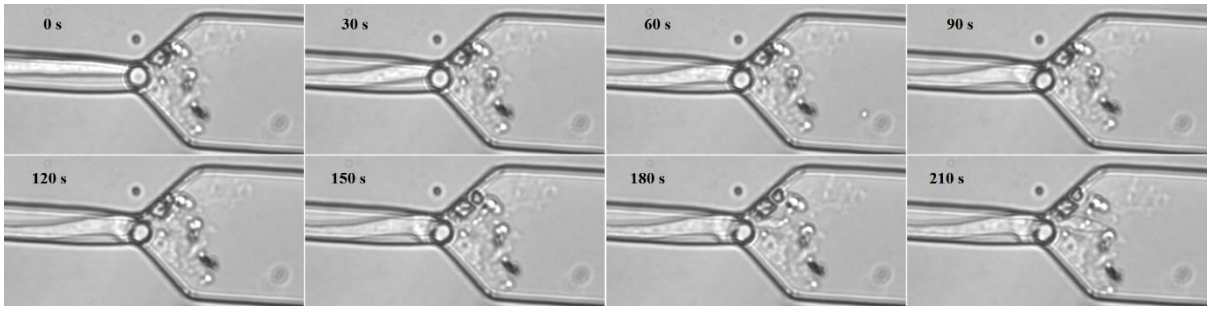

Figure 3.43. Appressoria-like structures formed in LOC devices with adhered pillars over time. When the hypha encountered the pillar, it began to push against the pillar, causing the hypha to bend, seen between 0 and 30 s. The hypha then appeared to stop growing, following which the hyphal tip began to swell, seen between 30 and 90 s, before branching and pushing two hyphal tips out from either side of the pillar.

This morphological change resembles the formation of appressoria during host tissue invasion by hyphal organisms. While the LOC devices in this research were designed to measure the forces exerted by hyphae, this observation highlights potential future applications of the LOC devices.

Chapter 4. Discussion

Although the impact of oomycete diseases is well known, strategies for effective prevention and control of many of these pathogens is limited, identifying the urgent need for an increase in scientific knowledge and development (Panabières et al 2016). An increased understanding of the molecular mechanisms behind invasive growth may allow for the development of novel oomycides that are effective against target pathogens. This would increase the efficiency of pathogen control and help protect species that are being targeted by these pathogenic species.

Force production, a key component of invasive hyphal growth, was examined in this thesis. Methods previously employed to measure force exertion by hyphal organisms have included both direct and indirect methods. Until recently, the most successful of these methods has been strain gauges. However, the validity of results obtained from this method have been questioned (Money 2007, Nezhad 2014, Nezhad & Geitmann 2013, Tayagui et al 2017). Because of this, microfluidic LOC devices have been developed as an alternative approach (Nezhad et al 2013, Nock et al 2015, Sun et al 2018, Tayagui et al 2016, Tayagui et al 2017). The applicability of micropillar-based LOC devices for measurements of force, growth rates and hyphal widths of *P. nicotianae*, *P. cinnamomi* and *P. sojae* was assessed in this thesis. Additionally, the mechanisms responsible for force production in *P. nicotianae* hyphae were investigated using the actin cytoskeletal inhibitor latB. The effectiveness of these micropillar-based LOC devices to investigate the molecular mechanisms involved in hyphal growth and force production is discussed in this chapter.

4.1 LOC device design

Three versions of LOC devices were tested and successfully used throughout this research to measure hyphal growth rates, hyphal widths and exerted forces of *P. nicotianae*, *P. cinnamomi* and *P. sojae*. This supports the hypothesis that the *Phytophthora* species will be able to grow on the designed LOC devices and shows promise for future applications with other *Phytophthora* and oomycete species. Force measurements were able to be collected for both squeezing and hyphal tip forces of *P. nicotianae* hyphae, increasing the amount of data that can be successfully collected from a single LOC device design.

Version 1 devices had a channel width of 15 µm whereas version 2 and 3 devices had a channel width of 17 µm. This difference had no impact on the growth rate or width of *P. nicotianae*

hyphae (Figs. 3.7 and 3.12, respectively). As a channel width of 17 µm was used successfully in the final design (version 3 devices), it would be advised to use the same width in future designs.

Similar to growth of *A. bisexualis* hyphae in LOC devices by Tayagui et al (2017), *P. nicotianae* hyphae were found to reach the central channels before the outer channels. This was likely due to the shorter distance required to reach these central channels from the seeding area. In version 1 devices with 24 channels, this meant that approximately 12 central channels often had hyphae approaching them concurrently. As *P. nicotianae* had a fast growth rate and only three channels could be recorded concurrently, a large proportion of the hyphal deflections were unable to be recorded. As such, 12 channels were implemented into version 2 and 3 devices. This meant that there were only six central channels. Hyphae which approached these channels concurrently were therefore able to be measured easier than in version 1 devices, with less deflections being missed.

While using 12 channels in version 2 and 3 devices was most successful, version 1 pillar 5 devices had an advantage in that two gap widths could be tested (3 and 5 µm). In these devices, squeezing forces produced by *P. nicotianae* hyphae on devices with a gap size of 3 µm were significantly greater than forces produced on devices with a gap size of 5 µm (Fig. 3.32). This highlights the importance of device design for force data collection. While a gap size of 3 µm would be preferable to obtain higher force values, with higher signal-to-noise, the gap size is limited by fabrication restrictions. When integration of a gap size of 3 µm was attempted in version 2 devices, the pillars adhered to the walls of these channels. Therefore, due to variations in device fabrication, the integration of a gap size of 3 µm was not feasible. As such, this gap size was only successfully integrated into version 1 pillar 5 devices. For this reason, version 3 devices incorporated gap widths of 5 µm in channels alongside the general design of version 2 devices.

Version 3 devices were the most successful device designed as such were used most frequently. When *P. nicotianae* hyphae were treated with the cytoskeletal inhibitor latB, hyphal growth rates significantly decreased (Fig. 3.8). Therefore, a version 4 device could be designed for experiments utilising latB or other cytoskeletal inhibitors, incorporating 24 channels from the version 1 design into the version 3 design. While not suitable for normal hyphae, for hyphae treated with latB with a significantly slower growth rate, an increase in channels would potentially increase the amount of force data collected from a single device. In addition, the

quantity of inhibitors, devices, time and cost required to obtain the same quantity of data would be significantly reduced.

4.2 Growth rates of *P. nicotianae*

4.2.1 Impact of PDMS and LOC device design on the growth rate of *P. nicotianae* hyphae

Initial growth experiments used culture dishes to determine whether PDMS had an impact on the growth of *P. nicotianae* hyphae. The culture dishes were set up with agar, broth or broth with a PDMS layer. When growth rates were compared between broth and broth with PDMS there was no significant difference in growth rate detected (Fig. 3.5). This identified that PDMS had no effect on the growth rate of *P. nicotianae* hyphae. As such, this meant that the results obtained on LOC devices were not altered by the presence of PDMS and were therefore valid measurements.

When growth rates of *P. nicotianae* hyphae under normal conditions (broth) in PDMS LOC device channels were compared to growth rates in culture dishes (broth and PDMS), a significant difference was observed (Fig. 3.9). The growth rate of hyphae in channels was found to be significantly faster than the growth rate of hyphae grown in culture dishes. This increase was expected, as there is less opportunity for hyphal branching and less competition by other hyphae in channels compared to culture dishes. In channels, the hyphae grow in a predefined direction, where they are guided by the device design. Additionally, there is no clustering of hyphae in channels, with each channel primarily having only one hypha. This allows the leading hypha to grow without competition. This is contrasted in culture dishes where hyphae grow radially from the mycelium plug, causing hyphae to cluster together and remain in continual competition with other hyphae for nutrients and space.

It is evident from these experiments that *P. nicotianae* hyphae are not affected by the presence of PDMS, nor are they negatively impacted by device design. Instead, *P. nicotianae* hyphae have an increased growth rate on devices compared to culture dishes. This supports the hypothesis that LOC devices will not negatively impact the growth rate of *P. nicotianae* hyphae. In contrast, Tayagui et al (2017) found no significant difference in the growth rate of *A. bisexualis* when grown on peptone yeast glucose (PYG) agar plates compared to channels containing PYG broth on LOC devices. While the experiment by Tayagui et al (2017) compared growth rate in channels to growth rate on a solid medium, rather than a liquid

medium in this research, it is unlikely that the liquid medium was the cause of the observed difference in growth rate between channels and dishes. This is because in dishes, growth on agar was significantly slower than growth on broth with PDMS (Fig. 3.5).

To determine whether channel width in LOC devices affected the growth rate of hyphae, the growth rate in version 1 devices (width = 15 µm) was compared to version 2 and 3 devices (width = 17 µm) (Fig. 3.7). Analysis showed that there was no statistically significant difference in the growth rate of *P. nicotianae* hyphae when grown in channels with widths of 15 and 17 µm. Similarly, the growth rate of *Camellia japonica* pollen tubes grown in PDMS LOC microchannels did not change when channel widths were varied (Agudelo et al 2013). Taken together, these findings indicate that the growth rate of tip growing cells is not affected by variations in channel width in PDMS LOC devices.

Different organisms and species may have different responses to the restraints imposed by LOC devices. Pollen tubes from *Lilium longiflorum*, which grow through the process of tip growth, were grown in PDMS LOC device microchannels by Hu et al (2017). It was found that the growth rate of pollen tubes varied in channels but that the growth rates did not differ from growth rates obtained in a conventional *in vitro* culture assay (Hu et al 2017). Similarly, the growth rates of *C. japonica* pollen tubes in LOC device microchannels were also comparable to results from conventional *in vitro* assays (Agudelo et al 2013). In addition, growth rates of *N. crassa* in LOC device channels were found to vary between hyphae and were dependent upon the hypha's position in the channel (Geng et al 2015).

While the results from this research identify that *P. nicotianae* hyphae are not affected by the presence of PDMS, or negatively impacted by device design, other species may be more sensitive to alterations in growth conditions. The impact of LOC devices on growth rate and other cell morphologies should therefore be independently determined for each species grown on the device to examine any potential impacts from LOC device composition and design.

4.2.2 Impact of latB on the growth rate of *P. nicotianae* hyphae

In culture dishes, latB was found to significantly decrease the growth rate of *P. nicotianae* hyphae when compared to normal and DMSO control conditions (Fig. 3.6). While there was no significant difference between normal and 0.05 µM latB and normal and 0.075 µM latB, there was a significant difference between normal and 0.1 µM latB. This suggests that there is a concentration dependent impact of latB on growth rate. Additionally, the growth rate in the

DMSO control was significantly different to that in all latB conditions (Fig. 3.6). This strongly suggests that latB decreases the growth rate of *P. nicotianae* hyphae on culture dishes. While it appears that DMSO may increase growth rate in culture dishes compared to the normal condition, this increase was not statistically significant. However, if there was an increase, as all latB conditions contained the same concentration of DMSO and were all significantly slower than the DMSO control this would only further support the results obtained.

LatB was also found to significantly decrease the growth rate of *P. nicotianae* hyphae in LOC devices (Fig. 3.8). When grown in LOC device channels, there was a significant difference in the growth rate of *P. nicotianae* hyphae between all conditions except for between normal and DMSO, between 0.05 µM latB and 0.075 µM latB and between 0.075 µM latB and 0.1 µM latB. Similar to the results obtained in culture dishes, this suggests that there is a concentration dependent impact of latB on growth rate.

When the growth rates in culture dishes were compared with the growth rates in channels, the growth rates were found to be significantly faster in channels than in dishes under all latB conditions tested, except for under 0.075 µM latB (Fig. 3.9). Although the growth rate of hyphae grown in channels under 0.075 was faster than in culture dishes, this difference was not significant. This is likely a result of small sample sizes for this data, as the sample sizes were the smallest of all conditions in both channels and dishes. This identifies a negative impact of latB on the growth rate of *P. nicotianae* hyphae.

LatB has been found to decrease hyphal growth rates in a concentration dependent manner in other oomycete species. Ketelaar et al (2012) identified that in the presence of increasing latB concentrations, the growth rate of *P. infestans* hyphae decreased. Additionally, mycelial growth was shown to be inhibited altogether at increasingly higher concentrations of latB (0.75 and 1 µM latB) (Ketelaar et al 2012). Research conducted by Gupta and Heath (1997) on the oomycete *S. ferax* also identified a reduction in hyphal growth rate in the presence of latB, followed by a cessation of growth after 60 s. Interestingly, turgor levels were shown to play a role in the growth rate in the first 10 s following latB addition, with normal turgor hyphae displaying an increase in growth rate and low turgor hyphae displaying a decrease in growth rate (Gupta & Heath 1997). Subsequent experiments with *S. ferax* for longer time periods identified that following growth cessation as a result of latB addition, growth resumed after 1.5 hours (Bachewich & Heath 1998). While no growth rate changes following addition of latB to an already growing culture were observed in this research, as latB was present throughout the

experiments, the observed decrease in *P. nicotianae* hyphal growth rate due to latB addition is consistent with findings from other oomycete species. This further highlights the importance of the actin cytoskeleton in hyphal growth, with actin polymerisation inhibition by latB causing hyphae to grow slower.

4.3 Hyphal widths of *P. nicotianae*

4.3.1 Impact of PDMS and LOC device design on the width of *P. nicotianae* hyphae

Initial growth experiments used culture dishes to determine whether PDMS had an impact on the width of *P. nicotianae* hyphae. The culture dishes were set up with agar, broth or broth with a PDMS layer. When hyphal widths were compared between broth and broth with PDMS there was no significant difference (Fig. 3.10). This identified that PDMS had no effect on the width of *P. nicotianae* hyphae.

When hyphal widths of *P. nicotianae* hyphae under normal conditions (broth) in PDMS LOC device channels were compared to hyphal widths in culture dishes (broth and PDMS), a significant difference was observed (Fig. 3.14). The width of hyphae in culture was found to be significantly wider than the width of hyphae grown in channels. Similarly, when hyphal widths were compared with the addition of latB in LOC device channels and culture dishes, hyphal width was also found to be significantly wider in dishes than in channels under all latB conditions tested (Fig. 3.14). This does not support the hypothesis that the width of *P. nicotianae* hyphae will not change when grown on LOC devices compared to culture dishes. The observed decrease in hyphal width in channels is likely a result of the hyphae being restrained by the channel width in LOC devices and unrestrained in culture dishes.

Similarly, Tayagui et al (2017) found that the width of *A. bisexualis* hyphae was narrower in channels grown in PYG broth than on PYG agar plates. However, it does not appear that this difference was statistically significant. As discussed in section 4.2.1, Tayagui et al (2017) compared the hyphae between a liquid medium in channels and a solid medium in plates. In this research, the hyphal width was compared between a liquid medium in channels and a liquid medium in dishes. When comparing these dishes to agar dishes, the hyphae were significantly wider when grown on agar (Fig. 3.10), and as such would give an even greater difference in width if compared with channels. This indicates that it is not the medium, but the constraints of the channels that is causing the observed decrease in width in *P. nicotianae* hyphae. It is unclear whether this is also true for *A. bisexualis* hyphae. Similar to growth rates in LOC

devices, it appears that the influence of the LOC devices on growth may be dependent upon the species, with some species affected more than others.

4.3.2 Impact of latB on the width of *P. nicotianae* hyphae

In culture dishes, latB was found to significantly increase the width of *P. nicotianae* hyphae when compared to normal conditions at latB concentrations of 0.075 µM and 0.1 µM (Fig. 3.11). This suggests that there is a concentration dependent impact of latB on *P. nicotianae* hyphal width. However, there was no significant difference in *P. nicotianae* hyphal width between DMSO and any latB treatments. This suggests that the significant difference identified under normal conditions may not be a real effect. However, as hyphal widths under latB conditions were calculated at the leading edge of the mycelium, it is possible that the width of *P. nicotianae* hyphae did change with treatment of latB but that this was not detected in most cases as hyphae which were wider and more greatly affected by latB may have had a slower growth rate.

Additionally, latB did not significantly affect the width of *P. nicotianae* hyphae in LOC devices (Fig. 3.13). However, hyphae grown under latB conditions were observed to have altered morphologies including extreme swelling at the hyphal tips and in some cases the whole hypha was enlarged (subapical swelling) (Fig. 3.42 and Table 3.3). As hyphal widths were only measured for hyphae that were growing in the channels, the widths of these hyphae were not recorded. In culture dishes, it was also unlikely that these hyphae were measured as they would have likely been growing within the mycelium and not at the leading edge.

In other oomycete species, latB has been found to alter hyphal width in a concentration dependent manner in the form of tip and subapical swelling. Ketelaar et al (2012) identified that in the presence of increasing latB concentrations, *P. infestans* hyphal tips swelled, increasing hyphal widths. When maximum hyphal widths were measured, widths of 10.38 ± 2.66 µm were calculated for hyphae treated with 0.5 µM of latB compared to 3.54 ± 0.47 µm without latB treatment (Ketelaar et al 2012). While statistical significance was not reported, it is apparent that latB treatment resulted in an increase in the width of *P. infestans* hyphae.

While hyphal widths were not measured in other studies, latB addition to oomycete species led to swelling of hyphae and germ tubes in a concentration dependent manner. Research conducted by Gupta and Heath (1997) on the oomycete *S. ferax* observed apical and subapical swelling of hyphae in the presence of latB. This swelling occurred following a cessation in

hyphal growth. Interestingly, turgor levels were shown to play a role in swelling, with low turgor hyphae displaying little or no hyphal swelling compared to hyphae with normal turgor (Gupta & Heath 1997). Subsequent experiments with *S. ferax* for longer time periods also observed hyphal tip and subapical swelling (Bachewich & Heath 1998). Tip swelling as a result of latB treatment was also observed in *P. infestans* hyphae (Meijer et al 2014). In addition to swelling of hyphae, Deora et al (2008) observed swelling of the tips of germ tubes in *A. cochlioides*. These studies further highlight the importance of the actin cytoskeleton in hyphal growth, suggesting that actin may play a restraining structural role at the hyphal tip.

4.4 Force measurements for *P. nicotianae* on LOC devices

Throughout this research, a total of 117 force deflections were recorded, 76 of which were squeezing forces and 41 of which were hyphal tip forces. This supports the hypothesis that the forces exerted by *Phytophthora* species can be measured using the LOC devices. On average, 2.5 squeezing and 1.5 hyphal tip forces were collected per device, averaging 4 deflections per device across all experiments. While up to 24 measurements could be collected for version 1 devices and 12 for version 2 and 3 devices, many factors influenced the number of successful deflections recorded.

Recorded data was not used for analysis in instances where the data was inaccurate, or pillar deflection did not occur due to hyphae growing down channel walls and avoiding pillar contact. Data inaccuracies were the result of multiple uncontrollable factors. In some instances, multiple hyphae grew down a channel and deflected the pillar concurrently. This data was excluded as an individual hyphal deflection was not measured. Additionally, as discussed previously, half of the channels in version 2 devices were unable to be recorded as pillars were found to adhere to the channel walls. Deflections could therefore only be recorded for half of the total channels in these devices.

On occasion, remnant debris from device fabrication were left in the device. When hyphae deflected a pillar with debris behind it, the debris would sometimes move onto the pillar, blocking the view of the pillar top. As a result, the pillar was unable to be accurately tracked through time and the data was excluded.

Unfortunately, as result of ongoing construction at the time of this research, on occasion the microscope would move during sequential image collection. In the resulting image sequences obvious movement of the microscope slide was observed with the device moving significantly

throughout the sequence. Because of this, the location of the pillar was not constant throughout the sequence. This meant that pillar deflection could not be accurately determined in these sequences and the data was excluded.

Although the obtained sample sizes are small, the nature of this research means that it takes a lot of time to obtain data. Collecting raw data alone took hundreds of hours, with each device taking approximately 8 hours to complete under normal conditions and even longer when hyphae were treated with latB. In addition, fabricating devices and data analysis were heavily time consuming. As sample sizes were small, force measurement data was analysed in two ways; maximum and half point values. This allowed for a more thorough examination of the collected data.

4.4.1 Squeezing force measurements

4.4.1.1 Squeezing forces on pillar 5 LOC devices with and without latB treatment

P. nicotianae squeezing forces differed under latB conditions in pillar 5 devices (Fig. 3.33). While it was determined that in pillar 5 devices there was a statistically significant difference in the squeezing forces exerted by hyphae treated with latB, post hoc analysis did not identify a significant difference. The inability of the post hoc test to detect which groups differed significantly from one another was likely due to the small sample sizes in the latB treatment groups. To accurately determine which groups differed significantly from one another would require a greater sample size with reduced standard errors.

The squeezing forces calculated for normal conditions were much greater than the forces obtained from the two highest latB concentrations (Fig. 3.33). While these forces were not identified as being significantly different, they suggest that latB negatively impacts squeezing force generation. This does not support the hypothesis that the force exerted by *P. nicotianae* hyphae will increase when actin microfilaments are inhibited. The reduction in squeezing force production may be explained by a reduction in hyphal structure and rigidity caused by sequestration of actin by latB. With reduced cytoskeletal support, the hyphal body would likely be less rigid and as a result the force exerted by the hyphal body onto the pillar when squeezing through the gap would be lower than the force exerted with cytoskeletal support.

4.4.1.2 Squeezing forces on pillar 7 LOC devices with and without latB treatment

P. nicotianae squeezing forces differed under latB conditions in pillar 7 devices (Fig. 3.34). These significant differences were identified between normal conditions and the two highest concentrations of latB using maximum force values. Half point force values identified an additional significant difference between normal conditions and the lowest concentration of latB in addition to the two higher concentrations. Similar to squeezing force analysis in pillar 5 devices, an increase in sample size would increase the accuracy of the data. This would likely result in agreement between the significance testing of the maximum and half point forces.

The squeezing forces calculated for normal conditions were significantly greater than the forces obtained from the two highest latB concentrations (Fig. 3.34). This suggests that latB negatively impacts squeezing force generation, as was seen in pillar 5 devices.

4.4.1.3 Comparison of squeezing forces on pillar 5 and pillar 7 LOC devices with and without latB treatment

P. nicotianae squeezing forces differed under latB conditions between pillar 5 and pillar 7 devices (Fig. 3.35). These significant differences were identified in all conditions except for 0.05 µM latB and 0.1 µM latB using maximum force values. Half point force values identified a significant difference in all conditions except for 0.075 µM latB. When comparing maximum and half point forces between pillar sizes, there is a significant difference in all latB conditions between the two analyses. As mentioned for pillar 5 and pillar 7 force values, an increase in sample sizes would increase the power of the squeezing force data analysis. This would likely reduce differences between the results when using maximum or half point force values.

In pillar 7 devices, squeezing forces are significantly higher than on pillar 5 devices (Fig. 3.35). This difference could be explained by the hyphae having a larger surface area onto which they can exert force (contact area) on pillars that are 7 µm in diameter than on pillars that are 5 µm in diameter. With a larger pillar diameter, more of the hypha can be in contact with the pillar, allowing more of the hyphal body to push against the pillar and exert force. Considering all factors, devices with a pillar size of 7 µm would be recommended for *P. nicotianae* hyphae in future experiments.

Measuring squeezing forces on the designed LOC devices has similarities with measuring forces on PDMS LOC devices with microgaps. In these LOC devices, long microchannels with a series of narrow gaps, called microgaps, are used to quantify force exertion by tip growing

cells. Nezhad et al (2013) designed this technique and used it to quantify force production of *C. japonica* pollen tubes. In this approach, pollen tubes grew down the channel and through the gaps. When the pollen tube was larger than the gap size it encountered, it would exert force onto the PDMS walls on either side of the gap. This deformation was quantified into force production and further into pressure exerted by the pollen tube using finite element analysis (Nezhad et al 2013). As the squeezing forces for *P. nicotianae* hyphae were only measured on one side of the hypha, as opposed to both sides in the microgap approach, they could not be accurately converted into pressures. Squeezing forces for *P. nicotianae* hyphae do however provide an idea of the magnitude of the squeezing forces that may be exerted by *P. nicotianae* when growing inside host tissue.

4.4.2 Hyphal tip force measurements

4.4.2.1. Hyphal tip forces on pillar 5 LOC devices with and without latB treatment

P. nicotianae hyphal tip forces did not differ under latB conditions in pillar 5 devices (Fig. 3.36). The hyphal tip forces for normal conditions are comparable with the forces under all latB treatment conditions. While no statistically significant difference was observed, the inability of the test to detect significance may have been due to the small sample sizes in the latB treatment groups and the absence of any values for 0.075 µM latB. To accurately determine which groups differed significantly from one another would require a greater sample size with reduced standard errors.

4.4.2.2 Hyphal tip forces on pillar 7 LOC devices with and without latB treatment

P. nicotianae hyphal tip forces differed under latB conditions in pillar 7 devices (Fig. 3.37). These significant differences were identified between all conditions and 0.075 µM latB, using maximum force values. In contrast, half point force values did not identify a significant difference between any conditions. This is likely due to the small sample sizes in the latB treatment groups and the absence of any values for 0.1 µM latB. Additionally, as the half point force values had unequal variances and data transformations were unable to homogenise them, a non-parametric test was performed, decreasing the power of the analysis. An increase in sample size and addition of values for 0.1 µM latB should reduce standard errors and may homogenise the variances. This would allow for a stronger parametric test to be employed and would increase the confidence of any conclusions drawn.

While differences in the results are inconclusive, the large increase in force with 0.075 µM latB is interesting (Fig. 3.37). When hyphal tip deflections were observed throughout all experiments, the hyphal tip would push into the pillar and once it had exerted force and encountered resistance, the hypha would effectively jump off the pillar. In contrast, both hyphae under 0.075 µM latB did not jump off the pillar but continued to push into it, one of which continued for the whole duration of the recorded sequence (Fig. 3.28). This observation suggests that these hyphae may have had increased compliance at the tip due to the effect of latB on the cytoskeleton, allowing the hyphae to push into the pillar without being pushed back when encountering resistance. This supports the hypothesis that the force exerted by *P. nicotianae* hyphae will increase when actin microfilaments are inhibited. However, the small sample size and absence of any values for 0.1 µM latB render the impact of latB on hyphal tip forces in pillar 7 devices and this observation inconclusive. To further explore any potential changes in hyphal tip compliance from latB treatment would require the collection of additional data.

4.4.2.3 Comparison of hyphal tip forces on pillar 5 and pillar 7 LOC devices with and without latB treatment

P. nicotianae hyphal tip forces differed under latB conditions between pillar 5 and pillar 7 devices (Fig. 3.38). A significant difference was identified under normal conditions but not under DMSO or 0.05 µM latB. As discussed previously, an increase in sample size would increase the power of the analysis. Additionally, an absence of values for 0.075 µM and 0.1 µM latB for pillar 7 and pillar 5 devices respectively, prevented these conditions from being compared. As hyphal tip forces were higher with pillar 7 devices under normal conditions, these devices would be recommended for *P. nicotianae* hyphae in future experiments, to obtain maximum hyphal tip forces. As pillar 7 devices were also most appropriate for obtaining squeezing force data, this would allow for direct comparisons between squeezing and hyphal tip forces, without the need to categorise data into different pillar sizes. Furthermore, using a single pillar size would increase the sample sizes obtained over the same experimental time, effectively combatting the main issue with the hyphal tip data collected in this research.

Hyphal tip forces have been also been measured on PDMS LOC devices using *A. bisexualis* (Tayagui et al 2017). When measuring forces exerted by individual hypha, a maximum force of 10 µN was recorded. The maximum hyphal tip force recorded for *P. nicotianae* was 13.73 µN (Fig. 3.22). While these values are comparable, no average maximum hyphal tip values

were reported by Tayagui et al (2017), making it difficult to draw conclusions on the similarities between species using force measurements. However, the ability to compare forces exerted by hyphae of different oomycete species on micropillar containing LOC devices holds potential for future comparative studies.

Another method used to obtain quantitative hyphal tip forces for oomycete species is the strain gauge. While forces for *P. nicotianae* have not been obtained using this approach, forces have been obtained for other oomycete species. MacDonald et al (2002) used the strain gauge method to calculate hyphal tip forces of two oomycete species; *Pythium graminicola* and *Pythium insidiosum*. Hyphal tip forces for *P. graminicola* and *P. insidiosum* were calculated to be 1.9 ± 0.2 µN (mean ± S.E.M., n = 34) and 1.8 ± 0.2 µN (mean ± S.E.M., n = 41), respectively (MacDonald et al 2002). In comparison, the maximum hyphal tip forces exerted by *P. nicotianae* were 4.33 ± 1.26 µN (mean ± S.E.M., n = 9).

When using different methods to calculate hyphal tip forces, such as LOC device pillars and strain gauges, the forces are exerted onto systems with differing characteristics. As such, forces were converted into pressures using Equations 2.1 and 2.2 to normalise the measurements and allow for better comparisons between forces calculated using different methods. Similarly, as pillar 5 and pillar 7 devices have differing pillar diameters and therefore differing contact areas, comparisons are best done using pressures. By comparing hyphal tip forces on pillar 5 and pillar 7 devices without converting to pressures, the forces differed significantly under normal conditions (Fig. 3.38). However, when converted to pressures, no significant difference was identified as the contact area on the pillar had been accounted for (Fig. 3.41).

4.5 Pressure measurements in LOC devices

In addition to applied pressures, pressure can be presented as a percentage of total turgor pressure in hyphae. When *P. nicotianae* hyphal tip pressures were converted into the percentage of total turgor pressure using Equation 2.3, the maximum percentage under normal conditions was 21% (Table 3.2). When compared to the maximum percentage under latB treatment of 45% (Table 3.2, 0.075 µM latB), this suggests that latB treatment increased the compliance of the hyphal tip.

As forces and therefore pressures of *P. nicotianae* hyphae have not been reported previously, the values obtained in this research cannot be compared to other results for *P. nicotianae*. However, pressures and the percentage of total turgor pressure have been reported for other

oomycete species using a strain gauge (MacDonald et al 2002, Money et al 2004, Ravishankar et al 2001). The pressures as a percentage of total turgor pressure for these species were summarised by Money et al (2004). Similarities are seen between values for *A. bisexualis* (16%), *P. graminicola* (20%) and *P. insidiosum* (25-54%) obtained using the strain gauge and the obtained value for *P. nicotianae* (21%) on LOC devices. As these values are comparable, it appears that the designed LOC devices can measure pressures with reasonable accuracy. Additionally, the percentage of total turgor pressure exerted onto pillars by *A. bisexualis* in LOC devices was 14% (Tayagui et al 2017). As the accuracy of pressure measurements using strain gauges has been questioned previously with regards to the reorientation of hyphal growth upon contact (Money 2007, Nezhad 2014, Nezhad & Geitmann 2013, Tayagui et al 2017), future experiments with LOC devices may increase the accuracy of pressures obtained for other oomycete species.

Pressures calculated under latB treatment suggest that actin microfilament modification may have led to an increase in compliance at the hyphal tip which allowed for the generation of greater force and pressure on the pillars. Although this is based on a very small sample size, this notable increase in compliance at the tip was not observed in the other 39 measurements taken with lower concentrations of latB and the smaller pillar size. The generation of increased force and pressure through cell cytoskeletal modifications was proposed by Walker et al (2006) regarding hyphae grown invasively. Walker et al (2006) examined the actin cytoskeleton in *P. cinnamomi* and *A. bisexualis* hyphae grown in invasive and non-invasive conditions and identified an actin depleted zone at the tip of hyphae grown in invasive but not non-invasive conditions. They suggested that this actin depleted zone is a modification of the actin cytoskeleton that, along with cell wall softening, plays a role in the generation of force by oomycetes to enable invasive growth (Walker et al 2006). While *P. nicotianae* hyphae were grown under non-invasive conditions in this research, treatment with latB appeared to simulate invasive conditions by inducing actin structure depletion. An increase in tip yielding through alteration of the actin cytoskeleton in hyphae may be a process through which hyphae produce the force and pressure required to invade hosts, along with cell wall softening and enzymatic degradation of host tissue.

4.6 Force, growth rate and hyphal width measurements for *P. cinnamomi* and *P. sojae*

Preliminary experiments with *P. cinnamomi* and *P. sojae* used version 2 pillar 5 LOC devices (Fig. 3.31). These experiments identified that these species can grow on the LOC devices and that force data can be collected. Growth rates and hyphal widths of *P. cinnamomi* and *P. sojae* hyphae were also successfully measured (Table 3.1). While no reliable conclusions can be drawn from this data as the sample size was only two for each species, it appears that *P. sojae* had a slower growth rate than *P. cinnamomi* and the hyphal widths were very similar. When compared to *P. nicotianae*, both species appear to have a slower growth rate but comparable hyphal widths.

In addition to successful growth on the devices, force measurements, growth rates and hyphal width data can be collected. This highlights the success of the devices and identifies their potential for use with other oomycete species.

4.7 Relationships between growth rate, hyphal width, force and pressure of *P. nicotianae* hyphae in LOC devices

Three potential relationships were tested to understand the extent to which the obtained variables were related. Relationships between growth rate and hyphal width, between growth rate and pressure and between growth rate, hyphal width and force were examined.

No relationship between growth rate and hyphal width was found. This suggests that hyphal width and growth rate are independent variables; growth rate is not affected by hyphal width and vice versa. The large sample sizes of these variables give confidence to this result.

While a potential relationship was found between growth rate and pressure using regression analysis, the low R^2 value combined with the correlation result which did not detect a relationship suggests that there is no relationship between growth rate and pressure. As the sample sizes for pressures were low, this result is inconclusive. Greater sample sizes are required to further explore this potential relationship.

A relationship was found between growth rate, hyphal width and force for both squeezing forces and hyphal tip forces. However, the relationship for hyphal tip forces was only detected on pillar 7 devices with maximum forces. The R^2 values obtained for these relationships were low, indicating that the relationship between growth rate, hyphal width and force is weak.

Larger sample sizes for these forces, particularly hyphal tip forces, are required to determine the actual strength of this relationship. However, the results suggest that these variables are dependent upon one another; the force generated by *P. nicotianae* hyphae is affected by the width and growth rate of the hyphae.

Similarly, Tayagui et al (2017) compared the force generated by *A. bisexualis* hyphae with hyphal width. They found that the force generated by a hypha appears to be related to its width, with smaller hyphae generating a smaller force than larger hyphae (Tayagui et al 2017). While growth rate was not examined in the relationship as for *P. nicotianae*, the result obtained by Tayagui et al (2017) suggests that the relationship detected between growth rate, width and force in *P. nicotianae* is real.

While strong relationships between growth rate, hyphal width, force and pressure were not found, this does not mean that no relationships were present. Throughout the experiments, sample sizes for forces, in particular hyphal tip forces, were inherently low. As such, the identification of strong relationships may be difficult.

4.8 Morphological observations in LOC devices

4.8.1 Hyphal morphologies observed with latB treatment

Treatment of *P. nicotianae* hyphae with latB in LOC devices caused latB dependent morphological changes (Table 3.3 and Fig. 3.42). Furthermore, these morphologies appeared to be concentration dependent. Morphological changes as a result of latB addition have also been reported in previous studies of oomycete species including changes to hyphal widths in the form of apical and subapical swelling (discussed in Section 4.3.2), cell wall deposition (Bachewich & Heath 1998) and organelle distribution (Bachewich & Heath 1998, Gupta & Heath 1997, Ketelaar et al 2012). In addition, subapical branch formation (Bachewich & Heath 1998, Ketelaar et al 2012), hyphal tip bifurcation (Ketelaar et al 2012) and extreme loss of growth polarity, resulting in curling of the hyphal tip onto itself in some cases (Ketelaar et al 2012) have been reported. While cell wall deposition and organelle distributions were not examined in this research, all other morphological changes were observed in hyphae treated with latB. These changes identify the substantial role of the actin cytoskeleton in maintaining normal hyphal morphology.

The loss of growth polarity through actin sequestration by latB strongly affected hyphal morphologies. While the distribution of actin was not examined in this research, latB disruption of actin populations in studies with *S. ferax* (Bachewich & Heath 1998, Gupta & Heath 1997) and *P. infestans* (Hua et al 2015, Ketelaar et al 2012, Meijer et al 2014) identified that different actin structures within the hypha are affected differently. In *S. ferax* hyphae, latB was found to disrupt apical actin caps, then subsequently disrupt the subapical actin cables before disrupting actin plaques (Bachewich & Heath 1998, Gupta & Heath 1997). Similarly, in *P. infestans* hyphae, where no actin cap has yet been observed, actin cables were found to be more sensitive to actin depolymerisation by latB than actin plaques (Hua et al 2015, Ketelaar et al 2012, Meijer et al 2014). The different and increasingly observed morphologies in *P. nicotianae* at higher concentrations of latB are likely a result of actin populations being affected differently. This could be determined more conclusively by performing experiments with actin staining at different concentrations of latB.

4.8.2 Appearance of appressoria-like formations

Appressoria-like formations were observed in version 2 LOC devices (Fig. 3.43). These structures occurred when hyphae encountered pillars that were adhered to the channel walls. Following initial contact with the pillar, the hypha would try to push the pillar and appeared to stop growth. Following this, the hypha swelled considerably, before branching into two hyphal branches which pushed out onto either side of the pillar. This morphological process resembles the formation of appressoria during host tissue invasion by hyphal organisms (Fig. 1.1). Recently, Kots et al (2017) identified a novel actin aster-like actin configuration in a Lifeact-eGFP strain of *P. infestans*. This actin configuration was observed during appressoria formation on hyphal contact with a physical barrier. The hyphal tips were observed to swell following contact, following which growth was halted and occasional new outgrowths formed (Kots et al 2017). This formation of appressoria is very similar to the changes observed in *P. nicotianae*.

While LOC devices were designed to measure the forces exerted by hyphae, the observation of an appressoria-like structure highlights potential future applications. In particular, LOC devices with adhered pillars could be designed specifically to examine the formation of appressoria structures further.

4.9 Conclusions

The results obtained and discussed in this thesis identify the capability of the designed LOC devices to measure the growth rate, hyphal width and force production of oomycete species, while simultaneously enabling morphological observations. The growth rate of *P. nicotianae* hyphae was shown to increase in devices compared to culture dishes, while hyphal width decreased. These changes did not appear to negatively impact the hyphae. Additionally, two types of force measurements were successfully obtained; squeezing forces and hyphal tip forces.

The results obtained from the latB experiments identify that latB decreases the growth rate of *P. nicotianae* hyphae. Additionally, morphological changes suggest that latB also severely disrupts the polarity of hyphal growth, with abnormal swellings and multiple branch formations observed. Taken together, these results show that the actin cytoskeleton is vitally important for the maintenance of hyphal growth and morphology.

In addition, although preliminary, the force and pressure results obtained for *P. nicotianae* hyphae under 0.075 µM latB treatment suggests that disruption of the actin cytoskeleton increases tip yielding, leading to the production of greater forces and pressures at the hyphal tip. This may be a process through which hyphae produce the force and pressure required to invade hosts, along with cell wall weakening and enzymatic degradation of host tissue.

Future experiments using the LOC devices with cytoskeletal actin staining, modelled invasive growth conditions and Lifeact-eGFP are of interest. Cytoskeletal actin staining with different concentrations of latB would allow for visualisation of the disruption of actin populations in *P. nicotianae*. Modelling invasive conditions by adding low melting point agar to the device, through which the hyphae would grow, would provide information on the forces produced under invasive conditions and the magnitude by which they differ to non-invasive conditions. Furthermore, actin staining under invasive conditions would allow for comparisons between actin structures formed in invasive and non-invasive growth. Unfortunately, as actin staining requires cell fixation, cytoskeletal modifications and concurrent measurements of force would not be observed. However, concurrent measurements may be possible with Lifeact-eGFP. While *P. nicotianae* has not been modified with Lifeact-eGFP to allow for live cell imaging, a group has successfully modified a *P. infestans* strain (Meijer et al 2014). As Lifeact-eGFP expression does not affect the growth of the modified strain, live imaging of hyphae in the devices could be used to obtain force measurements and concurrently observe cytoskeletal

processes occurring during force exertion. Additionally, this modified strain could be used with LOC devices with purposely adhered pillars to investigate the underlying dynamics of actin structures involved in the formation of appressoria.

In conclusion, the designed LOC devices are suitable for the growth and manipulation of pathogenic oomycete species. Using *P. nicotianae*, two types of force were quantified, and cytoskeletal manipulations were performed. The devices have the potential to provide new knowledge on the mechanisms that enable pathogenic oomycetes to cause disease. Additionally, as fungi grow through the process of tip growth and are morphologically similar to oomycetes, the designed devices would likely be able to be appropriately modified for the examination of fungal species. This information could be used to improve treatment strategies for disease caused by the invasive growth of these organisms to minimise further economic and biodiversity loss.

References

Ackerveken G. 2017. Seeing is believing: imaging the delivery of pathogen effectors during plant infection. *New Phytologist* 216: 8-10

Agudelo CG, Sanati Nezhad A, Ghanbari M, Naghavi M, Packirisamy M, Geitmann A. 2013. TipChip: a modular, MEMS-based platform for experimentation and phenotyping of tip-growing cells. *The Plant Journal* 73: 1057-68

Asai S, Shirasu K. 2015. Plant cells under siege: plant immune system versus pathogen effectors. *Current Opinion in Plant Biology* 28: 1-8

Bachewich C, Heath IB. 1998. Radial F-actin arrays precede new hypha formation in *Saprolegnia*: implications for establishing polar growth and regulating tip morphogenesis. *Journal of Cell Science* 111: 2005-16

Bastmeyer M, Deising HB, Bechinger C. 2002. Force exertion in fungal infection. *Annual Review of Biophysics and Biomolecular Structure* 31: 321-41

Bebber DP, Holmes T, Gurr SJ. 2014. The global spread of crop pests and pathogens. *Global Ecology and Biogeography* 23: 1398-407

Bebber DP, Ramotowski MAT, Gurr SJ. 2013. Crop pests and pathogens move polewards in a warming world. *Nature Climate Change* 3: 985-88

Beever RE, Waipara NW, Ramsfield TD, Dick MA, Horner IJ. 2009. Kauri (*Agathis australis*) under threat from *Phytophthora*? *Phytophthoras in Forests and Natural Ecosystems* 74-85

Bouwmeester K, Van Poppel P, Govers F. 2009. Genome biology cracks enigmas of oomycete plant pathogens in: Molecular aspects of plant disease resistance. Oxford, UK: Wiley-Blackwell: 102-34

Brand A, Gow NA. 2009. Mechanisms of hypha orientation of fungi. *Current Opinion in Microbiology* 12: 350-57

Chakraborty S, Murray G, Magarey P, Yonow T, O'Brien R, et al. 1998. Potential impact of climate change on plant diseases of economic significance to Australia. *Australasian Plant Pathology* 27: 15-35

Chen H, Bernstein BW, Bamburg JR. 2000. Regulating actin-filament dynamics *in vivo*. *Trends in Biochemical Sciences* 25: 19-23

Deora A, Hashidoko Y, Tahara S. 2008. Actin filaments predominate in morphogenic cell stages, whereas plaques predominate in non-morphogenic cell stages in *Peronosporomycetes*. *Mycological Research* 112: 868-82

Derevnina L, Petre B, Kellner R, Dagdas YF, Sarowar MN, et al. 2016. Emerging oomycete threats to plants and animals. *Philosophical Transactions of the Royal Society* 371: 20150459

Dick MA, Williams NM, Bader MK-F, Gardner JF, Bulman LS. 2014. Pathogenicity of *Phytophthora pluvialis* to *Pinus radiata* and its relation with red needle cast disease in New Zealand. *New Zealand Journal of Forestry Science* 44: 6

Dodds PN, Rathjen JP. 2010. Plant immunity: towards an integrated view of plant-pathogen interactions. *Nature Reviews Genetics* 11: 539-48

Duffy DC, McDonald JC, Schueller OJA, Whitesides GM. 1998. Rapid prototyping of microfluidic systems in poly(dimethylsiloxane). *Analytical Chemistry* 70: 4974-84

Duniway J. 1983. Role of physical factors in the development of *Phytophthora* diseases in: *Phytophthora*: Its Biology, Taxonomy, Ecology, and Pathology. St. Paul, Minnesota: The American Phytopathological Society: 175-187

Ecroyd C. 1982. Biological flora of New Zealand 8. *Agathis australis* (D. Don) Lindl. (Araucariaceae) Kauri. *New Zealand Journal of Botany* 20: 17-36

Eddington DT, Puccinelli JP, Beebe DJ. 2006. Thermal aging and reduced hydrophobic recovery of polydimethylsiloxane. *Sensors and Actuators B: Chemical* 114: 170-72

Eisenstein M. 2017. Mechanobiology: a measure of molecular muscle. *Nature* 544: 255-257

Erwin DC. 1983. Variability within and among species of *Phytophthora* in: *Phytophthora*: Its Biology, Taxonomy, Ecology, and Pathology. St. Paul, Minnesota: The American Phytopathological Society: 149-65

Erwin DC, Ribeiro OK. 1996. *Phytophthora* diseases worldwide. St. Paul, Minnesota: The American Phytopathological Society

Fawke S, Doumane M, Schornack S. 2015. Oomycete interactions with plants: infection strategies and resistance principles. *Microbiology and Molecular Biology Reviews* 79: 263-80

Fisher MC, Henk DA, Briggs CJ, Brownstein JS, Madoff LC, et al. 2012. Emerging fungal threats to animal, plant and ecosystem health. *Nature* 484: 186-194

Geitmann A, Cresti M, Heath IB. 2001. Cell biology of plant and fungal tip growth. Amsterdam, Netherlands: IOS Press.

Geng T, Bredeweg EL, Szymanski CJ, Liu B, Baker SE, et al. 2015. Compartmentalized microchannel array for high-throughput analysis of single cell polarized growth and dynamics. *Scientific Reports* 5: 16111

Ghanbari A, Nock V, Blaikie R, Chase JG, Chen X, et al. 2010. Force pattern characterisation of *Caenorhabditis elegans* in motion. *International Journal of Computer Applications in Technology* 39: 137-44

Ghanbari A, Nock V, Johari S, Blaikie R, Chen X, Wang W. 2012. A micropillar-based on-chip system for continuous force measurement of *C. elegans*. *Journal of Micromechanics and Microengineering* 22: 095009

Grenville-Briggs LJ, Anderson VL, Fugelstad J, Avrova AO, Bouzenzana J, et al. 2008. Cellulose synthesis in *Phytophthora infestans* is required for normal appressorium formation and successful infection of potato. *The Plant Cell* 20: 720-38

Grenville-Briggs LJ, van West P. 2005. The biotrophic stages of oomycete-plant interactions. *Advances in Applied Microbiology* 57: 217-43

Gupta GD, Heath IB. 1997. Actin disruption by latrunculin B causes turgor-related changes in tip growth of *Saprolegnia ferax* hyphae. *Fungal Genetics and Biology* 21: 64-75

Hardham AR. 2007. Cell biology of plant-oomycete interactions. *Cellular Microbiology* 9: 31-39

Heath IB, Gupta G, Bai S. 2000. Plasma membrane-adjacent actin filaments, but not microtubules, are essential for both polarization and hyphal tip morphogenesis in *Saprolegnia ferax* and *Neurospora crassa*. *Fungal Genetics and Biology* 30: 45-62

Heath IB, Kaminskyj SG. 1989. The organization of tip-growth-related organelles and microtubules revealed by quantitative analysis of freeze-substituted oomycete hyphae. *Journal of Cell Science* 93: 41-52

Held M, Edwards C, Nicolau DV. 2011. Hyphal responses of *Neurospora crassa* to micron-sized beads with function chemical surface groups in: Imaging, Manipulation, and Analysis of Biomolecules, Cells, and Tissues IX, 7902: International Society for Optics and Photonics.

Howard RJ, Ferrari MA, Roach DH, Money NP. 1991. Penetration of hard substrates by a fungus employing enormous turgor pressures. *Proceedings of the National Academy of Sciences* 88: 11281-84

Hu C, Munglani G, Vogler H, Fabrice TN, Shamsudhin N, et al. 2017. Characterization of size-dependent mechanical properties of tip-growing cells using a lab-on-chip device. *Lab on a Chip* 17: 82-90

Hua C, Kots K, Ketelaar T, Govers F, Meijer HJ. 2015. Effect of flumorph on F-actin dynamics in the potato late blight pathogen *Phytophthora infestans*. *Phytopathology* 105: 419-23

Jamieson A, Bassett IE, Hill LMW, Hill S, Davis A, et al. 2014. Aerial surveillance to detect kauri dieback in New Zealand. *New Zealand Plant Protection* 67: 60-65

Jing C, Gou J, Han X, Wu Q, Zhang C. 2017. *In vitro* and *in vivo* activities of eugenol against tobacco black shank caused by *Phytophthora nicotianae*. *Pesticide Biochemistry and Physiology* 142: 148-54

Jo BH, Lerberghe LMV, Motsegood KM, Beebe DJ. 2000. Three-dimensional micro-channel fabrication in polydimethylsiloxane (PDMS) elastomer. *Journal of Microelectromechanical Systems* 9: 76-81

Johari S, Nock V, Alkaisi MM, Wang W. 2012a. Elastomeric pillar arrays for integrated measurement of *C. elegans* locomotion forces. 16th international conference on miniaturized systems for chemistry and life sciences. In MicroTAS 2012 proceedings, Okinawa, Japan.

Johari S, Nock V, Alkaisi MM, Wang W. 2012b. High-throughput microfluidic sorting of *C. elegans* for automated force pattern measurement. *Materials Science Forum* 700: 182-87

Johari S, Nock V, Alkaisi MM, Wang W. 2013. On-chip analysis of *C. elegans* muscular forces and locomotion patterns in microstructured environments. *Lab on a Chip* 13: 1699-707

Judelson HS, Blanco FA. 2005. The spores of *Phytophthora*: weapons of the plant destroyer. *Nature Reviews Microbiology* 3: 47-58

Jung T, Cooke DEL, Blaschke H, Duncan JM, Oßwald W. 1999. *Phytophthora quercina* sp. nov., causing root rot of European oaks. *Mycological Research* 103: 785-98

Kamoun S, Furzer O, Jones JD, Judelson HS, Ali GS, et al. 2015. The top 10 oomycete pathogens in molecular plant pathology. *Molecular Plant Pathology* 16: 413-34

Keeling PJ, Burger G, Durnford DG, Lang BF, Lee RW, et al. 2005. The tree of eukaryotes. *Trends in Ecology & Evolution* 20: 670-76

Ketelaar T, Meijer HJ, Spiekerman M, Weide R, Govers F. 2012. Effects of latrunculin B on the actin cytoskeleton and hyphal growth in *Phytophthora infestans*. *Fungal Genetics and Biology* 49: 1014-22

Kots K, Meijer HJ, Bouwmeester K, Govers F, Ketelaar T. 2017. Filamentous actin accumulates during plant cell penetration and cell wall plug formation in *Phytophthora infestans*. *Cellular and Molecular Life Sciences* 74: 909-20

Kroon LP, Brouwer H, de Cock AW, Govers F. 2012. The genus *Phytophthora* anno 2012. *Phytopathology* 102: 348-64

Lamour K, Kamoun S. 2009. Oomycete genetics and genomics: diversity, interactions and research tools. Wiley-Blackwell

Latijnhouwers M, de Wit PJ, Govers F. 2003. Oomycetes and fungi: similar weaponry to attack plants. *Trends in Microbiology* 11: 462-69

Lew RR. 2011. How does a hypha grow? The biophysics of pressurized growth in fungi. *Nature Reviews Microbiology* 9: 509-18

Lew RR, Levina NN, Walker SK, Garrill A. 2004. Turgor regulation in hyphal organisms. *Fungal Genetics and Biology* 41: 1007-15

MacDonald E, Millward L, Ravishankar J, Money NP. 2002. Biomechanical interaction between hyphae of two *Pythium* species (Oomycota) and host tissues. *Fungal Genetics and Biology* 37: 245-49

Madoui MA, Bertrand-Michel J, Gaulin E, Dumas B. 2009. Sterol metabolism in the oomycete *Aphanomyces euteiches*, a legume root pathogen. *New Phytologist* 183: 291-300

McDonald JC, Duffy DC, Anderson JR, Chiu DT, Wu H, et al. 2000. Fabrication of microfluidic systems in poly(dimethylsiloxane). *Electrophoresis* 21: 27-40

Meijer HJ, Hua C, Kots K, Ketelaar T, Govers F. 2014. Actin dynamics in *Phytophthora infestans*; rapidly reorganizing cables and immobile, long-lived plaques. *Cellular Microbiology* 16: 948-61

Meng Y, Huang Y, Wang Q, Wen Q, Jia J, et al. 2015. Phenotypic and genetic characterization of resistance in *Arabidopsis thaliana* to the oomycete pathogen *Phytophthora parasitica*. *Frontiers in Plant Science* 6: 378

Meng Y, Zhang Q, Ding W, Shan W. 2014. *Phytophthora parasitica*: a model oomycete plant pathogen. *Mycology* 5: 43-51

Miyoshi M. 1895. Die durchbohrung von membranen durch pilzfäden. *Jahrbiicher fur Wissenschaftliche Botanik* 28: 269-89

Monahan J, Gewirth AA, Nuzzo RG. 2001. A method for filling complex polymeric microfluidic devices and arrays. *Analytical Chemistry* 73: 3193-97

Money N. 2007. Biomechanics of invasive hyphal growth in: Biology of the fungal cell. Berlin, Heidelberg: Springer: 237-49

Money NP. 2006. The triumph of the fungi: a rotten history. New York, USA: Oxford University Press

Money NP, Davis CM, Ravishankar J. 2004. Biomechanical evidence for convergent evolution of the invasive growth process among fungi and oomycete water molds. *Fungal Genetics and Biology* 41: 872-76

Nezhad AS. 2014. Microfluidic platforms for plant cells studies. *Lab on a Chip* 14: 3262-74

Nezhad AS, Geitmann A. 2013. The cellular mechanics of an invasive lifestyle. *Journal of Experimental Botany* 64: 4709-28

Nezhad AS, Naghavi M, Packirisamy M, Bhat R, Geitmann A. 2013. Quantification of cellular penetrative forces using lab-on-a-chip technology and finite element modeling. *Proceedings of the National Academy of Sciences* 110: 8093-98

Nock V, Tayagui A, Garrill A. 2015. Elastomeric micropillar arrays for the study of protrusive forces in hyphal invasion. 19th international conference on miniaturized systems for chemistry and life sciences. In MicroTAS 2015 proceedings, Gyeongju, South Korea.

Panabières F, Ali GS, Allagui MB, Dalio RJ, Gudmestad NC, et al. 2016. *Phytophthora nicotianae* diseases worldwide: new knowledge of a long-recognised pathogen. *Phytopathologia Mediterranea* 55: 20-40

Park E, Nedo A, Caplan JL, Dinesh-Kumar SP. 2017. Plant-microbe interactions: organelles and the cytoskeleton in action. *New Phytologist* 217: 1012-28

Presti LL, Kahmann R. 2017. How filamentous plant pathogen effectors are translocated to host cells. *Current Opinion in Plant Biology* 38: 19-24

Qiu Z, Tu L, Huang L, Zhu T, Nock V, et al. 2015. An integrated platform enabling optogenetic illumination of *Caenorhabditis elegans* neurons and muscular force measurement in microstructured environments. *Biomicrofluidics* 9: 014123

Qiu Z, Xue X, Li Y, Tu L, Zhu T, et al. 2014. Optogenetic manipulation of freely moving *C. elegans* in an elastomeric environment-mimicking and force-measuring chip. 18th International Conference on Miniaturized Systems for Chemistry and Life Sciences, San Antonio, Texas, USA.

Ravishankar J, Davis CM, Davis DJ, MacDonald E, Makselan SD, et al. 2001. Mechanics of solid tissue invasion by the mammalian pathogen *Pythium insidiosum*. *Fungal Genetics and Biology* 34: 167-75

Schindelin J, Arganda-Carreras I, Frise E, Kaynig V, Longair M, et al. 2012. Fiji: an open-source platform for biological image analysis. *Nature Methods* 9: 676-82

Scott P, Williams N. 2014. *Phytophthora* diseases in New Zealand forests. *New Zealand Journal of Forestry* 59: 14-21

Sietsma J, Wessels J. 2006. Apical wall biogenesis in: Growth, Differentiation and Sexuality. Berlin, Heidelberg: Springer: 125-41

Stanley CE, Grossmann G, i Solvas XC, deMello AJ. 2016. Soil-on-a-Chip: microfluidic platforms for environmental organismal studies. *Lab on a Chip* 16: 228-41

Suei S, Garrill A. 2008. An F-actin-depleted zone is present at the hyphal tip of invasive hyphae of *Neurospora crassa*. *Protoplasma* 232: 165-72

Sun Y, Tayagui A, Shearer H, Garrill A, Nock V. 2018. A microfluidic platform with integrated sensing pillars for protrusive force measurements in *Neurospora crassa*. *Micro Electrical Mechanical Systems*. Belfast, Northern Ireland.

Tayagui A, Collings D, Garrill A, Nock V. 2016. On-chip measurement of protrusive force exerted by individual hyphal tips during hyphal growth. 20th international conference on miniaturized systems for chemistry and life sciences. In MicroTAS 2016 proceedings, Dublin, Ireland.

Tayagui A, Sun Y, Collings DA, Garrill A, Nock V. 2017. An elastomeric micropillar platform for the study of protrusive forces in hyphal invasion. *Lab on a Chip* 17: 3643-53

Tinevez JY, Perry N, Schindelin J, Hoopes GM, Reynolds GD, et al. 2017. TrackMate: An open and extensible platform for single-particle tracking. *Methods* 115: 80-90

Tyler BM. 2002. Molecular basis of recognition between *Phytophthora* pathogens and their hosts. *Annual Review of Phytopathology* 40: 137-67

Tyler BM. 2007. *Phytophthora sojae*: root rot pathogen of soybean and model oomycete. *Molecular Plant Pathology* 8: 1-8

Waipara NW, Hill S, Hill LMW, Hough EG, Horner IJ. 2013. Surveillance methods to determine tree health, distribution of kauri dieback disease and associated pathogens. *New Zealand Plant Protection* 66: 235-41

Walker SK, Chitcholtan K, Yu Y, Christenhusz GM, Garrill A. 2006. Invasive hyphal growth: An F-actin depleted zone is associated with invasive hyphae of the oomycetes *Achlya bisexualis* and *Phytophthora cinnamomi*. *Fungal Genetics and Biology* 43: 357-65

Wang H, Yang S, Wang M, Xia H, Li W, et al. 2013. Sensitivity of *Phytophthora parasitica* to mandipropamid: *In vitro* determination of baseline sensitivity and *in vivo* fungitoxicity. *Crop Protection* 43: 251-55

Wang S, Boevink PC, Welsh L, Zhang R, Whisson SC, Birch PR. 2017. Delivery of cytoplasmic and apoplastic effectors from *Phytophthora infestans* haustoria by distinct secretion pathways. *New Phytologist* 216: 205-15

Wang Y, Meng Y, Zhang M, Tong X, Wang Q, et al. 2011. Infection of *Arabidopsis thaliana* by *Phytophthora parasitica* and identification of variation in host specificity. *Molecular Plant Pathology* 12: 187-201

Xia Y, Whitesides GM. 1998. Soft lithography. *Annual Review of Materials Science* 28: 153-84

Yang L, Hao X, Wang C, Zhang B, Wang W. 2014. Rapid and low cost replication of complex microfluidic structures with PDMS double casting technology. *Microsystem Technologies* 20: 1933-40

Yang X, Tyler BM, Hong C. 2017. An expanded phylogeny for the genus *Phytophthora*. *IMA Fungus* 8: 355-98

Yu YP, Jackson SL, Garrill A. 2004. Two distinct distributions of F-actin are present in the hyphal apex of the oomycete *Achlya bisexualis*. *Plant and Cell Physiology* 45: 275-80